UNIVERSIDADE DE SÃO PAULO

FACULDADE DE CIÊNCIAS FARMACÊUTICAS

Programa de Pós-graduação em Tecnologia Bioquímico-Farmacêutica

Área de Tecnologia Químico-Farmacêutica

Incorporation of the antitumor drug miltefosine into polymeric micelles

Valker Araujo Feitosa

Tese para obtenção do título de Doutor

Orientadora: Profa. Dra. Carlota de Oliveira Rangel Yagui

Co-orientadora: Dra. Natália Neto Pereira Cerize

São Paulo

2019

UNIVERSIDADE DE SÃO PAULO

FACULDADE DE CIÊNCIAS FARMACÊUTICAS

Programa de Pós-graduação em Tecnologia Bioquímico-Farmacêutica

Área de Tecnologia Químico-Farmacêutica

Incorporation of the antitumor drug miltefosine into polymeric micelles

Valker Araujo Feitosa

Versão original

Tese para obtenção do título de Doutor

Orientadora: Profa. Dra. Carlota de Oliveira Rangel Yagui

Co-orientadora: Dra. Natália Neto Pereira Cerize

São Paulo

2019

Valker Araujo Feitosa

Incorporation of the antitumor drug miltefosine into polymeric micelles

Comissão julgadora da tese

para obtenção do título de Doutor:

_____

Profa. Dra. Carlota de Oliveira Rangel Yagui

Orientadora/Presidente

_____

1º. examinador

_____

2o. examinador

_____

3o. examinador

São Paulo, _____ de _____ de 2019.

Ficha Catalográfica elaborada eletronicamente pelo autor, utilizando o programa desenvolvido pela Seção Técnica de Informática do ICMC/USP e adaptado para a Divisão de Biblioteca e Documentação do Conjunto das Químicas da USP
Bibliotecária responsável pela orientação de catalogação da publicação:
Marlene Aparecida Vieira - CRB - 8/5562

Feitosa, Valker Araujo
F311i Incorporation of the antitumor drug miltefosine into polymeric micelles / Valker Araujo Feitosa. - São Paulo, 2019.
132 p.

Tese (doutorado) - Faculdade de Ciências Farmacêuticas da Universidade de São Paulo. Departamento de Tecnologia Bioquímico-Farmacêutica.
Orientador: Rangel-Yagui, Carlota de Oliveira
Coorientador: Cerize, Natalia Neto Pereira

1. Nanotecnologia Farmacêutica. 2. Sistemas Coloidais. 3. Câncer. 4. Quimioterapia. 5. Alquilfosfocolinas. I. T. II. Rangel-Yagui, Carlota de Oliveira , orientador. III. Cerize, Natalia Neto Pereira, coorientador.

“Se vim ao mundo, foi para desenhar
meus próprios pés na areia inexplorada!”

José Régio

Dedico...

À minha amada mãe, ***Francy****.*
Meu o maior exemplo de coragem,
força, luta e superação.
Te amo, mainha!

Ao meu irmão e grande amigo, ***Valkercyo****.*
Pelo apoio incondicional e por me ensinar
a sempre fazer o melhor.

Às minhas queridas orientadoras, ***Carlota e Natália****.*
Pela acolhida e confiança e por todo empenho neste trabalho.
Parabéns pela dedicação à Ciência e à Tecnologia!
Vocês duas me inspiram diariamente.

Agradeço...

À minha família, especialmente aos meus pais, Francy e Valdemiro, ao meu irmão, Valkercyo, à minha cunhada, Tereza e à minha irmã, Neta;

Às minhas orientadoras, Carlota e Natália;

Aos meus supervisores estrangeiros, Paul e Agi;

Aos meus companheiros dos laboratórios;

Aos amigos que ganhei por onde passei;

Aos funcionários, técnicos, professores e pesquisadores da Universidade de São Paulo (USP), do Instituto de Pesquisas Tecnológicas (IPT) e do King's College London (KCL);

Às agências de fomento à pesquisa, especialmente à Coordenação de Aperfeiçoamento de Pessoal de Nível Superior (CAPES) e à Fundação de Apoio ao Instituto de Pesquisas Tecnológicas (FIPT / Novos Talentos);

A todos que me acompanharam e torceram por mim...

Muito obrigado!

List of contents

List of figures

Chapter 1

Chapter 2

Chapter 3

List of tables

Introduction

Chapter 1

Chapter 2

Chapter 3

Resumo

FEITOSA, V. A. ***Desenvolvimento de nanoestruturas poliméricas para encapsulação do antitumoral miltefosina****. 2019. 133f. Tese (Doutorado) – Faculdade de Ciências Farmacêuticas, Universidade de São Paulo, São Paulo, 2019.*

Miltefosina (hexadecilfosfocolina, HePC), um fármaco antitumoral sintético desenvolvido a partir de fosfolipídios naturais, é clinicamente aprovada para o tratamento tópico de metástases de câncer de mama e linfomas cutâneos. Atua principalmente nas membranas celulares, onde se acumula e interfere no metabolismo lipídico e nas vias de sinalização dependentes de lipídios levando as células à apoptose. No entanto, quando administrada sistemicamente ou oralmente a HePC induz hemólise e toxicidade de mucosas, respectivamente. Para superar estas reações adversas investigamos os efeitos protetores conferidos por micelas poliméricas coloidais (PM) compostas por Pluronics, copolímeros tribloco de poli(óxido de etileno) e poli(óxido de propileno). Inicialmente, encontramos que a composição e concentração do Pluronic modulam o perfil hemolítico do fármaco encapsulado (HePC-PM), aumentando a quantidade necessária de HePC para causar hemólise in vitro. Além disso, utilizamos o espalhamento de raios-X a baixo ângulo (SAXS) para obter informações estruturais das interações entre HePC e PM. Em seguida, mostramos que HePC-PM preveniu a irritação da mucosa, diminuindo a hemorragia e a vasoconstricção em membrana corioalantóica de ovos embrionados. Estudos in vitro demonstraram que a HePC-PM aumentou seletivamente a citotoxicidade contra células de carcinoma HeLa em relação a fibroblastos saudáveis, sugerindo captação diferencial dessas nanoestruturas pelas células tumorais. Além disso, relatamos que, in vitro, a HePC induz citotoxicidade, diminui a sobrevivência, migração e proliferação osteossarcomas. Esta citotoxicidade está associada à ativação da caspase-3, fragmentação do DNA, formação de corpos apoptóticos e inibição da fosforilação de Akt/PKB. Adicionalmente, HePC-PM reduz os efeitos citotóxicos nestas linhagens. Finalmente, demonstramos que as micelas poliméricas de Pluronic F127 são eficientes para a entrega intracelular fármacos preferencialmente em células tumorais, e em menor grau em células saudáveis. Em conjunto, os dados sugerem que este sistema nanoestruturado reduz a toxicidade da HePC e representa uma alternativa potencial para a administração sistêmica deste e de outros fármacos anfifílicos.

Palavras-chave: *Alquilfosfolipídios, alquilfosfocolinas, poloxamer, nanoesturutras, sistemas para entrega de fármacos, sistemas coloidais.*

Abstract

FEITOSA, V. A. ***Incorporation of the antitumor drug miltefosine into polymeric micelles****. 2019. 133f. Tese (Doutorado) – Faculdade de Ciências Farmacêuticas, Universidade de São Paulo, São Paulo, 2019.*

Miltefosine (hexadecylphosphocholine, HePC), a synthetic antitumor designed from natural phospholipids, is clinically approved for cutaneous metastases of breast cancer and cutaneous lymphoma. This drug acts mainly at cellular membrane level, where it accumulates and interferes with lipid metabolism and lipid-dependent signaling pathways leading the cells to apoptosis. However, HePC systemic and peroral administration induces hemolysis and mucosal toxicity, respectively. To overcome these limitations, we investigated the protective properties of colloidal polymeric micelles (PM) composed by Pluronics, triblock copolymers of poly(ethylene oxide) and poly(propylene oxide). We found that both Pluronic composition and concentration modulate the hemolytic profile of incorporated drug (HePC-PM) by increasing the drug amount to cause in vitro hemolysis. Moreover, small-angle X-ray scattering (SAXS) was used to assess structural information of interactions between HePC and PM. Additionally, we showed that HePC-PM prevented mucosal irritation, decreasing bleeding and lysis of blood vessels in a chicken chorioallantoic membrane model. Interestingly, HePC-PM increased the in vitro selective cytotoxicity against cervix tumor cells rather healthy fibroblasts, suggesting a differential uptake of these nanostructures by tumor cells. Furthermore, we also found that HePC induces cytotoxicity and decrease cell survival, migration and proliferation in osteosarcoma cells in vitro. We showed that cytotoxicity by HePC is associated with caspase-3 activation, DNA fragmentation, apoptotic-like body's formation and inhibition of both constitutive and cytokine-stimulated Akt/PKB phosphorylation. HePC-PM clearly reduces the drug cytotoxic effects. Finally, we demonstrated that Pluronic F127 polymeric micelles are efficient for cargo delivering the encapsulated drug preferentially into tumor cells rather than healthy cells. These findings together suggest that Pluronic F127 PM reduce drug side effects and provide a potential alternative for systemic delivery of HePC, as well as other amphiphilic drugs.

Keywords: *Alkylphospholipids, alkylphosphocholines, poloxamer, nanoestrutures, drug-delivery systems, colloidal system.*

Introduction

Cancer is a heterogeneous group of more than 100 proliferative diseases, in which abnormal cells divide uncontrollably forming tumors and leading to the destruction of surrounding health tissue. Besides, these malignant cells may disseminate into blood or lymphatic stream, reaching secondary sites (*i.e.* tissues and organs); this process is known as metastasis (Estanqueiro, *et al*., 2015).

Tumor cells acquired evolutionary-advantageous characteristics that complementarily promote transformation of phenotypically normal cells into malignant ones, and promote progression of malignant cells while sacrificing/exploiting host tissue. In general, cancer shares the following characteristics (*i.e.* hallmarks): (i) selective growth and proliferative advantage, (ii) altered stress response favoring overall survival, (iii) vascularization, (iv) invasion and metastasis, (v) metabolic rewiring, an abetting microenvironment, and (vi) immune modulation (Fouad and Aanei, 2017).

Regarding cancer treatments, these diseases remain one of the most common causes of death globally. Cancers are most likely curable at the earlier stages through conventional treatments such as surgical resection, chemotherapy and radiotherapy. However, at a later stage when cancer becomes progressive and metastasized, worse outcomes and prognosis are common. In addition, even if the cancer is diagnosed and treated early, some residual cells still remain and may cause recurrence (Ayob and Ramasamy, 2018).

Surgery and radiation, which are considered local therapy, were the main antitumor treatments up to the 1960s when it became clear that combination with drugs could bring the cure of several patients with various advanced cancers (DeVita and Chu, 2008). However, to date, anticancer drugs have reached very low success rate (~5%) in clinical development and application, which is significantly lower than other classes of drugs (Pan *et al*., 2016).

The chemotherapeutic drugs can be functionally classified based on their mechanism of action and some examples of these drugs are listed in the **Table 1.** These chemotherapeutic agents generally have a narrow margin of safety and are used in combination, usually given at a maximum tolerated dose to achieve maximum efficacy (Pan *et al*., 2016). Despite the clinical use of more than 200 anticancer drugs, dose-limiting host toxicity and drug resistance are the major obstacles for the success of cancer chemotherapy and cure. For most anticancer drugs, a large inter-individual variability in pharmacokinetics is observed resulting in unpredictable toxicity and variable antitumor effects (Pan *et al*., 2016).

As shown in **Table 1**, most of the antineoplastic agents present cytotoxicity by interacting with the genetic material (*i.e.* DNA and RNA) and, therefore, present poor selectivity only based on the accelerated growth rate of neoplastic cells. These drugs are associated to side effects that have a severe impact on patients' quality of life (Estanqueiro, *et al*., 2015).

Table 1. Chemotherapeutic drugs based on their mechanism of action. According to Estanqueiro, et al. (2015) and Pan et al. (2016).

Groups	***Mechanism of Action***	***Examples***
Alkylating agents	*Directly damage DNA to prevent the cancer cell from reproducing*	*Cyclophosphamide, ifosfamide, carmustine, dacarbazine,* *-Platinum drugs (cisplatin, carboplatin, oxalaplatin)*
Antimetabolites	*Interfere with DNA and RNA growth (during the phase S) by substitution of the normal building blocks of RNA or DNA*	*5-Fluorouracil, 6-mercaptopurin, capecitabine, cytarabine, gemcitabine, thioguanine*
Antitumor antibiotics	*Anthracyclines interfere with enzymes involved in DNA replication*	*Daunorubicin, doxorubicin, epirubicin, idarubicin, actinomycin-D, bleomycin, mitomycin-C*
Topoisomerase inhibitors	*Interfere with topoisomerases, enzymes that separate DNA strands for duplication*	*Topoisomerase I inhibitors (topotecan, irinotecan)* *Topoisomerase II inhibitors (etoposide, teniposide)*
Mitotic inhibitors	*Stop mitosis or inhibit enzymes from making proteins needed for cell reproduction (acts during the phase M but can damage cells in all phases)*	*Taxanes (paclitaxel and docetaxel)* *Epothilones (exabepilone)* *Vinca alkaloids (vinblastine, vincristine and vinorelbine, estramustine)*
Proteasome inhibitors	*Inhibit proteasome and prevent p53 degradation*	*Bortezomib, carfilzomib, ixazomib*
Tyrosine kinase inhibitors (TKIs)	*Block tyrosine kinase enzymes*	*Bcr-Abl TKIs (imatinib, nilotinib, dasatinib, bostutinib)* *VEGF/VEGFRs TKIs (axitinib, leflunomide, neratinib, pazopanib, regorafenib, semaxinib, vandetanib, vatalanib, crizotinib, sorafenib, bevacizumab, lucentis, aflibercept, ramucirumab, motesanib)* *PDGF/PDGFRs TKIs (axitinib, cediranib, imatinib, leflunomide, pazopanib, sunitinib, tandutinab)* *EGFR/HER2/HER3 TKIs (panitumumab, trastuzumab, cetuximab, pertuzumab, erlotinib, gefitinib, canertinib, lapatinib, afatinib, trastuzumab emtansine)* *ALK TKI (crizotinib, ceritinib, alectinib)*
Corticosteroids	*Natural hormones and hormone-like drugs useful in treating some types of cancer*	*Prednisone, methylprednisolone; desamethasone*
Alkylphospholipids (APLs)	*Cause direct destruction of tumor cells and this effect was associated with disturbance of the membrane phospholipid metabolism*	*Edelfosine, miltefosine (HePC), perifosine, erucylphosphocholine, erufosine*
Miscellaneous	*Drugs that act in slightly different ways and do not fit well into any of the other categories*	*L-asparaginase*

1

Synthetic alkyl-lysophospholipids (APLs), originated from the naturally occurring cell membrane phospholipids, were developed as a new type of antitumor drugs. The amphiphilic nature of APLs allows them to easily insert into membranes and interfere with both lipid-based metabolism and signaling. Miltefosine (hexadecylphosphocholine, HePC), is one of the first drugs of the APL class and the prototype of alkylphosphocholines subclass (APCs). HePC presents anti-tumor effect both in cell culture and *in vivo* models. It is clinically used for topical treatment of cutaneous metastases of breast cancer as well as cutaneous lymphoma. Additionally, HePC exhibits potent leishmanicidal activity (Hildmann and Danker, 2014).

Unfortunately, owing to the amphiphilic nature HePC causes cell lysis at high concentrations and cannot be intravenously administered due to the strongly hemolytic effect. Additionally, it may cause severe gastrointestinal toxicity (*i.e.* nausea, vomiting and diarrhea), resulting in a narrow tolerable oral dose (Ríos-Marco, et al., 2017). These side effects limit the broader utilization of HePC as a systemic anticancer drug.

Taking into account all the aforementioned, we propose that incorporation of HePC intro colloidal polymeric nanostructures, namely Pluronic micelles could reduce the drug toxicity. Pluronics are amphiphilic triblock block copolymers of poly(ethylene oxide)-poly(propylene oxide)-poly(ethylene oxide) that above a certain concentration (critical aggregation concentration) self aggregate into polymeric micelles in aqueous solutions. These polymeric micelles have been receiving increasing interest as drug delivery systems because of their distinct advantages including easy production (*i.e* formed by self-assembly), adequate size for drug delivery (*e.g.* less than 50 nm), improved solubility of hydrophobic

drugs, long circulation *via* evading recognition by reticuloendothelial system (RES) and passive targeting ability of tumor tissues by the enhanced permeability and retention (EPR) effect (Estanqueiro, *et al*., 2015).

To address this hypothesis, the present thesis was structured in three chapters with aim to demonstrate that the proposed nanostructures decrease both hemolytic and mucosal toxicity while preserving the cytotoxic effect of HePC against tumor cells rather than healthy cells.

References

Ayob and Ramasamy. Cancer stem cells as key drivers of tumour progression. Journal of Biomedical Science (2018) 25:20.

DeVita and Chu. A History of Cancer Chemotherapy. Cancer Res 2008; 68: (21).November 1, 2008.

Ríos-Marco, et al., Alkylphospholipids: An update on molecular mechanisms and clinical relevance. Biochimica et Biophysica Acta, 1859, (2017) 1657-1667.

Estanqueiro, *et al*. Nanotechnological carriers for cancer chemotherapy: The state of the art. Colloids and Surfaces B: Biointerfaces 126 (2015) 631–648.

Fouad and Aanei, Revisiting the hallmarks of cancer. Am J Cancer Res. 2017; 7(5): 1016–1036.

Hildmann and Danker. Modified phospholipids: From detergents towards smallmolecular response modifiers. Eur. J. Lipid Sci. Technol. 2014,116, 1108–1113.

Pan et al., Molecular mechanisms for tumour resistance to chemotherapy. Clinical and Experimental Pharmacology and Physiology, 2016; 43: 723–737.

Chapter I

This first chapter, entitled "Polymeric micelles of Pluronic F127 reduce hemolytic potential of amphiphilic drugs", were submitted to publication on the Journal Colloids and Surfaces B: Biointerfaces.

Polymeric micelles of Pluronic F127 reduce hemolytic potential of amphiphilic drugs

Valker Araujo Feitosa[1,2], Vinícius Cordeiro de Almeida[1], Barbara Malheiros[3], Raphael Dias de Castro[3], Leandro Ramos Souza Barbosa[3], Natalia Neto Pereira Cerize[2], Carlota de Oliveira Rangel-Yagui[1]

[1]Department of Biochemical and Pharmaceutical Technology, School of Pharmaceutical Sciences, University of São Paulo (USP), São Paulo, Brazil
[2]Bionanomanufacturing Center, Institute for Technological Research (IPT), São Paulo, Brazil
[3]Institute of Physics, University of São Paulo (USP), São Paulo, Brazil

Abstract

One of the main toxicities associated to intravenous administration of amphiphilic drugs is pronounced hemolytic activity. To overcome this limitation, we investigated the anti-hemolytic properties of polymeric micelles of Pluronics, triblock copolymers of poly(ethylene oxide) and poly(propylene oxide). We studied the encapsulation of the amphiphilic compounds miltefosine (HePC), cetrimonium bromide and cethylpyridinium chloride into polymeric micelles of Pluronics F108, F68, F127, L44, and L64. In vitro hemolysis indicated that, among the five copolymers studied; only F127 completely inhibited hemolytic effect of the compounds at 50 µg/mL. To better understand this interaction, we analyzed the HC_{50} (concentration causing 50% of hemolysis) for HePC free and loaded into F127 micelles. Copolymer concentration influenced the hemolytic profile of encapsulated HePC; for F127 the HC_{50} increased relative to free HePC (40 µg/mL) up to 184, 441, 736 and 964 µg/mL, for 1, 3, 6 and 9% F127, respectively. Interestingly, a linear relationship was found between HC_{50}-HePC and F127 concentration. At 3% F127, it is possible to load up to 300 µg/mL HePC with no hemolytic effect. By achieving this level of hemolysis protection, a promising application is on the view, bringing the parenteral use of HePC and other amphiphilic drugs. Additionally, small-angle X-ray scattering (SAXS) was used to assess structural information of interactions between HePC and micelles.

Keywords: *Triblock copolymer, poloxamer, miltefosine, cetrimonium bromide, cethylpyridinium chloride, hemolysis, anti-hemolytic.*

1. Introduction

Hemolysis refers to the rupturing membrane of erythrocytes (*i.e.* red blood cells, RBCs), ultimately causing the release of hemoglobin and other internal component into the surrounding fluid (Shah *et al.,* 2009). The intravascular releasing of massive amounts of hemoglobin into the blood stream (*i.e.* hemoglobinemia) usually can result in adverse clinical signs and symptoms such as pain (*e.g.* local, abdominal and sternal), vascular alterations (*e.g.* endothelial irritation, phlebitis, platelet activation, thrombosis, vasoconstriction, blood pressure increase, pulmonary hypertension), jaundice, kernicterus, esophageal spasm, dysphagia, erectile dysfunction, inflammation, renal dysfunction (*e.g.* hemoglobinuria and acute renal failure), and in severe cases mortality (Rother *et al.,* 2005, Amin and Dannenfelser 2006).

Hemolytic events may occur *in vivo* under clinical-pathophysiological conditions, including paroxysmal nocturnal hemoglobinuria, sickle-cell disease, thalassemias, hereditary spherocytosis and stomatocytosis, microangiopathic hemolytic anemias, paroxysmal cold hemoglobinuria, severe idiopathic autoimmune hemolytic anemia, cardiopulmonary bypass, mechanical heart valve–induced anemia, enzymatic deficiency (*e.g.* pyruvate kinase and glucose-6-phosphate), blood transfusion (*e.g.* ABO mismatch and improperly stored red blood cells), infection-induced anemia (*e.g. Staphylococcus, Plasmodium,* and influenza virus) as well as drug-induced intravascular hemolysis (Rother *et al*., 2005, Shah *et al.,* 2009, Lee and Ding, 2013).

Hemolysis has been a concern during intravenously drug administration and can be caused by the direct interaction of chemical compounds with RBCs'

membrane surface. Substantial hemolysis is found after RBCs' contact with amphiphilic drugs (Schreier *et al*., 2000).

These effects of a drug on the erythrocyte membrane can be attributed to two main phenomena: (i) its insertion into the membrane and (ii) the intensity of the membrane-perturbing action of the molecule (Malheiros *et al.*, 2000). The hemolytic process induced by amphiphilic compounds can be described as a bilayer-to-micelle transition depending on the amphiphile:lipid ratio, in which the concentration of amphiphilic compound required to induce membrane saturation (the onset of hemolysis) and total membrane solubilization (100% lysis) determines the limits for the co-existence of mixed-membranes and mixed-micelles (Prete *et al.*, 2002; Domingues *et al.*, 2008). Important events resulting from the interaction of amphiphilic drugs with cell membranes include: (i) change in bilayer organization affecting permeability, change in membrane proteins structure and function; (ii) lipid or drug flip-flop; (iii) change in cells shape (iv) endo/exovesiculation; (v) non-bilayer drug-lipid domains (non-bilayer phase formation); (vi) interdigitation; and (vii) membrane disruption and even solubilization (Schreier *et al.*, 2000).

Classes of amphiphilic drugs include phenothiazine, benzodiazepine, tranquilizers, analgesics, peptides and non-peptide antibiotics, tricyclic antidepressants, antihistamines, anticholinergics, β-blockers, local anesthetics, non-steroidal anti-inflammatories, and anticancer drugs (Schreier *et al.*, 2000). Among these, we highlight miltefosine (hexadecylphosphocholine, HePC, **Figure 1A)**, the main representative of the class of anti-tumor synthetic alkylphospholipids (ALPs) clinically approved by the FDA for topical treatment of skin metastases of breast cancer, as well as cutaneous lymphoma

(Pachioni *et al.*, 2013). HePC is also widely used as an effective peroral treatment for visceral leishmaniasis (Alonso and Alonso, 2016).

A

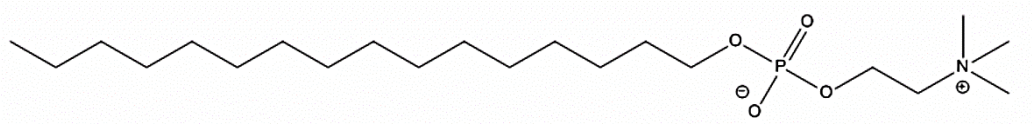

***Miltefosine (HePC)**, MW 407.6*

B

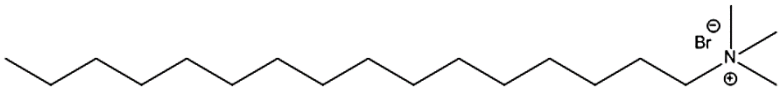

***Cetrimonium bromide (CTAB)**, MW 364.4*

C

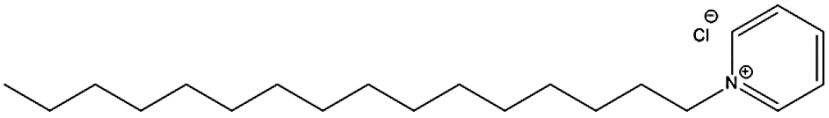

***Cetylpyridinium chloride (CPC)**, MW 339.9*

D

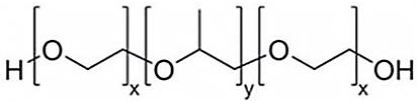

Pluronic

L44, x=12 and y=20
L64, x=13 and y=30
F68, x=78 and y=30
F108, x=132 and y=50
F127, x=106 and y=70

Figure 1. Chemical structure of the investigated amphiphilic molecules. ***(A)*** *miltefosine, HePC;* ***(B)*** *cetrimonium bromide, CTAB;* ***(C)*** *cetylpyridinium chloride, CPC; and* ***(D)*** *Pluronic. MW: molecular weight.*

One of the most studied alternatives to reduce drugs hemolytic effect is nanoencapsulation and an interesting alternative refers to polymeric micelles, which are colloidal nanostructures (~10-100 nm) of amphiphilic block copolymers, which spontaneously self-aggregate in aqueous environments (Rangel-Yagui *et al.*, 2005). Almost all routes of drug administration (*e.g.* parenteral, peroral, nasal, ocular, topical, among others), have benefited from drug encapsulation into polymeric micelles, mainly in terms of reduction of side effects and/or increase in bioavailability. Also, these supramolecular structures can

accumulate in cancer tissues owing to the enhanced permeation and retention (EPR) effect (Movassaghian *et al.*, 2015).

Synthetic and natural copolymers, with different biodegradable and biocompatible characteristics, have been explored for micelle formation. Among them, Pluronics **(Figure 1D)**, amphiphilic copolymers composed of polyethylene oxide (PEO) and polypropylene oxide (PPO), are well-known to form spherical micelles. The PEO-PPO-PEO triblock copolymers are biocompatible, FDA-approved and commonly used for cosmetic and pharmaceutical applications (Talelli and Hennink, 2011). Many types of Pluronics are available differing in the degree of polymerization of both PEO and PPO chains, thereby resulting in different molecular weights, physicochemical properties, and solubility profiles.

Polymeric micelles as drug carriers are already under clinical evaluation. The formulation *SP1049C* (Supratek Pharma®), composed by mixed-micelles of Pluronics (F127/L61) carrying doxorubicin is at international phase-III clinical trials for treating multidrug-resistant adenocarcinoma tumors (Oerlemans *et al.*, 2010; Guo and Huang, 2014; Movassaghian *et al.*, 2015). Similar Pluronic formulations containing docetaxel (*SP1012C*) and cabazitaxel (*SP1015C*) are under preclinical studies (Guo and Huang, 2014). Another interesting feature is the ability of some Pluronics to inhibit the P-glycoprotein (P-gp), a protein drug efflux transporter related to drug resistance development in some tumors (Wei *et al.*, 2013).

Understanding the erythrocyte solubilization process and finding effective protecting hemolysis agents are crucial challenges in pharmaceutical research. In this work, we investigated the interaction between HePC and polymeric micelles of Pluronics, as well as its effect on erythrocytes, envisioning reduction

of drug-hemolytic effect. To better understand the behavior of amphiphilic drugs and Pluronics micellar aggregates, we also investigated conventional surfactants cetrimonium bromide (CTAB, **Figure 1B**) and cetylpyridinium chloride (CPC, **Figure 1C**). While the first has been investigated for its antimicrobial and antitumor activities (Ito *et al.*, 2009; Wissing *et al.*, 2013; Pan *et al.*, 2015), the last is used as a bacterial antiseptic in several commercially-available mouthwashes, throat sprays and nasal sprays (Eley, 1999; Sreenivasan and Gaffar, 2002; Madaan and Tyagi, 2008).

2. Material and methods

HePC was obtained from Avanti Polar Lipids®, Alabaster, USA, CTAB and CPC were obtained from Sigma®, USA. Fresh defibrinated sheep blood was purchased from NewProv®, Brazil. Pluronics® block copolymers L44, L64, F68, F108 and F127, were kindly provided by Basf®, Brazil. The molecular characteristics of all Pluronics used in this study are presented in **Table 2**. All materials were used as received without additional purification.

2.1. Preparation of polymeric micelles

Polymeric micelles were prepared by direct dissolution method, whereby a required amount of the Pluronic (*i.e.* 0.1 to 9.0%) and drug ranging from 5 to 1500 µg/mL were solubilized in 154 mM NaCl (normal saline), and stirred at 37 ºC for one hour to reach thermodynamic equilibrium. For all polymeric micelles' formulations % of Pluronic always refers to their weight (in grams) per 100 mL.

2.2. Hemolysis bioassay

The effect of the amphiphilic compounds (HePC, CTAB and CPC), copolymers and polymeric micelles on the integrity of erythrocyte membranes was investigated by *in vitro* hemolysis assay. The release of hemoglobin from the erythrocytes was used as a measure of toxicity of these samples. Stock solutions of each compound were prepared in 154 mM NaCl aqueous solution. Two methods (A and B) were applied for *in vitro* evaluation of RBCs lysis. These methods differ in the concentration of RBCs, contact time, and dilution factor of the system. The first one is most commonly applied to compare hemolytic substances as well as for screening of hemolysis protectors, while method B simulates an intravenous administration.

2.2.1 Method A

According to (Rangel-Yagui *et al.*, 2007), the systems were prepared with 5% (v/v) of commercially available sheep RBCs and increasing concentrations of drugs (free or loaded into polymeric micelles) in normal saline. The test tubes were kept in a water bath at 37 ºC for one hour, under gentle agitation every 5-10 min. Following the incubation time, the tubes were then centrifuged at 3000 rpm for 3 min at room temperature. Hemoglobin released into the supernatant (A_{sample}) was measured by spectrophotometer analysis at 540 nm. The absorbance of samples was compared to normal saline as negative control (A_{saline} means 0% hemolysis) and distilled water as positive control (A_{water} means 100% hemolysis). All hemolysis data were presented as the percentage of the complete hemolysis given by **Eq 1.**; values are reported as mean ± standard deviation.

$$\%hemolysis = 100\ \frac{A_{Sample} - A_{Saline}}{A_{water} - A_{Saline}} \qquad \textbf{(Eq.1)}$$

Where, A_{sample} is the absorbance of the unknow sample, A_{saline} is the average absorbance of the negative without drug, and A_{water} is the average absorbance of the lysed samples.

2.2.1 Method B

Variable amounts of sheep blood were added to 100 µL of test solution in ratios from 1:1 to 12:1 (v:v). The mixture was homogenized and incubated at 37 ºC for 2 min. After this time, 5 mL of 154 mM saline solution was added. The hemoglobin concentration released, related to hemolysis, was determined at the same manner as described for method A (Reed and Yalkowsky, 1985).

2.3 Small angle X-ray scattering (SAXS) characterization

SAXS experiments were performed as SAXS1 beamline at the National Synchrotron Light Laboratory, LNLS, Campinas, SP (LNLS, Campinas, Brazil). The X-ray wavelength used was λ=0.1488 nm, and the sample-to-detector distance was ~1000 mm, providing a q-range of $0.1 < q < 4.0$ nm^{-1}, for the scattering vector q equal to $4\pi/\lambda \sin(\theta)$, being 2θ the scattering angle. A bidimensional PILATUS 300k detector was used. Samples were set between two flat mica walls with a 1 mm spacer and a thermal bath was used for temperature control, set to 37.0 ± 0.5 ºC. Scattering data were normalized for time acquisition (100 s each frame) and checked for radiation damage by measuring several consecutive frames. Indeed, no radiation damage effect was observed in the present study. The final scattering curves were subtracted from the buffer contribution and corrected by the sample's attenuation. SAXS measurements

were carried out in systems composed by 9% F127 in the absence and presence of increasing HePC concentration up to 1400 µg/mL. Furthermore, one single measurement at 4.5% was performed, just to check the possible effect of micelle-micelle interaction over the SAXS curves.

For spherical particles, it is possible to describe the scattering intensity as Bergmann, Fritz, and Glatter (2000) and Heike, *et al*., (2013):

$$I(q) = kn_pP(q)S(q) \qquad \textbf{(Eq. 2)}$$

Where, *k* is a constant related to the experimental setup, n_p is the particle number density (in this study is the concentration of polymeric micelles in solution) and P(q) and S(q) are the form and interference factors, respectively. P(q) in Eq. 2 is the orientational average of the particle form factor and was evaluated using the indirect Fourier transform (IFT) methodology (Bergmann, Fritz, and Glatter, 2000), where the pair distance distribution function, p(r), is calculated. The p(r) function is related to the probability of finding a pair of scattering elements, inside your scattering particle, at a distance *r*, thus for distances larger than the maximum dimension (D_{max}) of your scattering particle, $p(r > D_{max}) = 0$.

S(q) tends to 1 for noninteracting particles, this is the case for low concentrated dispersions of scattering particles. Nevertheless, as will be shown below, the concentration of 4.5 and 9% cannot be considered as diluted systems, thus it is clearly evidenced the appearance of an interference function over the SAXS curves. In order to calculate the S(q) function, the Perkus-Yevich approximation was used herein (Percus and Yevick, 1958). Under this approximation, the interference function, S(q), is treated with the hard sphere (being σ its diameter) potential. Thus, S(q) can be written as a function of the

volume fraction (Φ), which can be written as $\Phi = {n_p \pi \sigma^3}/{6}$ and is the total volume that the micelles occupies in the solution. Under this approximation, the interference function, S(q), can be written as Percus and Yevick, (1958) and Vrij (1979):

$$S(q) = \frac{1}{1+\frac{48\Phi G(q)}{q\sigma}} \qquad \textbf{(Eq. 3)}$$

The function G(q) is:

$$G(q) = \frac{(1+2\Phi)^2}{(1-\Phi)^4}\left(\frac{\sin(q\sigma) - q\sigma\cos(q\sigma)}{(q\sigma)^2}\right)$$

$$-\frac{3}{2}\Phi\frac{(2+\Phi)^2}{(1-\Phi)^4}\left(\frac{2q\sigma\sin(q\sigma) + (2-(q\sigma)^2)\cos(q\sigma) - 2}{(q\sigma)^3}\right)$$

$$+\frac{(1+2\Phi)^2}{(1-\Phi)^4}\frac{\Phi}{2}.\left(\frac{4[(3(q\sigma)^2-6)\cos(q\sigma)+\left((q\sigma)^3-6q\sigma\right)\sin(q\sigma)+6]-(q\sigma)^4\cos(q\sigma)}{(q\sigma)^5}\right) \qquad \textbf{(Eq. 4)}$$

Furthermore, it is possible to calculate the micellar aggregation number, using the volume fraction of the hard spheres and using some algebraic equations, resulting in:

$$N_{agg} \cong \frac{\pi\sigma^3([F127]-CMC)}{10\Phi\, M_W} \qquad \textbf{(Eq. 5)}$$

Where, [F127] is the polymer concentration (in g/L) CMC is the polymer critical micellar concentration (also in g/L), M_W is the polymer molecular weight, which is 12600 g/mol for F127. At 37 ºC it is known that the CMC of F127 is ~0.1% (Valenzuela-Oses, García, Feitosa et al., 2017, **Appendix A**). Using such procedure, it is possible to infer about the micelle aggregation number, N_{agg}.

3. Results and discussion

3.1. Hemolitic potential of HePC, CTAB and CPC

Hemolysis is the disruption of the RBCs and can be caused by the interaction of amphiphilic compounds with the cell membrane altering their composition, shape and stability. These compounds could solubilize lipids or insert into phospholipid membranes to destabilize them. The hemolytic curves, reported as %hemolysis, obtained with increasing concentrations of HePC, CTAB, and CPC in erythrocyte suspensions are shown in **Figure 2**. All compounds tested produced a dose-response hemolysis and the hemolytic behavior is similar, hemolysis was not observed up to 20 µg/mL, thereafter increasing drug concentration results in immediate hemolysis.

The hemolytic parameters HC_{50} (concentration needed to induce 50% of hemolysis), C^{sat} (concentration required to induce saturation - the onset of hemolysis) and C^{sol} (concentration of total membrane solubilization/lysis) are presented in **Table 1.** Approximately similar parameter settings are observed, regardless of the compound tested. However, HePC shows higher values for all parameters, indicating its ability to accommodate at greater amounts into erythrocytes membrane, prior to leading to hemolysis.

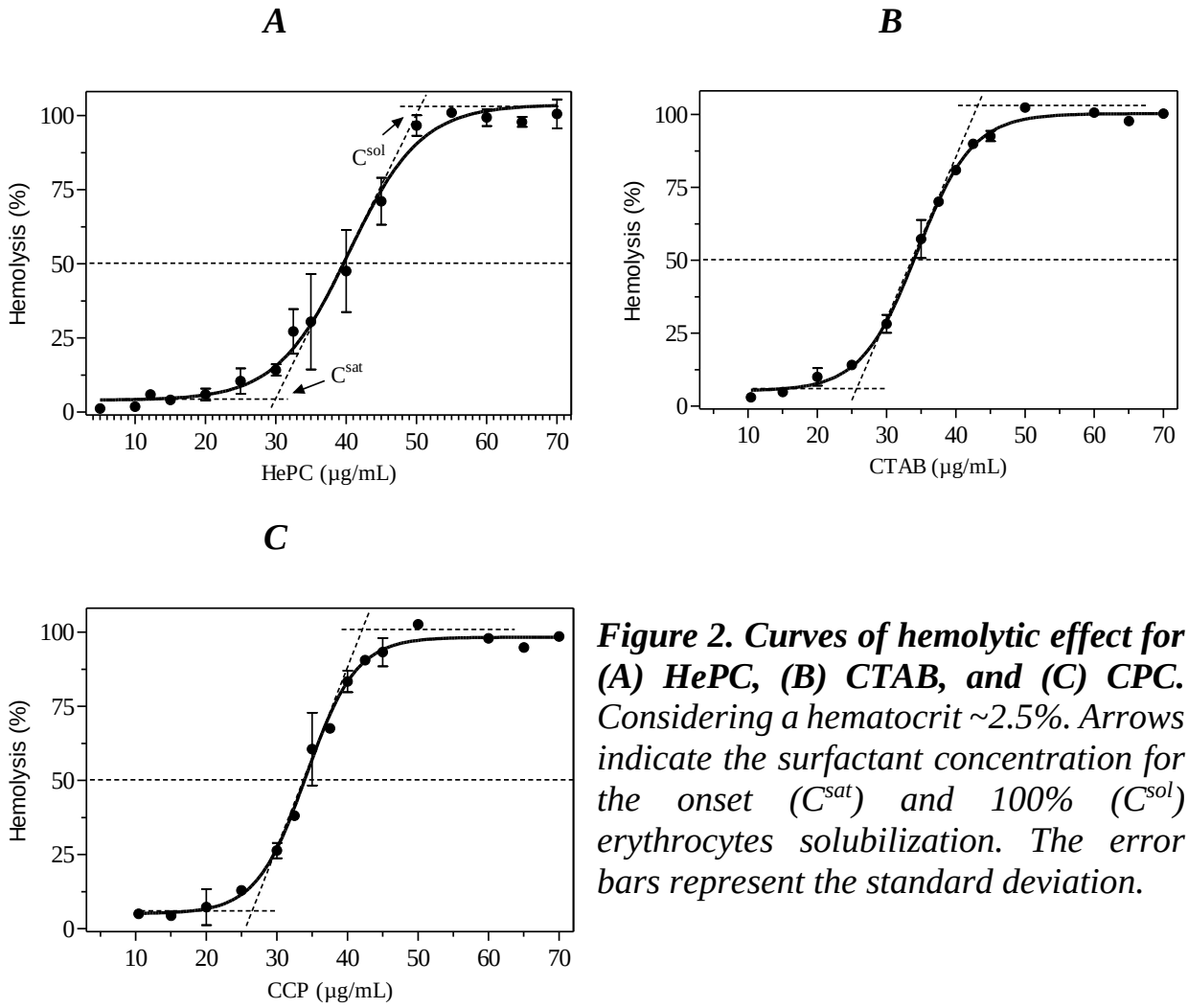

Figure 2. Curves of hemolytic effect for (A) HePC, (B) CTAB, and (C) CPC. *Considering a hematocrit ~2.5%. Arrows indicate the surfactant concentration for the onset (C^{sat}) and 100% (C^{sol}) erythrocytes solubilization. The error bars represent the standard deviation.*

Table 1. Hemolytic effect parameters of HePC, CTAB and CCP upon sheep erythrocyte membranes.

Drug	*C^{sat} (µg/mL)*	*HC_{50} (µg/mL)*	*C^{sol}(µg/mL)*
HePC	*30*	*40.4*	*50*
CTAB	*26*	*34.4*	*43*
CTCP	*27*	*34.2*	*42*

Considering a hematocrit ~2.5%. HC_{50}: drug concentration needed to induce 50% hemolysis; C^{sat}: drug concentration required to induce saturation; and C^{sol}: drug concentration required to total membrane solubilization.

HePC monomers in aqueous solutions self-assemble in small micelles (~6 nm) that can interact non-specifically with bilayer membranes leading to cell disruption, including gastrointestinal cells and erythrocytes (Van Blitterswijk and Verheij, 2008).

The aggregation state of HePC, *i.e.* self-organization into classical small micelles, has proven to be an indicator of hemolytic toxicity. Considering the CMC of 50 µM (*i.e.* 20.4 µg/mL), proposed by Marioni *et al*. (2015), our results show that HePC begins to induce hemolysis above 20 µg/mL **(Figure 2A)**, thus suggesting that the drug hemolytic effect is linked to it self-assemble into micelles, which interact nonspecifically with cell membranes leading to its solubilization.

3.2. Incorporation of HePC, CTAB and CPC into Pluronic F127 micelles suppress drug-induced hemolysis

While lipid membrane solubilization triggered by surfactants is a well-described phenomenon (Schreier *et al.*, 2000) and the hemolytic effect of HePC has been studied (Moreira *et al.*, 2013; Munoz *et al.*, 2013; De Sa *et al.*, 2015; Alonso and Alonso, 2016), polymeric micellar formulations to inhibit surfactant-drug hemolysis has not been investigated to any great extent.

Considering the clinical relevance of HePC, our group has been working to understand the interaction between this drug and polymeric micelles. Previously, we demonstrated that HePC incorporation into F127 micelles reduces hemolytic effects while maintaining anti-tumor activity *in vitro* (Valenzuela-Oses, García, Feitosa *et al.,* 2017, **Appendix A**). Here we evaluated the performance of others copolymers (*i.e.* F108, F68, L44, and L64) to increase possibilities of formulation. The interest in using Pluronic polymeric micelles as drug delivery systems is not recent, and the first anticancer micellar formulation to reach clinical evaluation was doxorubicin loaded into Pluronics L61/F127 mixed micelles (SP1049C) (Valle *et al.*, 2004; Armstrong *et al.*, 2006; Valle *et al.*, 2011; Alakhova *et al.*, 2013; Pitto-Barry and Barry, 2014).

We studied Pluronics formulations to lower the hemolytic effect of surfactant drugs. In **Figure 3,** we show the hemolytic effect of HePC, CTAB and CPC loaded into several Pluronics solutions above the CMC. Pluronic F127 at 1% was able to protect erythrocytes from hemolysis for all three amphiphilic molecules at 50 µg/mL; the hemolytic percentage was always near to 0%, which is in very good agreement with our previous findings (Valenzuela-Oses, García, Feitosa *et al.,* 2017, **Appendix A**). The most notable feature of these new results is that protective interaction is surprisingly selective for F127 and is not observed, or much reduced, with other Pluronics (F68, F108, L44, and L64). Additionally, hemolysis was not observed in none of the empty Pluronic micelles **(data not shown)**. The locus of drug/compound binding is probably near to micellar core but with the hydrophilic portion towards the palisade layer (core/corona interface), as HePC, CTAB and CPC are amphiphilic. Nonetheless, to assert the specific compound localization refined analyzes, such as SANS and NMR, are required (Valero *et al.*, 2016).

The reason for the increase incorporation of amphiphilic molecules only into Pluronic F127 micelles, and not into other tested Pluronics, may be due to the unique physicochemical and structural properties of each Pluronic. We propose that low toxicity of drugs incorporated only into F127 micellar formulation possibly involving the coaggregation of these drugs themselves with the colloidal nanostructures, thus forming mixed micelles, and ultimately protecting the erythrocyte from drug-induced hemolysis. In contrast, erythrocyte protection was not observed for the other four copolymers studied (*i.e.* F108, F68, L44, and L64) in which the drugs may not readily bind inside these polymeric micelles, under

experimental conditions (*i.e.* Pluronic 1%, drug 50 µg/mL, at 37 ºC), resulting in an inability to block hemolysis.

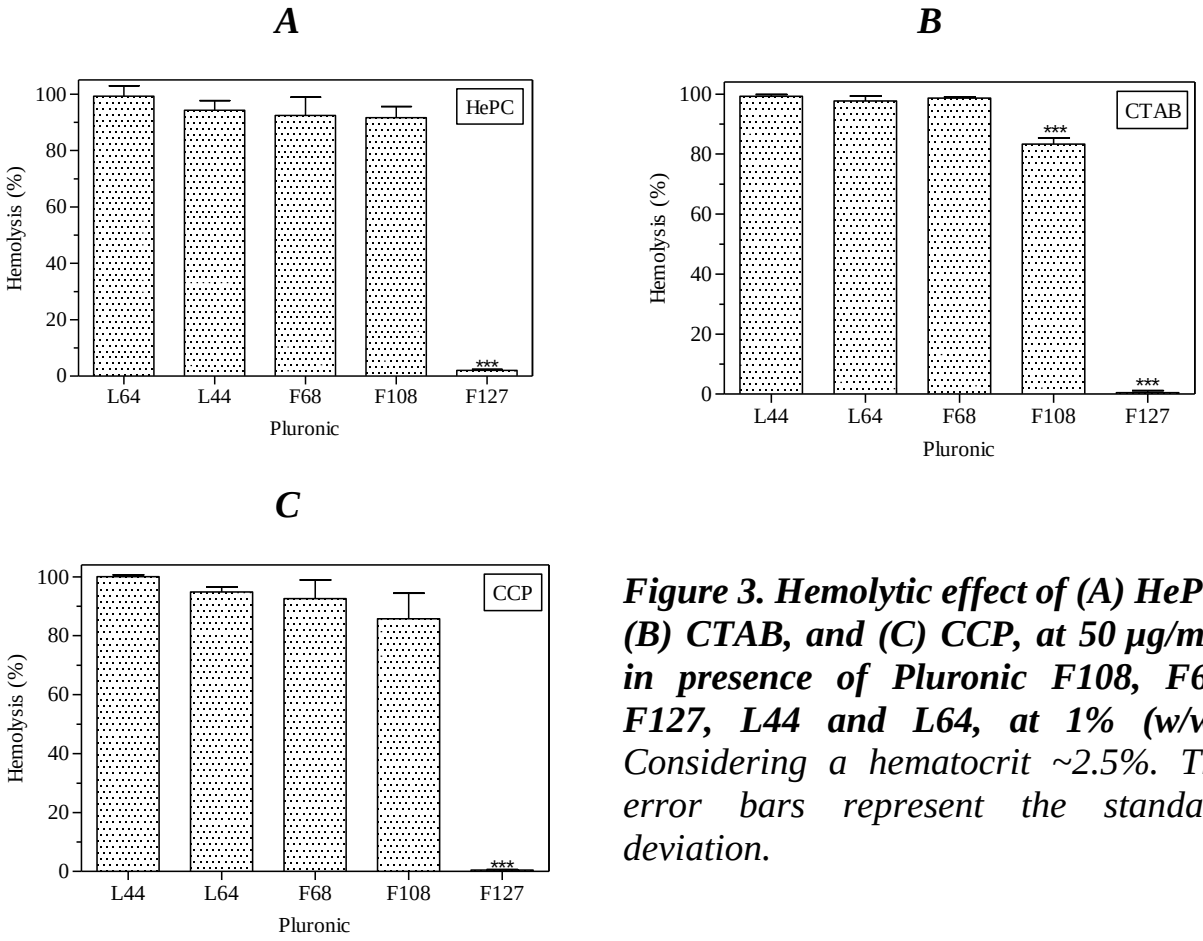

Figure 3. Hemolytic effect of (A) HePC, (B) CTAB, and (C) CCP, at 50 µg/mL, in presence of Pluronic F108, F68, F127, L44 and L64, at 1% (w/w). *Considering a hematocrit ~2.5%. The error bars represent the standard deviation.*

Table 2 and **Figure 4** present some physicochemical and structural properties of the Pluronics studied and, interestingly, Pluronic F127 stands out due to high molecular length of PPO chain and the weight percent of PEO chain. This feature can facilitate both self-aggregation of the copolymer into polymeric micelles as well as drug interaction with hydrophobic PPO core.

Comparatively to F127, Pluronics F108, F68, L44, and L64 have PPO chains of reduced length, therefore to explain the lower or non-protection of hemolysis it is possible to speculate two competitive processes of amphiphiles interaction, or a combination of both: (i) with reduced PPO units they are less favorable for hydrophobic interactions as well as (ii) are more susceptible to

formation of “pearl-necklace” aggregate complexes. This is a well-known phenomenon in which hydrophobic tails of classic surfactants (*e.g.* SDS) interact with PPO segments of triblock copolymers leading to the “solubilization” of polymeric micelles, *i.e.* disruption of micellar organization (Li *et al*., 2011). This interaction pattern between the amphiphilic drug/molecule (HePC, CTAB or CPC) and the pre-formed polymeric micelles of Pluronics F108, F68, L44, and L64, may provide major drug availability in the aqueous phase and in this way promote the total hemolysis observed in **Figure 2**.

Small organic molecules and hence drugs, have been shown to modify the CMC, CMT (*i.e.* critical micellar temperature), aggregate size and shape, phase behavior (*e.g.* gelation boundaries), and stability of Pluronic micelles. Stability of the micelles and, therefore, CMC and aggregation number (N_{agg}), is known to be the result of a repulsive-attractive balance of forces between the hydrophobic chains and the hydrophilic head-groups of the surfactant, acting mainly on the interfacial region of the aggregates (Valero and Dreiss 2010).

Table 2. Physicochemical and structural properties of the Pluronic copolymers studied. *According to Alexandridis and Hatton, 1995; Batrakova et al., 1999 and Kurahashi et al., 2012.*

Pluronic	*Molecular structure*	*MW*	*PEO wt (%)*	*PPO:PEO ratio*	*HLB*	*CMC (mol/L)*
L44	EO_{12}-PO_{20}-EO_{12}	*~2200*	*40*	*0.83*	*16*	3.6×10^{-3}
L64	EO_{13}-PO_{30}-EO_{13}	*~2900*	*40*	*1.15*	*15*	4.8×10^{-4}
F68	EO_{78}-PO_{30}-EO_{78}	*~8400*	*80*	*0.19*	*29*	4.8×10^{-6}
F108	EO_{132}-PO_{50}-EO_{132}	*~14600*	*80*	*0.19*	*27*	2.2×10^{-5}
F127	EO_{106}-PO_{70}-EO_{106}	*~12600*	*70*	*0.33*	*22*	2.8×10^{-6}

EO and PO denote ethylene oxide and propylene oxide, respectively; MW: molecular weight; and HLB: hydrophile–lipophile balance.

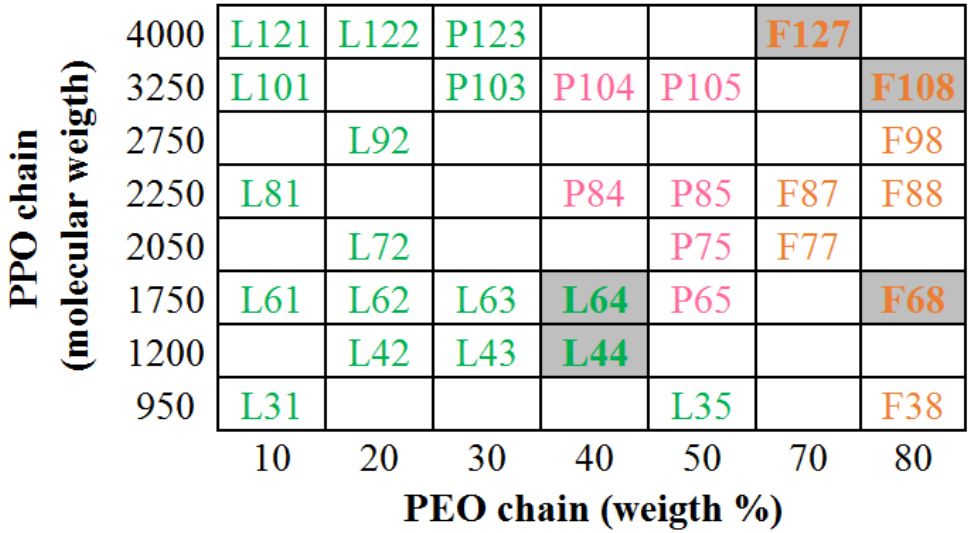

Figure 4. Pluronics arranged in the "copolymer grid". *Copolymers along the vertical lines have the same PPO:PEO ratio, while copolymers along the horizontal lines have PPO blocks of the same length. Color code refers to the physical state of copolymers under ambient conditions: green (liquid), pink (paste), and orange (flake). Pluronics used in this study are highlighted in gray. Adapted from Alexandridis and Hatton, 1995; Pitto-Barry and Barry, 2014.*

3.3. Understanding the intrinsic relationship of HePC-F127 micelles

To better understand the interaction between an amphiphilic drug and F127 copolymer/polymeric micelles, we have extensively studied the hemolytic protection of HePC-F127 mixed micelles in two complementary scenarios. In the first one, the hemolytic activity of HePC was determined as a function of F127 concentration **(Figure 5)**. In the second one we fixed different amount of F127 looking at incorporating the maximum drug without having hemolysis (see next section).

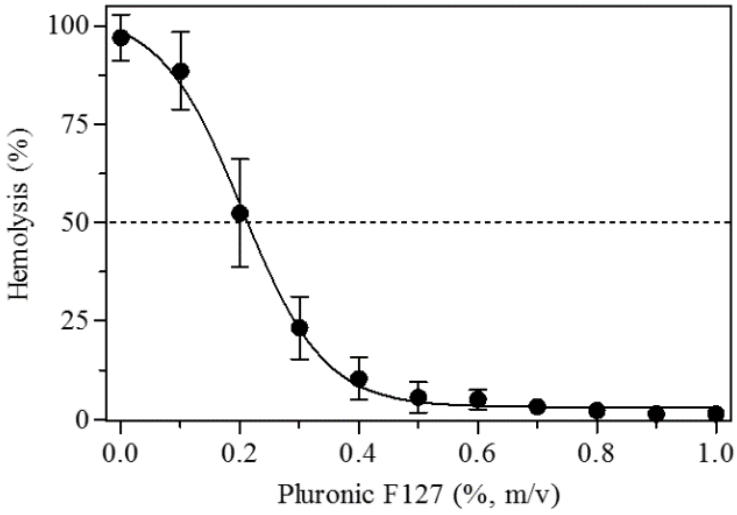

Figure 5. Hemolytic effect as a function of F127 concentration in the presence of HePC 50 µg/mL. *Considering a hematocrit ~2.5%. The error bars represent the standard deviation.*

Initially, we tested different concentrations of Pluronic F127, below and above its CMC (*i.e.* from 0.1 to 1.0%) in the presence of fixed HePC at C^{sol} (*i.e.* 50 µg/mL). The results in **Figure 5** confirm that increasing the concentration of F127 leads to reduction of hemolysis due to incorporation of HePC into polymeric micelles. A mild reduction of hemolysis (~10%) was observed below the CMC of F127 (*i.e.* ~0.15%, Valenzuela-Oses, García, Feitosa *et al.,* 2017, **Appendix A**),

suggesting that HePC may be interacting with Pluronic unimers in solution, more specifically with the more hydrophobic PPO moieties. This effect gradually increases with F127 concentration up to 0.5%, when hemolysis is suppressed. At Pluronic 0.2% we observed 50% of hemolysis and, therefore, can estimate a concentration of HePC free in aqueous phase around 40 µg/mL (*i.e.* HC_{50}). Based on this assumption, the concentration of drug self-aggregated with the polymeric micelles is 10 µg/mL. In the same way, we estimated a total micellar incorporation of HePC at Pluronic 0.5%, expressed by negligible hemolysis.

3.4. Achieving maximum drug-load in HePC-F127 formulations

From the practical point of view, aiming for an *in vivo* application, it is important to achieve higher drug loading inside the polymeric micelles and, therefore, the hemolytic protection of F127 micelles was determined as a function of HePC concentration. Thus, we tested different concentrations of HePC (*i.e.* from 5 to 1500 µg/mL) loaded into polymeric micelles prepared with 1, 3, 6 and 9% copolymer. As can be seen in **Figure 6**, similar sigmoidal profiles were obtained for all F127 concentration. As already mentioned, with accumulative HePC entrapment into polymeric micelles the hemolysis proceeds at a more gradual rate. Also, as expected, by increasing F127 concentration from 1% up to 9% the concentration of HePC in the system without causing hemolysis increases, consequently improving the safety of the drug intravenous administration. According to Amin and Dannenfelser (2006) formulations with *in vitro* hemolysis below 10% are nonhemolytic while hemolysis more 25% should not be used intravenously. So, additionally, data from **Figure 6** were expressed as the concentration of HePC that produce negligible hemolysis, *i.e.* below 5% (represent by dashed lines).

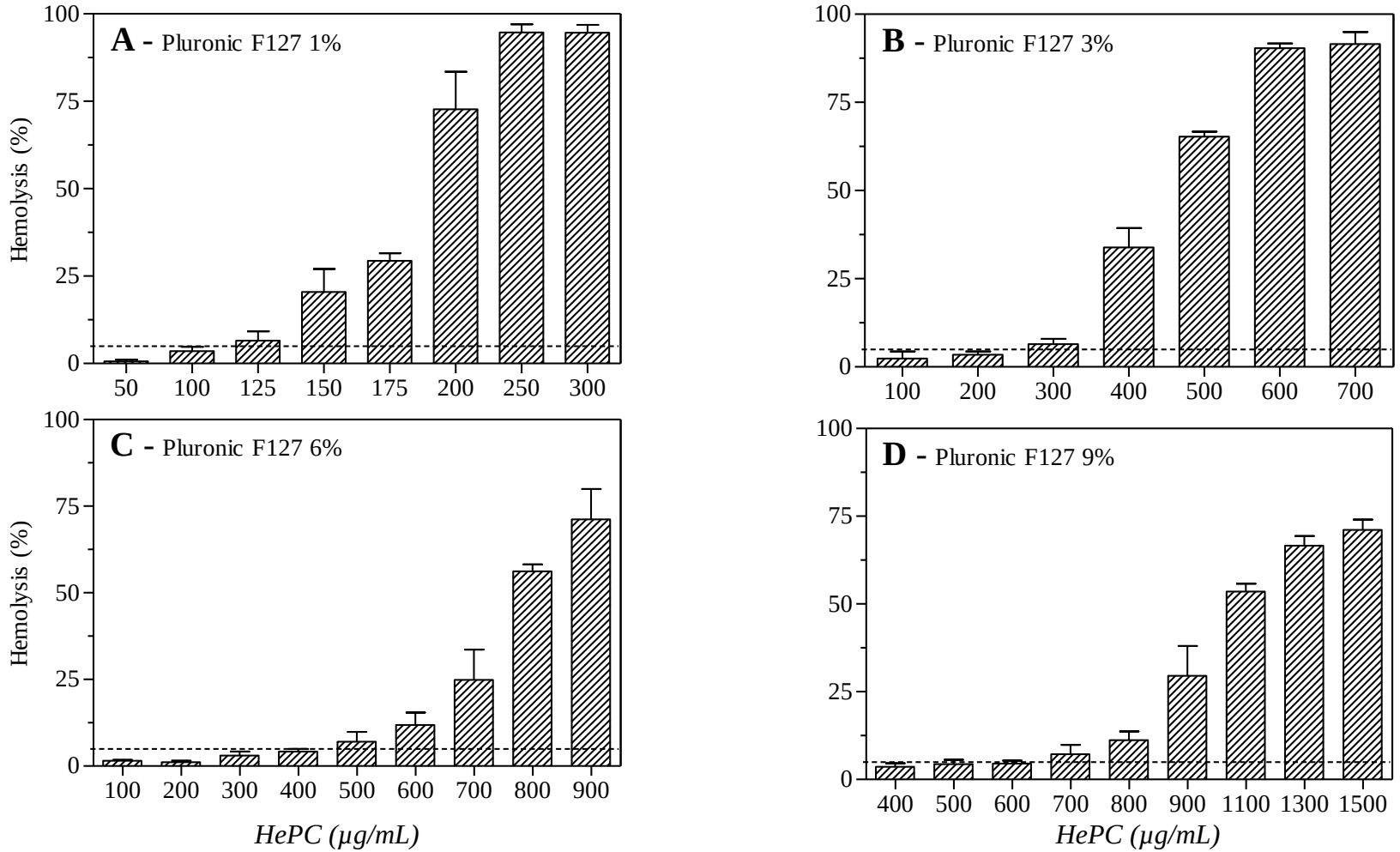

Figure 6. Panel of hemolytic effect as a function of HePC concentrations in the presence of (A) 1%, (B) 3%, (C) 6%, and (D) 9% (w/w) of Pluronic F127*. Considering a hematocrit ~2.5%. Dashed lines indicate 5% of erythrocyte hemolysis. The error bars represent the standard deviation.*

The hemolytic parameters HC_{50} and HC_5 are presented in **Figure 7A** and a proportional relation between F127 concentration and HePC concentration resulting in 50% and 5% of lysis was observed. Thus, increasing F127 on the formulation is a simple way to efficiently enhance HePC administration with minimal hemolytic side-effect. Indeed, in contrast with free drug, which causes 5-10% of hemolysis at 20-25 µg/mL, HePC-F127 mixed formulations increase this value 30-fold, *i.e.* up to 600 µg/mL **(Figure 7-B)**, encouraging us to propose this system as an alternative for parenteral administration of this drug.

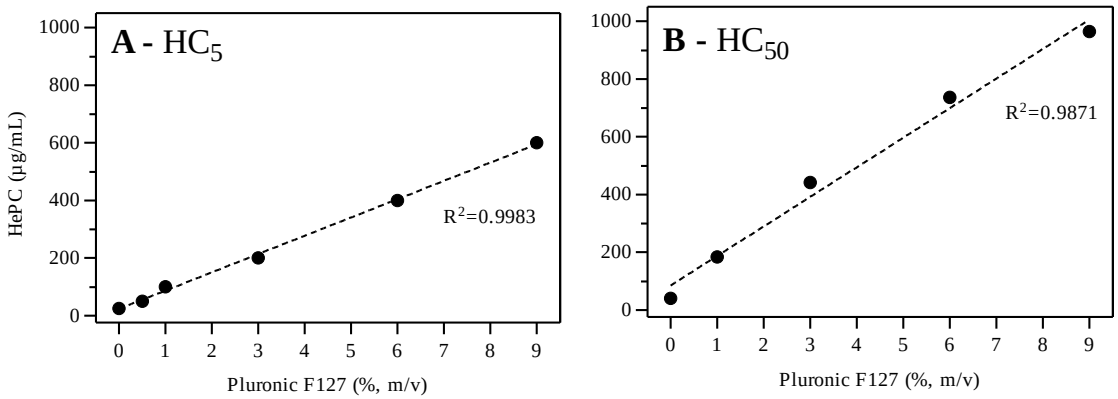

Figure 7. Correlation between HePC concentration and Pluronic F127 concentration required to HC_5 (A) and HC_{50} (B). *Considering a hematocrit ~2.5%. Closed circles and dashed lines denote sample data from* ***Figure 6*** *and linear regression models, respectively.*

3.5. Extrapolating the mass balance of HePC-F127 mixed micelles

If we take the micellar system composed of F127 1% (10000 µg/mL) which corresponds to ~794 µM **(Figure 6A),** it is possible to incorporate up to 100 µg/mL of HePC (306.7 µM), corresponding to a total molar ratio of ~2.6 or ~2.8 if we discount the CMC of F127 and consider drug interacting only with the polymeric micelles (*i.e.* 0.85%, 8500 µg/mL, ~677 µM). Due to the large difference of MW between HePC (407.6 g/mol) and F127 (~12600 g/mol), the drug cargo is 1% (m/m), which means a ratio of 1 µg of HePC to 100 µg of F127. Considering the

Avogadro constant, the N_{agg} for F127polymeric micelles around 80 unimers **(see SAXS results, Table 3)**, and assuming that all Pluronic unimers above CMC are aggregated into micelles and all HePC is binding to F127 micelles (due to the negligible hemolysis up to 5%), and neglecting structural changes in F127 micelles after drug incorporation, we estimate about ~28 HePC molecules per polymeric micelle (N_{drug}).

No published data have been found on the physicochemical interaction of HePC with Pluronic micelles. The partitioning of charged compounds into Pluronic micelles is limited due to electrostatic repulsion by the drugs inside the micelles reducing the packing of the polymeric chains (Valero *et al*., 2016). HePC is zwitterionic **(Figure 1A)** presenting a permanently positive quaternary amine group and negatively charged phosphoryl group, pKa~2 (Dorlo *et al.,* 2012), thus the charged phosphorylcholine group may justify the limited partitioning of this drug to F127 polymeric micelles. Additionally, Valero and Dreiss (2010) proposed that the presence of heteroatoms (*e.g.* nitrogen) and electron pairs in drugs, added to the presence of charge, is likely to contribute to lower drug partitioning inside Pluronic micelles. Nagarajan, Barry, and Ruckenstein (1985) suggested an unusually high partitioning selectivity for aromatic molecules compared to aliphatic ones into diblock PEO-PPO polymeric micelles. In other words, the partitioning of aliphatic molecules into Pluronic micelles is limited. Yet regarding HePC structure **(Figure 1A)**, the long 16 carbons alkyl chain may be a limitation to incorporation into polymeric micelles of F127.

3.6. HePC slightly changes F127 micelle-micelle interaction

In order to check if the incorporation of HePC was effectively changing F127 micelle conformation, we performed SAXS measurements on samples composed by 4.5% and 9% F127 (dispersed in 154 mM NaCl solution) in the absence and presence of increasing HePC concentrations, up to 1400 µg/mL. **Figure 8** shows the scattering profiles of these samples. As one can see, two pronounced peaks are present on the SAXS curves, one at ~0.3 nm^{-1} and the second one around 0.65 nm^{-1}. Generally, peaks at small q position are due to particle-particle interaction potential and not due to form factor of the scattering particle. To check for these effects, we performed one measurement of F127 micelles at 4.5% (namely Diluted in **Figure 8**) in the absence of HePC. As one can clearly see in **Figure 8**, the first peak at q ~0.3 nm^{-1} vanishes, whereas the second one (at ~0.65 nm^{-1}) is less pronounced. This is a strong indication that the first peak was indeed due to particle-particle interaction potential, whereas the second one arises from the particle form factor. Furthermore, in the inset of **Figure 8** one can see a detailed information on the very small q range ($q<0.4\ nm^{1}$). In this region, as stated above, the micelle-micelle interaction potential takes place. Interestingly, as the HePC concentration, increases we observed a decrease in the very small q range (see the arrow in the inset of **Figure 8**); indicating that the presence of HePC is able to slightly changes the particle-particle interaction potential.

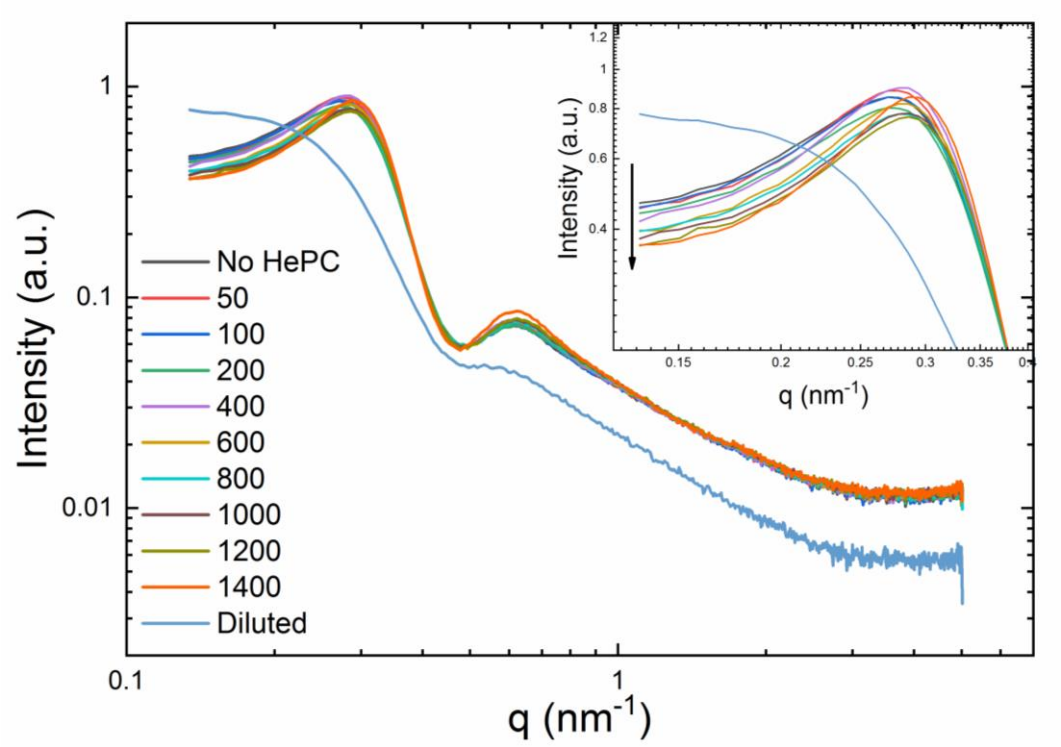

Figure 8. Small Angle X-ray Scattering curves of Pluronic F127 9% in the absence and presence of increasing HePC concentrations (in µg/mL, see figure legend). *In order to check for micelle-micelle interaction potential, a diluted measurement (Pluronic F127 4.5%) in the absence of HePC was also performed (see Diluted curve). In the inset the detailed information on the very small q range (q<0.4 n/m) can be appreciated. The arrow indicates the increasing of the HePC concentration.*

The peak at ~0.65 nm^{-1} could be due to the particle form factor. Indeed, micellar structures, with a core shell electron density profile (an inner core with an electron density smaller than the water and a polar region with a larger electron density as compared to the water) could give rise to a peak at this q range. Several papers in the literature report the presence of well pronounced peaks at middle q-values due to the presence of core-shell micellar structures (Santiago, *et al*., 2007; Rangel-Yagui, *et al*., 2007; Barbosa, *et al*., 2008; D'Andrea, *et al*., 2011), or even that polymeric micelles can indeed have a core-shell structure (Pedersen, 1997; Oda, *et al*., 2017).

Ivanova, Lindman and Alexandridis (2000) performed a detailed study on the phase behavior of the ternary systems: F127/water/propylene carbonate and F127/water/triacetin phase diagrams, using SAXS. According to the authors, considering the binary system F127/water, up to 17% the system is composed by isotropic micelles in a water-rich phase. Nevertheless, for polymeric concentrations >18% up to ~64% the system behaves like a crystalline cubic structure composed by micelles. A normal micellar cubic phase was thus identified, along the F127-water axis. The normal micellar cubic phase consists of discrete micelles crystallized in a cubic lattice. It should be stressed that the authors have not examined the F127 micellization process. However, the occurrence of a micellar cubic liquid crystalline phase at >18%, strongly indicates micelle formation at polymeric concentrations <18%. Moreover, several reports on the literature present evidences on the micelle formation by block copolymers, in particular F127 (Alexandridis, Holzwarth, 1997; Exerowa, *et al*., 1997; Alexandridis, Spontak, 1999).

In order to get more information on F127 micelles, we used the generalized indirect Fourier transformation (GIFT) methodology by means of GIFT software to get information on the pair distance distribution function, p(r), as well as in the micelle-micelle interaction potential, S(q). **Figure 9 A and B** shows the form and structure factors, respectively, for the system composed by F127 9% in the absence (black solid lines) and in the presence of 1400 µg/mL HePC (red solid lines) as well as the system composed by 4.5% of F127 in the absence of HePC (blue line). As one can see, regarding the micelles form factor, no crucial changes were observed due to the presence of HePC for the systems at 9% F127 concentrations (**Figure 9A**). However, a significant change may be observed as

the polymeric concentrations decreases 2-fold (see **Figure 9-A**), in particular in the region of the peak at ~0.65 nm^{-1}. This change as propose above is due to changes in the micellar form factor, as it will be discussed latter in the text. Regarding the micelle-micelle interaction potential, i.e., the S(q) functions, one can notice a slightly shift to larger q-values of the first peak position **(see Figure 9B and the inset)** due to the presence of HePC in the F127 9% systems. Such a small shift could be an indication of a small influence of HePC on the S(q) functions, inducing a small approximation of the micelles (due to the shift to larger q-values).

Our results show that the proposed model used to describe F127 micellar system at all studied conditions was able to describe these systems, as we can see on **Figure 9C**, where the final fitted curves can be found. Several approaches are used to analyze SAXS data. Most of them are based on the so-called geometric models, in which the particle geometry is defined a priori and could be spherical, elliptical, cylindrical, and so on. Here, we used a different approach with a model-free methodology by means of GIFT software, in which both form and structure factors are evaluated concomitantly, being the first one throws the p(r) and the last one using the Perkus-Yevich approximation. Interestingly, the p(r) analyses revealed that the micellar form factor changes significantly as the polymeric concentration decreases. Accordingly, F127 micelle swelled as its concentration decreases. Such effect could be due to a shrinking in the excluded volume effect.

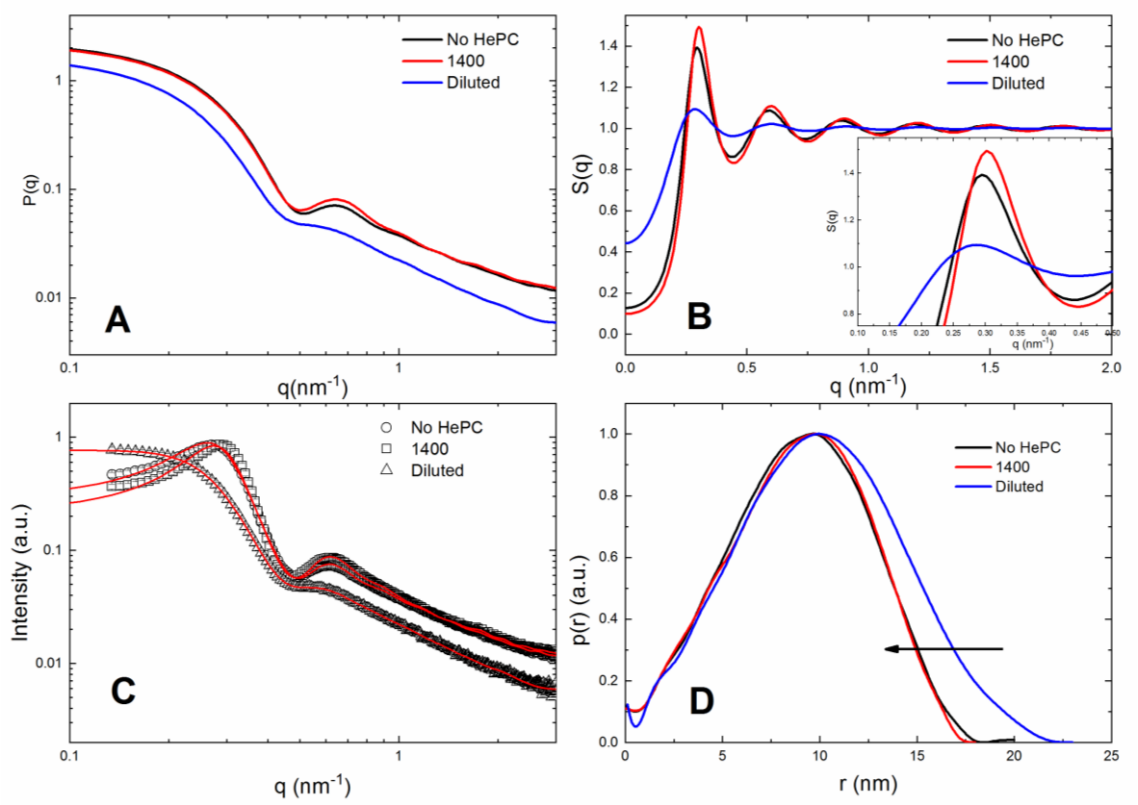

Figure 9. SAXS data analysis of the systems composed by Pluronic F127 9% in the absence (black solid line) and in the presence of 1400 µg/mL HePC (red solid line) as well as the diluted system at 4.5% (blue line). (A) *form factor functions, P(q),* ***(B)*** *interference micelle-micelle functions, S(q), in the inset the first peak of the S(q) functions can be appreciated.* ***(C)*** *Final fitting functions (solid red curves), along with the experimental SAXS data for Pluronic F127 at 9% in the absence (open circles) and in the presence of 1400 µg/mL HePC (open squares), as well as the diluted system at 4.5% of Pluronic F127 (open triangles).* ***(D)*** *Respective pair distance distribution functions, p(r).*

Analyzing the SAXS curves in the **Figure 9A** we propose that at 4.5% F127 micelles have a larger average distance among each other. At such conditions, the PEO molecules (hydrophilic at the outer shell of the micelle) can adopt a more extended conformation as compared to 9%, in which the average distance among the micelles is considerably smaller, inducing a decrease in the shell (hydrophobic) region. This fact is further supported by the presence of a well pronounced peak at the P(q) functions at q~0.65 nm^{-1} **(see the black line**

Figure 9A) for the system composed of 9% F127, as compared to the system of 4.5% F127 **(blue line in Figure 9A).**

Yet, based on hemolysis experiments and extrapolating the SAXS analysis, we propose a schematic representation of polymeric micelles, varying the F127 concentration in the presence of HePC, as shows in **Figure 10**. At lower F127 concentration **(Figure 10A)** we have the PEO corona more extended, this may favor the entrapment of HePC in the PPO core as well in the PEO chains themselves, impairing the HePC partition to erythrocyte membrane. Also, at high F127 concentration (**Figure 10B),** the corona compaction, resulting from the contraction of PEG chains, can drive to an inverse effect, that is, reduce the amount of HePC interacting with polymeric micelles evidenced by increased hemolysis at higher HePC concentrations.

Yet, based on hemolysis experiments **(Figure 6)** and extrapolating the SAXS analysis **(Figure 9)**, we propose a schematic representation of polymeric micelles, varying the F127 concentration in the presence of HePC, as shows in **Figure 10**. At lower F127 concentration "↓[F127]" the PEO corona appears to be extended, this may favor the entrapment of HePC in the PPO core, as well in the PEO chains themselves, impairing the HePC partition to erythrocyte membrane. Also, at high F127 concentration "↑[F127]", the corona compaction, resulting from the contraction of PEO chains, can drive to an inverse effect, that is, reduce the amount of HePC interacting with polymeric micelles evidenced by increased hemolysis at higher HePC concentrations.

The SAXS parameters obtained with the fitting of the scattering curves are presented in **Table 3.** Regarding the size of the F127 micelles, it was interesting that the radius of gyration decreases as the polymer concentration increases from

7.7 to 6.8 nm for the systems composed by 4.5 and 9%, respectively. Interestingly, despite the changes on the R_g values, our SAXS data suggested that the effective diameter (σ) of the micelles, which were obtained using the interference function, are quite similar for all studied systems. Valero *et al*., (2016) studied the ability of F127 in load different drugs, like lidocaine, pentobarbital sodium salt, sodium naproxen, and sodium at salicylate 4% and at 37 ^{o}C by means of small angle neutron scattering (SANS). In their study, the authors used a geometric model (spherical core-shell micelles) to analyze the scattering data. According to the authors, for 5% F127 micelles a core radius of 45 Å, whereas the shell thickness of 64 Å was observed. These values indicate an effective diameter of ~21.8 nm, in good agreement with the data obtained in the present study.

Table 3. SAXS parameters obtained with the fitting of the scattering curves displayed in Figure 9.

SAXS parameter	***F127 4.5%***	***F127 9%***	
		without HePC	***HePC (1400 µg/mL)***
R_g ***(nm)***^{a}	*7.7 ± 0.1*	*6.8 ± 0.1*	*6.8 ± 0.1*
σ ***(nm)***^{a}	*20.6 ± 0.2*	*21.2 ± 0.2*	*20.8 ± 0.2*
ϕ^{a}	*0.11 ± 0.01*	*0.26 ± 0.02*	*0.27 ± 0.02*
n_p ***(part/nm***^{3}***)x10***$^{-5}$	*2.40 ± 0.22*	*5.21 ± 0.41*	*5.73 ± 0.44*
C_{mic} ***(mol/L)x10***$^{-5}$	*3.99*	*8.65*	*9.51*
$N_{agg}{}^{b}$	*89.5 ± 8.3*	*82.5 ± 6.5*	*75.1 ± 5.7*

R_g: particle radius of gyration; σ: Hard Sphere diameter; ϕ: volume fraction of micelles; n_p: micellar numerical density concentration; C_{mic}: micellar concentration, N_{agg}: aggregation number of each micelle; (a): these parameters we obtained in the fitting process and (b) was calculated using ***Eq. 7****.*

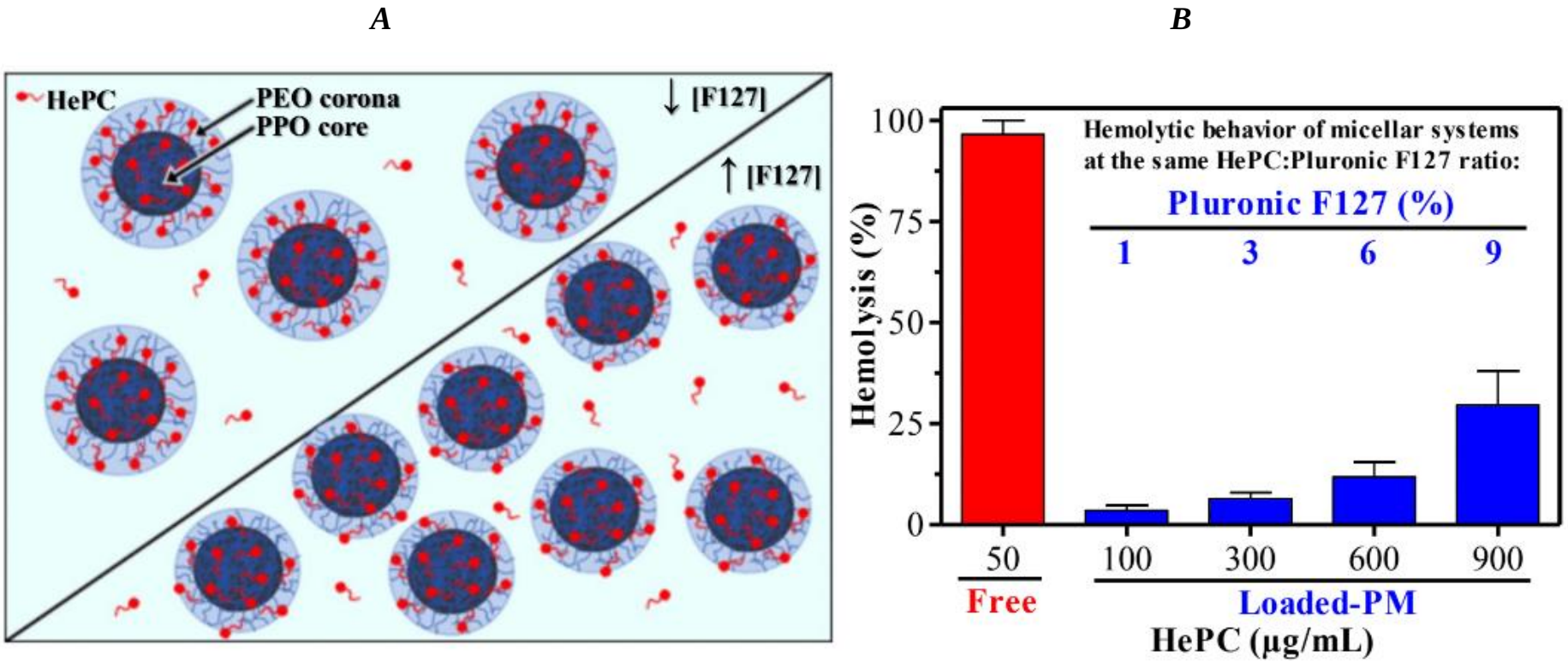

Figure 10. Schematic representation of HePC-loaded polymeric micelles at lower and higher Pluronic F127 concentration (A), according to the SAXS data analysis and hemolysis bioassays (B).

1

Mortensen and Talmon (1995) performed an interesting study regarding the structural features of F127 micelles, at different temperatures and concentrations, by means of SANS and cryogenic transmission electron microscopy (cryo-TEM). In particular, they used systems composed by 5, 12 and 20% of F127 at different temperatures. The authors also reported the values of Φ as a function of temperature, for these three concentrations. According to the data, there is almost a linear increasing for the volume fraction, Φ, as the concentration increases. According to the data, it is possible to infer that Φ at 37 ºC for 4.5 and 9% are 0.10 and 0.27, respectively. Both values are in really good agreement with the data reported herein.

Regarding the aggregation number, N_{agg}, there are several different values reported in the literature. Actually, one can find N_{agg} values in the 10-100 range (Kazunori, *et al*., 1993; Yokoyama, *et al*., 1998; Yu, *et al*., 1998; Torchilin, 2001; Kadam, Yerramilli and Bahadur, 2009). For instance, Valero *et al*., (2016) reported values in the 30-40 range for the aggregation number of F127, solubilized in water, in the absence of any loaded drug. Desai *et al*., (2001), on the other hand, determined the aggregation number of F127 micelles as 72. In a different study, Sharma *et al*. (2008) reported an aggregation number of 73 in water, in good agreement with Desai *et al*. (2001). These reported values are in good agreement with the data reported herein. Nevertheless, one should bear in mind that there is no consensus about the F127 aggregation number.

3.7. Hemocompatibility of Pluronic F127 micelles

When nanostructures are injected into the blood for drug delivery, negligible interaction of these particles with blood constituents is desired.

Therefore, the hemolysis assay would give additional information about the biocompatibility in the case of an *in vivo* application. For the mixed HePC-F127 micelles at 6 and 9% of F127, macroscopic changes in RBCs sediment were observed after centrifugation. Under these conditions, the cells adhered to the wall of the tubes, apparently forming aggregates. At F127 concentrations up to 3%, no significant macroscopic changes in RBCs sediment were observed. Therefore, we evaluated the influence of pure Pluronic F127 on RBCs. For this, we used the protocol proposed by Reed and Yalkowsky (1985), this method seems more realistic for intravenous injection since it follows the ratio between the injected substance and RBCs, as well as considers that the injected substance is rapidly diluted in the bloodstream. According to **Figure 11**, F127 in concentrations of up to 4.5% shows low hemolytic potential, whereas higher concentrations resulted in increased hemolysis. Surprisingly, concentrations of F127 higher than 10% apparently reduced the hemolysis. We believe that, at higher copolymer concentrations, aggregation of erythrocytes may occur due to the systems high viscosity.

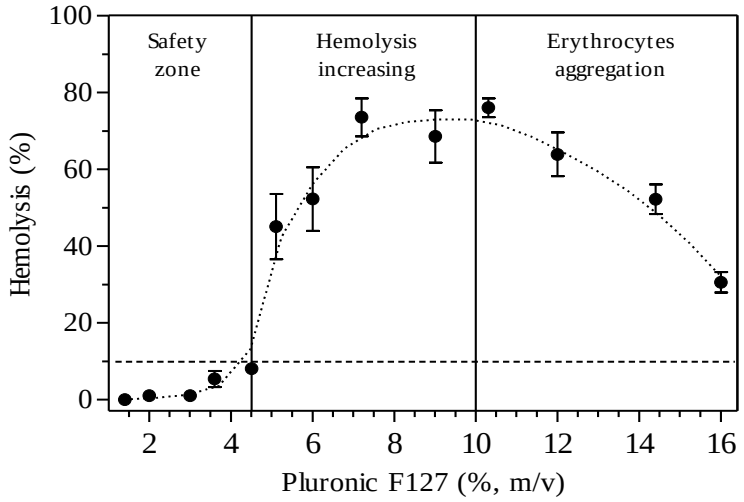

Figure 11. Hemolytic effect as a function of Pluronic F127 concentration, using the hemolysis bioassay (method B). *The error bars represent the standard deviation.*

These data suggest that the best concentration of Pluronic F127 for intravenous bolus administration of polymeric micelles is up to 4.5%. In addition, by interpolating the linear regression model of **Figure 7A**, incorporation of up to 300 µg/mL HePC in 4.5% F127 polymeric micelles can be considered safe in terms of hemolytic effect. Since HePC hemolytic activity is dependent on RBC concentration (Alonso and Alonso, 2016) and assuming a 40% hematocrit, it is possible to inject up to 4 mg/mL of HePC formulated in 4.5% F127 polymeric micelles. If we consider that plasmatic proteins provide extra protection to HePC action into erythrocytes, the amount of drug to be incorporated for bolus administration in whole blood could be even higher.

4. Conclusion

The interactions among amphiphilic drugs and with erythrocyte membranes and copolymers/polymeric micelles are quite complex. Consequently, the ability to modulate the equilibrium between the different aggregates is of primary concern for the rational development of amphiphilic drug formulation, such as HePC. Our study clearly demonstrates that the composition of Pluronic copolymers, expressed by differences on the weight percent of PEO and PPO moieties, influences the aggregation state of HePC and, therefore, *in vitro* erythrocytes lysis. In particular, Pluronic F127 copolymer concentration has a pronounced effect on the HePC hemolytic profile. Through manipulation of the polymer:drug ratio, it might be possible to design drug-delivery systems with properties tailored to the parenteral application. Specifically, it might be feasible to fine-tune the amount of HePC-loaded in polymeric micelles by adjusting the concentration of F127 copolymer, which can safely be administered at concentrations up to 4.5%. SAXS data indicates that the presence of HePC has a small effect on the F127 micelle at 9%, nevertheless, the polymeric concentration probably plays a major role on the micelle structure.

Acknowledgements

This study was financed by the *Coordination of Superior Level Staff Improvement* (CAPES/Brazil) - Finance Code 001, and by the *State of São Paulo Research Foundation* (FAPESP/Brazil, processes 2014/01983-0, 2015/15822-1, and 2018/17576-6) and *National Council for Scientific and Technological Development* (CNPq/Brazil). The authors wish to thank *Basf Company* (Brazil) for kindly supplying all Pluronic copolymers. The authors are also in debt with *Brazilian Synchrotron Light Source* (LNLS/Brazil), and its staff in the SAXS measurements. VAF also acknowledges to *IPT Foundation* for the "*Novos Talentos*" fellowship.

References

Alakhova, D.Y. et al. Effect of Doxorubicin/Pluronic SP1049C on Tumorigenicity, Aggressiveness, DNA Methylation and Stem Cell Markers in Murine Leukemia. Plos One, v. 8, n. 8, Aug 2013.

Alexandridis, P., Holzwarth, J.F. Differential Scanning Calorimetry Investigation of the Effect of Salts on Aqueous Solution Properties of an Amphiphilic Block Copolymer (Poloxamer) Langmuir 1997, 13, 6074- 6082

Alexandridis, P.; Hatton, T.A. Poly(ethylene oxide)-poly(propylene oxide)-poly(ethylene oxide) block copolymer surfactants in aqueous solutions and at interfaces: thermodynamics, structure, dynamics, and modeling. Colloids and Surfaces a-Physicochemical and Engineering Aspects, v. 96, n. 1-2, p. 1-46, Mar 1995.

Alexandridis, P.; Spontak, R. J. Solvent-regulated ordering in block copolymers. Curr. Opin. Colloid Interface Sci., 4, 130-139, 1999.

Alonso, L.; Alonso, A. Hemolytic potential of miltefosine is dependent on cell concentration: Implications for in vitro cell cytotoxicity assays and pharmacokinetic data. Biochimica Et Biophysica Acta-Biomembranes, v. 1858, n. 6, p. 1160-1164, Jun 2016.

Amin K., Dannenfelser, R.M. In vitro hemolysis: guidance for the pharmaceutical scientist. J Pharm Sci. Jun;95(6):1173-6, 2006.

Amin, K. and Dannenfelser, R.M. In vitro hemolysis: guidance for the pharmaceutical scientist. J Pharm Sci., Jun;95(6):1173-6, 2006.

Armstrong, A. et al. SP1049C as first-line therapy in advanced (inoperable or metastatic) adenocarcinoma of the oesophagus: A phase II window study. Journal of Clinical Oncology, v. 24, n. 18, p. 198S-198S, Jun 2006.

Barbosa, L.R.S. et al. Self-Assembling of Phenothiazine Compounds Investigated by Small-Angle X-ray Scattering and Electron Paramagnetic Resonance Spectroscopy. The Journal of Physical Chemistry B, 112 (14), 4261-4269, 2008.

Barbosa, L.R.S., et al. Interaction of Phenothiazine Compounds with Zwitterionic Lysophosphatidylcholine Micelles: Small Angle X-ray Scattering, Electronic Absorption Spectroscopy, and Theoretical Calculations. J. Phys. Chem. B, 110 (26), pp 13086–13093, 2006.

Barioni, M.B. Miltefosine and BODIPY-labeled alkylphosphocholine with leishmanicidal activity: Aggregation properties and interaction with model membranes. Biophysical Chemistry 196, 92–99, 2015.

Batrakova, E. et al. Fundamental Relationships Between the Composition of Pluronic Block Copolymers and Their Hypersensitization Effect in MDR Cancer Cells. Pharm Res, 16: 1373, 1999.

Bergmann, A., Fritz, G. and Glatter, O. Solving the generalized indirect Fourier transformation (GIFT) by Boltzmann simplex simulated annealing (BSSA). Appl. Cryst., 33, 1212-1216, 2000.

D'Andrea, M.G. et al., Thermodynamic and Structural Characterization of Zwitterionic Micelles of the Membrane Protein Solubilizing Amidosulfobetaine Surfactants ASB-14 and ASB-16. Langmuir, 27 (13), pp 8248–8256, 2011.

De Sa, M. M. et al. Alkylphosphocholines as Promising Antitumor Agents: Exploring the Role of Structural Features on the Hemolytic Potential. Molecular Informatics, v. 33, n. 1, p. 53-64, Jan 2014.

Desai, P.R. et al. Effect of additives on the micellization of PEO/PPO/PEO block copolymer F127 in aqueous solution. Colloids and Surfaces A, 178, 57–69, 2001.

Domingues, C.C.; Malheiros, S.V.P.; D Paula, E. Solubilization of human erythrocyte membranes by ASB detergents. Brazilian Journal of Medical and Biological Research, v. 41, n. 9, p. 758-764, Sep 2008.

Dorlo, T.P. et al., Miltefosine: a review of its pharmacology and therapeutic efficacy in the treatment of leishmaniasis. J Antimicrob Chemother., Nov;67(11):2576-97, 2012.

Eley BM. Antibacterial agents in the control of supragingival plaque - a review. British Dental Journal, 186(6):286-96, 1999.

Exerowa, D.; Sedev, R.; Ivanova, R.; Kolarov, T.; Thadros, Th. F. Transition from electrostatic to steric stabilization in foam films from ABA triblock copolymers of poly(ethylene oxide) and poly(propylene oxide).Colloids Surf. A, 123-124, 277-282, 1997.

Guo, S.; Huang, L. Nanoparticles containing insoluble drug for cancer therapy. Biotechnology Advances, v. 32, n. 4, p. 778-788, Jul-Aug 2014.

Heike M.A. et al. Generalized Indirect Fourier Transformation as a Valuable Tool for the Structural Characterization of Aqueous Nanocrystalline Cellulose Suspensions by Small Angle X-ray Scattering. Langmuir, 29 (11), 3740-3748, 2013.

Ito E, Yip, KW, Katz D, Fonseca SB, et al. Potential use of cetrimonium bromide as an apoptosis-promoting anticancer agent for head and neck cancer. Mol Pharmacol., Nov;76(5):969-83, 2009.

Ivanova, R., Lindman, B., Alexandridis, P. Evolution in Structural Polymorphism of Pluronic F127 Poly(ethylene oxide)−Poly(propylene oxide) Block Copolymer in Ternary Systems with Water and Pharmaceutically Acceptable Organic Solvents: From “Glycols” to “Oils”. Langmuir, 16 (23), pp 9058–9069, 2000.

Kadam, Y., Yerramilli, U. and Bahadur, A. Solubilization of poorly water-soluble drug carbamezapine in Pluronic® micelles: Effect of molecular characteristics, temperature and added salt on the solubilizing capacity. Colloids and Surfaces B: Biointerfaces, 72(1), pp.141-147, 2009.

Kazunori, K., Masayuki, Y., Teruo, O. and Yasuhisa, S. Block copolymer micelles as vehicles for drug delivery. Journal of Controlled Release, 24(1-3), pp.119-132, 1993.

Kurahashi, M. et al. Role of block copolymer surfactant on the pore formation in methylsilsesquioxane aerogel systems. Rsc Advances, v. 2, n. 18, p. 7166-7173, 2012. ISSN 2046-2069.

Lee, S.L. and Ding, J. L. A Perspective on the Role of Extracellular Hemoglobin on the Innate Immune System. DNA and cell biology, v. 32, n. 2, 2013.

Li, et al., Aggregation behavior and complex structure between triblock copolymer and anionic surfactants. Journal of Molecular Structure 985, 391–396, 2011.

Madaan P., Tyagi V.K. Quaternary pyridinium salts: a review. J Oleo Sci., 57(4):197-215, 2008.

Malheiros, , S.V.P.; Meirelles, N.C.; De Paula, E. Pathways involved in trifluoperazine-, dibucaine- and praziquantel-induced hemolysis. Biophysical Chemistry, v. 83, n. 2, p. 89-100, Jan 2000.

Moreira, R. A. et al. Interaction of miltefosine with the lipid and protein components of the erythrocyte membrane. Journal of Pharmaceutical Sciences, v. 102, n. 5, p. 1661-1669, May 2013.

Mortensen, K., Talmon, Y. Cryo-TEM and SANS Microstructural Study of Pluronic Polymer Solutions. Macromolecules, 28, 26, 8829-8834, 1995.

Movassaghian, S.; Merkel, O.M.; Torchilin, V.P. Applications of polymer micelles for imaging and drug delivery. Wiley Interdisciplinary Reviews-Nanomedicine and Nanobiotechnology, v. 7, n. 5, p. 691-707, Sep-Oct 2015.

Munoz, C. et al. Effect of miltefosine on erythrocytes. Toxicology in Vitro, v. 27, n. 6, p. 1913-1919, Sep 2013.

Nagarajan, R., Barry, M. and Ruckenstein, E. Unusual selectivity in solubilization by block copolymer micelles. Langmuir, 2 (2), pp 210–215, 1986.

Oda, C.M.R., et al. Synthesis, characterization and radiolabeling of polymeric nano-micelles as a platform for tumor delivering. Send to Biomed Pharmacother., May;89:268-275, 2017.

Oerlemans, C. et al. Polymeric Micelles in Anticancer Therapy: Targeting, Imaging and Triggered Release. Pharmaceutical Research, v. 27, n. 12, p. 2569-2589, Dec 2010.

Pachioni, J.D. et al. Alkylphospholipids - A Promising Class of Chemotherapeutic Agents with a Broad Pharmacological Spectrum. Journal of Pharmacy and Pharmaceutical Sciences, v. 16, n. 5, p. 742-759, 2013.

Pan, Y., Wang, Z., Shao, D. CTAB induced mitochondrial apoptosis by activating the AMPK–p53 pathway in hepatocarcinoma cells. Toxicol. Res.,4, 1359-1365, 2015.

Pedersen, J.S. Analysis of small-angle scattering data from colloids and polymer solutions: modeling and least-squares fitting. Adv. CoUoid Interface Sci. 70, 171-210, 1997.

Percus, J.K and Yevick, G.J. Analysis of Classical Statistical Mechanics by Means of Collective Coordinates. Phys. Rev. 110, 1, 1958.

Pitto-Barry, A.; Barry, N.P.E. Pluronic(r) block-copolymers in medicine: from chemical and biological versatility to rationalisation and clinical advances. Polymer Chemistry, v. 5, n. 10, p. 3291-3297, 2014.

Prete, P.S.C. et al. Quantitative assessment of human erythrocyte membrane solubilization by Triton X-100. Biophysical Chemistry, v. 97, n. 1, p. 1-5, May 2002.

Rangel-Yagui, C.O. et al. Novel potential drug against T-cruzi and its interaction with surfactant micelles. Pharmaceutical Development and Technology, v. 12, n. 2, p. 183-192, 2007.

Rangel-Yagui, C.O.; Pessoa, A.; Tavares, L.C. Micellar solubilization of drugs. Journal of Pharmacy and Pharmaceutical Sciences, v. 8, n. 2, p. 147-163, May-Aug 2005.

Reed, K.W., Yalkowsky, S.H. Lysis of human red blood cells in the presence of various cosolvents. J Parenter Sci Technol., Mar-Apr;39(2):64-9, 1985.

Rother, R.P. The Clinical Sequelae of Intravascular Hemolysis and Extracellular Plasma Hemoglobin. JAMA, April 6, v. 293, n. 13, 2005.

Santiago, P. S.; Neto, D. S.; Barbosa, L. R. S.; Itri, R.; Tabak, M. J. Coll. Interface Sci., 316, 730−740, 2007.

Schreier, S.; Malheiros, S.V.P.; De Paula, E. Surface active drugs: self-association and interaction with membranes and surfactants. Physicochemical and biological aspects. Biochimica Et Biophysica Acta-Biomembranes, v. 1508, n. 1-2, p. 210-234, Nov 2000.

Shah, K.G., et al. A retrospective analysis of the incidence of hemolysis in type and screen specimens from trauma patients. int J Angiol.,18(4):182-183, 2009.

Sharma, P.K. et al. The effect of pharmaceuticals on the nanoscale structure of PEO–PPO–PEO micelles. Colloids and Surfaces B, 53–60, 2008.

Sreenivasan P., Gaffar A. Antiplaque biocides and bacterial resistance: a review. J. Clin. Periodontol., ;29:965–974, 2002.

Talelli, M., Hennink, W.E. Thermosensitive polymeric micelles for targeted drug delivery. Nanomedicine, v. 6, n. 7, p. 1245-1255, Sep 2011.

Torchilin, V.P. Structure and design of polymeric surfactant-based drug delivery systems. Journal of controlled release, 73(2-3), pp.137-172, 2001.

Valenzuela-Oses, J., García, M., Feitosa, V.A., et al. Development and characterization of miltefosine-loaded polymeric micelles for cancer treatment. Mater Sci Eng C Mater Biol Appl. 2017.

Valero M, and Dreiss C.A. Growth, shrinking, and breaking of pluronic micelles in the presence of drugs and/or beta-cyclodextrin, a study by small-angle neutron scattering and fluorescence spectroscopy. Langmuir, Jul 6;26(13):10561-71, 2010.

Valero, et al. Competitive and Synergistic Interactions between Polymer Micelles, Drugs, and Cyclodextrins: The Importance of Drug Solubilization Locus. Langmuir, 32 (49), 2016.

Valle, J.W., et al. A phase 2 study of SP1049C, doxorubicin in P-glycoprotein-targeting pluronics, in patients with advanced adenocarcinoma of the esophagus and gastroesophageal junction. Investigational New Drugs, v. 29, n. 5, p. 1029-1037, Oct 2011.

Valle, J.W., et al. A phase II, window study of SP1049C as first-line therapy in inoperable metastatic adenocarcinoma of the oesophagus. Journal of Clinical Oncology, v. 22, n. 14, p. 362S-362S, Jul 2004.

Van Blitterswijk, W.J.; Verheij, M. Anticancer alkylphospholipids: Mechanisms of action, cellular sensitivity and resistance, and clinical prospects. Current Pharmaceutical Design, v. 14, n. 21, p. 2061-2074, Jul 2008.

Vrij, A. Mixtures of hard spheres in the Percus–Yevick approximation. Light scattering at finite angles J. Chem. Phys. 71, 3267, 1979.

Wei, Z. et al. Mechanism of inhibition of P-glycoprotein mediated efflux by Pluronic P123/F127 block copolymers: Relationship between copolymer concentration and inhibitory activity. European Journal of Pharmaceutics and Biopharmaceutics, v. 83, n. 2, p. 266-274, Feb 2013.

Wissing MD, Mendonca J, Kim E, et al. Identification of cetrimonium bromide and irinotecan as compounds with synthetic lethality against NDRG1 deficient prostate cancer cells. Cancer Biol Ther., ;14(5):401-10, 2013.

Yokoyama, M., Satoh, A., Sakurai, Y., Okano, T., Matsumura, Y., Kakizoe, T. and Kataoka, K. Incorporation of water-insoluble anticancer drug into polymeric micelles and control of their particle size. Journal of controlled release, 55(2-3), pp.219-229, 1998.

Yu, B.G., Okano, T., Kataoka, K. and Kwon, G. Polymeric micelles for drug delivery: solubilization and haemolytic activity of amphotericin B. Journal of controlled release, 53(1-3), pp.131-136. 1998.

Chapter II

This second chapter presents the pre-clinical safety, biocompatibility, and efficacy results of miltefosine incorporated into Pluronic F127-based polymeric micelles.

Safety and selective cytotoxicity of miltefosine-loaded polymeric micelles

Valker Araujo Feitosa[1,2], Camila Areias de Oliveira[1,2], Patrícia Leo[2], Natália Neto Pereira Cerize[2], Carlota de Oliveira Rangel-Yagui[1]

[1]Department of Biochemical and Pharmaceutical Technology, School of Pharmaceutical Sciences, University of São Paulo, [2]Institute for Technological Research (IPT), Brazil

Abstract

Miltefosine (hexadecylphosphocholine, HePC) is a synthetic antitumor alkylphosphocholine used clinically for the treatment of cutaneous metastases of breast cancer. This drug acts at cell membrane level, where it accumulates and interfere with lipid metabolism and lipid-dependent signaling pathways leading the cells to apoptosis. As a surface-active substance, high concentrations of HePC may cause cell lysis, limiting its intravenous administration and resulting in pronounced gastrointestinal toxicity when orally administered. To overcome these limitations, HePC was previously incorporated into polymeric micelles (PM) of Pluronic F127, a biocompatible triblock-copolymer approved by FDA. Here, using a chicken chorioallantoic membrane (CAM) model, we showed that HePC incorporation into PM prevented mucosal irritation, decreasing bleeding and lysis of blood vessels. This test confirmed the non-irritancy of HePC-PM demonstrating the ability of drug entrapment into PM and mucosal protection over free drug. The cytotoxic effect based on IC_{50} and selectivity index of free HePC and HePC-PM on HeLa cancer and L929 normal cell lines were studied, using the neutral red uptake test. We observed a dose-dependent reduction in viability of HeLa cell line when treated with HePC and a selective effect, since the drug was safe to normal L929 fibroblasts. Interestingly, HePC-PM increased the cytotoxicity against Hela cells, suggesting a differential uptake of these nanostructures by those cells. These data together demonstrate that HePC encapsulation into PM reduces side effects and increases selective cytotoxicity against tumor cells. Furthermore, empty-PM did not present any cytotoxicity and, therefore, this colloidal system could be further used for the administration of this important antitumor drug, as well as of other amphiphilic drugs.

***Keywords**: Pluronic; poloxamer; alkylphospholipids; alkylphosphocholines; hexadecilphosphocholine; HePC; chicken chorioallantoic membrane; Egg-CAM.*

1. Background

Synthetic alkylphospholipids (ALPs), such as edelfosine, miltefosine, perifosine, erucylphosphocholine and erufosine, are relatively new anticancer compounds (Blitterswijk and Verheij, 2013). Structurally, they are ether-derivatives from natural phospholipids of cell membrane, such as endogenous lysophosphatidylcholines (LysoPC or lysolecithins), in which the alkyl-ester linkage has been replaced by a more lipase-resistant ether bond, thus making APLs more metabolically stable.

Chemically APL family is divided into two main classes: (i) alkylglycerophosphocholines (AGPs), also known as alkyl-lysophospholipids or ether lipids, and (ii) alkylphosphocholines (APCs). The ether lipid edelfosine (1-O-octadecyl-2-O-methylglycero-3-phosphocholine, ET-18-OCH_3), first synthetized late 1960s, is considered the AGPs prototype, this compound closely resembles LysoPC with a glycerophospholipid head-group, contains an ether-linked 2-methyl-glycerol backbone and a single octadecyl alkyl chain. Miltefosine (hexadecylphosphocholine, HePC), on the other hand, dates back late 1980s and is a second-generation LysoPC-analogue and prototype of APCs having a single phosphoester-linked hexadecyl alkyl chain, but lacking the glycerol motif. HePC was the first antitumor lipid to be used clinically, in particular for the topical treatment of cutaneous metastases of breast cancer, and is the first effective peroral anti-leishmanial drug (Dorlo *et al*., 2012; Pachioni *et al*., 2013; Ríos-Marco *et al*., 2017).

APLs preferentially act on cell plasma membrane, which distinguishes them from the majority of anticancer drugs whose action mechanisms are mainly

based on interaction with the genetic material. Also, APLs have intracellular targets, implying their uptake within cells (Barratt *et al*., 2009; Pachioni *et al*., 2013).

Contrarily to LysoPC, ALPs resist catabolic degradation. Because of the ether bond, they are not degraded by phospholipases and, therefore, accumulates into cell membrane and cytosol interfering with lipid-dependent survival pathways, in particular membrane lipids – phospholipids and sterols (Barratt *et al*., 2009). ALPs insertion into membranes generate a biophysical perturbation, interfering with phospholipid metabolism, proliferation and cell survival signaling pathways, while simultaneously activating several stress pathways that promote apoptosis (Pachioni *et al*., 2013). It is proposed that molecular mechanisms of anticancer properties of these compounds is by affecting the phospholipid metabolism of the plasma membrane (*e.g.* de novo phospholipid biosynthesis), targeting membrane lipid-rafts and altering lipid-linked signaling (*e.g.* PI3K-Akt and Raf-Erk1/2) at the same time, stress pathways (e.g. stress-activated protein kinase/JNK) are activated inducing growth arrest and hence leading to apoptosis (Blitterswijk and Verheij, 2013; Ríos-Marco *et al*., 2017).

In particular, HePC is described as a lipid raft modulator interfering with the structural organization of surface receptors in the cell membrane. By modulating the cell membrane architecture, it alters receptor activation and/or downstream signaling events (Maurer *et al*., 2013).

The cytotoxic effect of HePC has been evaluated in a large variety of both tumor and normal cell types, showing selectivity towards tumor cells (Blitterswijk and Verheij, 2013). The uptake of HePC by cells begins by insertion into the

plasma membrane which may be followed by internalization (Barratt *et al*., 2009). Due to its amphiphilic nature and its similarity to LysoPC, APLs can be inserted into the outer leaflet of the cell membrane and cross the membrane with the help of a flippase complex. APLs have also been shown to internalize by cells targeting membrane lipid-rafts, suggesting that it has a high affinity to lipid-raft microdomains (Menez *et al*., 2007; Blitterswijk and Verheij, 2013).

HePC is also described to interferes with the functioning of a number of enzymes involved in phospholipid metabolism, including membrane-linked protein kinase C and the phospholipases A2, C and D (Barratt *et al*., 2009) as well as Akt signaling (Prêtre and Wicki, 2018).

Regarding its classical surfactant structure, when HePC concentration is above the critical micellar concentration (CMC), this drug spontaneously aggregates into small micelles. Therefore, HePC interacts with plasma membrane as monomers when its concentration is below to CMC and as both monomers and micelles when it is above the CMC (Barratt *et al*., 2009). Unfortunately, this interaction between HePC micelles and cell membranes causes cell lysis leading to drug side-effects. The mechanisms involves surfactant-membrane insertion and membrane disruption/solubilization (Pachioni *et al*., 2013).

HePC causes hemolysis and thrombophlebitis when administered parenterally and also its peroral administration was associated with gastrointestinal toxicity. The limiting peroral dose is 50 mg daily for adults weighing <25 kg and 100 mg daily for those who weigh >25 kg. In fact, at this low dose HePC is approved in some countries for visceral and cutaneous leishmaniasis treatment (Ríos-Marco *et al*., 2017).

HePC was clinically evaluated against soft tissue sarcomas, colorectal cancer and squamous cell carcinoma of the head and neck, however the severe side effects limited its maximum-tolerated daily dose, preventing observation of antiproliferative effects since the peroral doses required for systemic effects were toxic to the gastrointestinal tract (Ríos-Marco *et al*., 2017). Therefore, this dose-limiting gastrointestinal toxicity and hemolytic effects precludes its further use by the systemic routes for anticancer applications Consequently, the clinical use of HePC as anti-cancer has been limited mainly to the topical treatment of cutaneous tumors (Blitterswijk and Verheij, 2013).

Clinical trials have revealed that adverse reactions of HePC over the gastrointestinal system include nausea, vomiting and diarrhea. Another common symptom is fatigue (Ríos-Marco *et al*., 2017). Occasionally, hepatotoxicity and nephrotoxicity might occur. It also has teratogenic potential, so women of child-bearing age are advised contraception for the duration of treatment and for three additional months after the end of therapy (Sundar and Chakravarty, 2015b; Sundar and Singh *et al*., 2018). Additionally, elevation of serum creatinine and transaminases, hemoptysis, dyspnea, fatigue as well as lung toxicity have been described in clinical trials (Bhattacharya *et al*., 2007; Rahman *et al*., 2011; Silva *et al*., 2013; Ríos-Marco *et al*., 2017).

The development of a drug delivery system to protect gastrointestinal tract upon HePC peroral administration and to allow higher systemic drug concentrations would be of great interest to promote its use in anticancer therapy. Our group previously developed HePC loaded Pluronic F127 polymeric micelles (HePC-PM) with the purpose of lowering the drug toxicity. We have shown that HePC-PM significantly lowers the hemolytic effect of HePC while preserving the

in vitro cytotoxicity against HeLa cancer cell line (Valenzuela-Oses, García, Feitosa, *et al*., 2017, **Appendix A**). Taking into account our previous results, here we modified the HePC: Pluronic F127 ratio of HePC-PM and investigated its safety and selective cytotoxicity. We show that incorporation into PM reduces HePC irritation in a vascularized membrane model while increasing the selectivity index for tumor HeLa cells, rather than fibroblast cells. Additionally, we show that HePC-PM promote intracellular drug delivery.

2. Materials and methods

2.1. Chemicals and reagents

Miltefosine (HePC) was purchased from Avanti Polar Lipids, Inc. (Alabama, USA). Pluronic F127 (12.6 kDa) with the formula $(PEO)_{100}$-$(PPO)_{65}$-$(PEO)_{100}$ was donated by BASF (São Paulo, Brazil). All other chemicals were of analytical grade (Sigma-Aldrich, Brazil) unless otherwise stated.

2.2. Preparation of drug-loaded polymeric micelles (PM)

Drug-loaded PM were prepared by direct dissolution method, using 0.9% NaCl solution as the diluent, because it isotonic and physiologically biocompatible. Briefly, HePC was added to a 1 or 9% (w/v) Pluronic F127 micellar solution followed by smooth homogenization for 1 h at 37 ºC. The drug-loaded micelles were then sterilized by filtration through a 0.22 µm pore size membrane.

2.3. Irritation bioassay

The irritating potential of the free HePC, HePC-loaded PM and empty PM was assessed by modified hen's egg test, also called Hühner-Embryonen test on chorioallantoic membrane (HET-CAM) (Oliveira *et al* 2016). HET-CAM test evaluates the potential of mucous membranes irritancy of a test substance as measured by its ability to induce toxicity in the chick embryo CAM (Kanoujia *et al*., 2014). Briefly, freshly collected fertilized hen's eggs (White Leghorn), obtained from *School of Veterinary Medicine and Animal Husbandry* – University of São Paulo (Brazil). The eggs were kept horizontally in their trays of a climatic chamber, at 37 ºC and 65% relative humidity, equipped with an automatic rotation device to make sure that the embryo was positioned properly. After 10 days, the eggs were candled to ensure fertility and the air sac (*i.e.* air space) position was marked in the underside of the egg. The eggshell was partially opened by cracking around the marked air sac, and the outer membrane of the egg was exposed. Any non-fertilized eggs or those containing no live embryo were discarded. The inner membrane was wet with 0.9% NaCl solution and then carefully removed using blunt forceps and the CAM exposed.

Samples of 1 mL of the following treatments were applied directly onto the undamaged CAM surface: free HePC, HePC-loaded PM, empty PM and 0.9% NaCl solution as negative control. Then, the vasculature of CAM was monitored during 5 min for the appearance of any irritating event, *e.g.* hyperaemia (*i.e.* excess of blood in the vessels), hemorrhage (*i.e.* vessels bleeding), vascular lysis (*i.e.* vessels disintegrating) and coagulation (*i.e.* clotting/denaturalization of intra- and extravascular proteins). Images capturing, processing and analysis

were made using the DigiMicro 2.0 Scale Software. These assays were performed in triplicate.

2.4. Cell culture and viability assays

Cell viability after the treatment with free and encapsulated HePC was investigated for human cervix epithelial adenocarcinoma HeLa cells and mouse fibroblastic L929 according to recommendation of the “Biological evaluation of medical devices: tests for *in vitro* cytotoxicity” (IOS, 2009). This guideline was designed to measure the damage of *in vitro*-cultured mammalian cells after contact with a specific product and for calculation of the half-maximal inhibitory concentration (IC_{50}). For this, pre-cultured cells ($1x10^4$ cells/well) were seeded into 96-well plates and kept in Dulbecco’s modified Eagle’s medium (DMEM) with 10% fetal bovine serum (FBS), for 24 h (37 ºC, humidified, 5% CO_2) to form a semi-confluent monolayer. Afterwards, cell media was removed and replaced with increasing concentrations of HePC and HePC-PM, ranging from 0.4 to 100 µg/mL, diluted in DMEM (5% FBS). After 24 h, cells were exposed to neutral red (only live cells are able to uptake this vital dye). For each treatment, the percentage of growth inhibition (*i.e.* cytotoxic effect) was calculated and compared to DMEM negative control. Then, the IC_{50} were calculated from the concentration-response equation. Empty-PM (*i.e.* without HePC) were also tested as controls. All experiments were repeated at least three times.

3. Results and discussion

3.1. HePC-loaded Pluronic F127 prevents CAM mucosal irritation

HET-CAM was chosen as a preliminary safety test since it is easy to apply and the results are comparable to *in vivo* methods, *e.g.* Draize test (Dario *et al*., 2016. Grimaudo *et al*., 2018). It is a common preliminary organotypic method for the evaluation of mucous membranes irritability and has been recently reported as well-accepted for *in vitro* vascularized mucosae (Abdelkader *et al*., 2015). Free HePC and HePC-loaded into Pluronic-F127 (HePC-PM) were investigated in terms of mucosal irritancy using the modified HET-CAM test. Empty Pluronic PM formulation was also tested to confirm the tolerability and biocompatibility of this co-polymer (**Figure 1**).

Initially, increasing concentrations of free HePC were tested to determine a minimal dose with an irritant effect on this CAM model, which was found to be 3.7 mM, *i.e.* 1500 µg/mL **(Figure 1A)**. This same drug concentration was used in the formulation of HePC-PM with 9% (w/v) of Pluronic F127 **(Figure 1B)**. For the best our knowledge, here we present for the first time the toxic effects of APLs on egg's CAM.

As can be seen in the right-side **Figure 1A**, after administration of HePC at 3.7 mM, strong vascular irritation of CAM was observed in a few minutes. Clearly, HePC induces rapid bleeding vessels, with extensive hemorrhagic area owing to endothelial cell lysis, demonstrated by vasoconstriction as well as disintegrating vessels in the mucosa. These effects were more pronounced in smaller vessels but can also be observed in vessels of larger sizes.

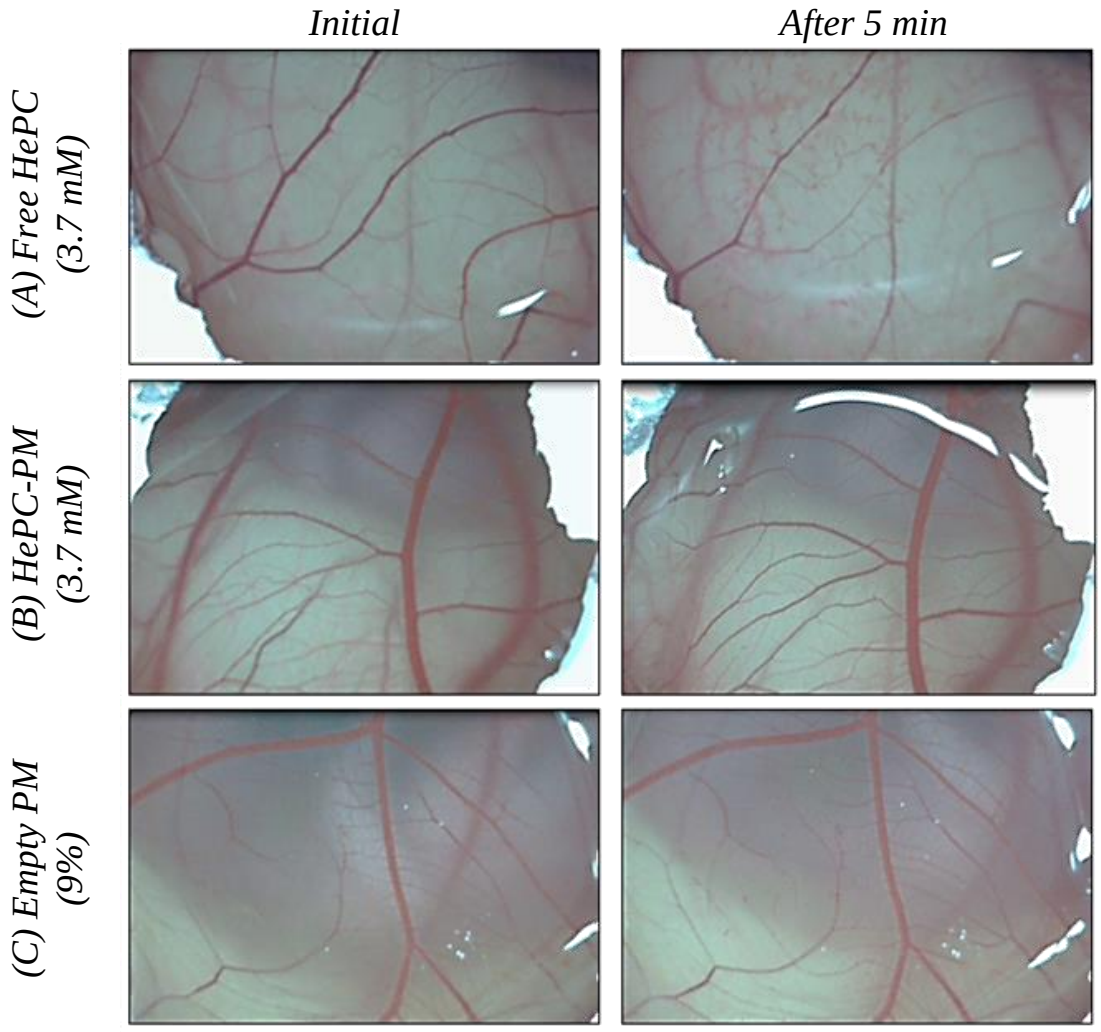

***Figure 1. HePC-loaded Pluronic F127 prevents CAM mucosal irritation**. Sequence of photographs illustrating the effect of free miltefosine (HePC) **(A)**, HePC-loaded Pluronic polymeric micelles (HePC-PM) **(B)** and empty PM **(C)** on the initial healthy CAM **(left side)** and over a 5 min after each treatment **(right side)**. These images are representative of triplicate experiments.*

The immediate appearance of irritating effects may be considered due to the surfactant effect of HePC on endothelial cells. Regarding the amphiphilic structure of HePC and other APLs such as edelfosine and ilmofosine, at concentrations higher than the critical micellar concentration (CMC) they form small micelles, and this aggregation in micelles governs its hemolytic effect,

which occur through mechanisms involving non-specific surfactant-membrane interactions following by lipid-solubilization and membrane lysis (Sá *et al*., 2013).

Similar to edelfosine and ilmofosine, HePC was originally developed as a peroral antineoplastic drug for treatment of breast cancer and other solid tumors, but its severe dose-limiting gastrointestinal toxicity outweighed its clinical benefits and so its use for cancer therapy was declined. Later HePC was repurposed for the peroral treatment of leishmaniasis. Nonetheless, even for antileishmanial therapy gastrointestinal toxicity is the most frequent drawback caused by peroral HePC administration, in which nausea, vomiting, diarrhea, abdominal pain, and anorexia have been consistently reported. Occasionally, the side effects can be severe, requiring treatment discontinuation.

These side effects, mainly caused by irritation of the gastric and enteric mucosa, were consistently reproduced in our HET-CAM model, which showed irritating events compatible with gastrointestinal effects caused by HePC. In fact, HET-CAM is a rapid, sensitive, technically easy and inexpensive test. Testing with incubated eggs is a borderline case between *in vivo* and *in vitro* systems and does not conflict with ethical and legal obligations. As the CAM of the chick embryo represents a vascular stratified tissue including veins, arteries, and capillaries, it responds to injury with a complete inflammatory process, similarly to the vascularized mucous membranes of mammalian tissues (Gupta *et al*., 2007; Kanoujia *et al*., 2014).

The incorporation of HePC into Pluronic-based polymeric micelles (HePC-PM) protected the CAM from vascular irritating side effects; the general physical appearance of egg's CAM kept normal during the test period **(Figure 1B)**. Indeed,

HePC-PM did not trigger any process of vascular change, no hemorrhage, lysis, coagulation, or any acute inflammatory reactions in the CAM occurred and the result was similarly to 0.9% NaCl **(data not shown)**.

The suppression of the side effects previously observed with free HePC strongly indicated that in HePC-PM most of the drug was incorporated into the polymeric nanostructures, limiting the interaction between HePC with the CAM and, therefore, preventing its vascular complications.

According to Lasa-Saracíbar *et al*. (2014), peroral administration of edelfosine in mice causes severe gastrointestinal tract irritation with degeneration, necrosis and peeling of the stomach and intestine walls. Necropsy of the animals showed gastrointestinal obstruction with accumulation of food in the stomach, swelling, fluid accumulation and thickness of the stomach and intestine walls. Histopathology revealed degeneration, necrosis and peeling of superficial cells in the stomach and the small intestine, accompanied by inflammation of the intestinal mucosa, which suggest an irritant effect of edelfosine over the gastric and duodenal mucosa. On the other hand, similarly to our findings, encapsulation of this drug into nanostructures (*i.e.* lipid nanoparticles) shown the protective effect that drug-loaded nanoparticles provide over the administration of the free-drug.

Regarding empty PM of Pluronic F127 at 9%, no signs of acute inflammation on the CAM were observed during the course of the assay. This finding is consistent with those reported in the literature. Kanoujia *et al* (2014) shows that Pluronic F127 PM (5%) with 0.5% gatifloxacin is nonirritant in HET-CAM. Grimaudo *et al*. (2018) reported that Pluronic F127/TPGS (1:1 molar ratio) mixed micelles formulated up to 20 mM (of total polymers) were seen to be also

nonirritant in HET-CAM. In addition, Gupta *et al*. (2007) tested a gel formulation composed by Pluronic F127 (9%), chitosan (0.25%), timolol (0.25%) and methylparaben (0.1%), demonstrating to be nonirritant to mild irritant and well tolerated. Similarly, Fathalla *et al*. (2017) demonstrated that polymeric gels based on Pluronic F127 (23%) and Pluronic F68 (15%) did not show any signs of CAM irritation.

Altogether, these is an indication that the Pluronic copolymers used in these formulations were not irritant to the CAM, exhibiting excellent mucous tolerability and biocompatibility.

3.2. Selective cytotoxicity of HePC-loaded polymeric micelles

To investigate the effect of HePC, free or loaded into polymeric micelles, cytotoxicity experiments were carried out against both tumor and healthy cell. For these following assays, we selected HePC-PM formulation consisting of 100 µg/mL HePC and 1% (w/v) Pluronic F127, in which we have previously demonstrated that most of the drug is incorporated into polymeric micelles **(Chapter 1)**.

We investigated HePC cytotoxicity against cervical carcinoma HeLa cells and healthy connective fibroblast L929 cells, as well as whether cytotoxicity could be modulated by HePC incorporation into polymeric micelles. Cytotoxicity of free HePC and HePC-PM was tested for 24 h by quantitative analysis using neutral red uptake assay and presented in **Figure 2 and Figure 3**.

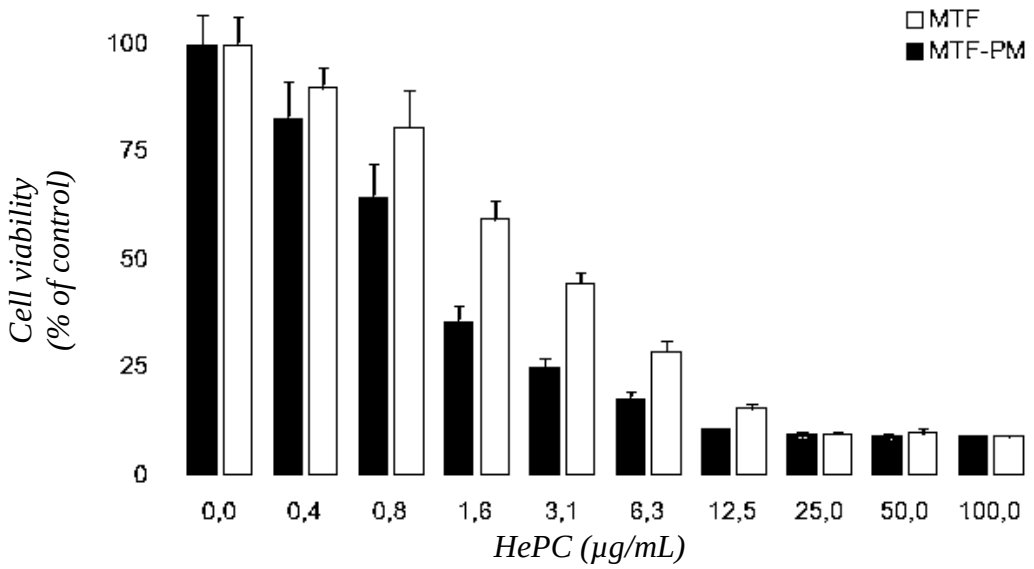

Figure 2. *In vitro cytotoxic effect of HePC treatment, free* ***(white bars)*** *or loaded into polymeric micelles* ***(black bars)****, against HeLa cervical carcinoma cells, measured by neutral red uptake assay.*

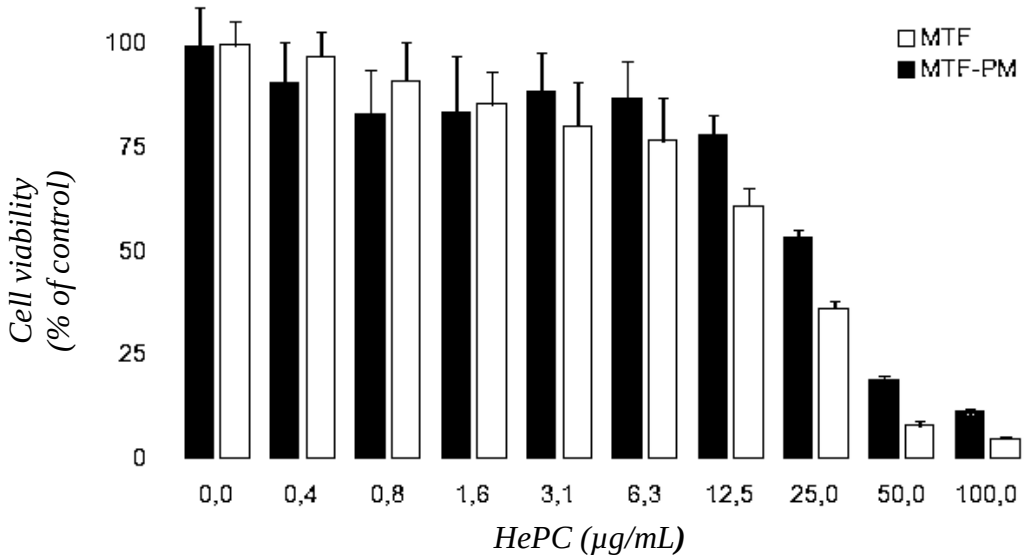

Figure 3. *In vitro cytotoxic effect of HePC treatment, free* ***(white bars)*** *or loaded into polymeric micelles* ***(black bars)****, agaist healthy L929 fibroblastic cells, measured by neutral red uptake assay.*

Treatment with both free HePC and HePC-PM for 24h caused a dose-dependent reduction in viability of HeLa and L929 cell lines. Under these conditions, tumor HeLa cells were very sensitive to the drug **(Figure 2)** and non-tumor L929 cells more resistant when treated with the same HePC concentration **(Figure 3).** Fibroblast cells were selected because they are the predominant tissue type. Moreover, many standard institutions recommend these cells.

Next, based on the presented dose-response curves, we calculated the IC_{50}, *i.e.* drug concentration required to decrease half of the cell viability, shown in **Table 1**.

***Table 1. Selective cytotoxicity of HePC-loaded polymeric micelles**. Comparison of cytotoxic activity of free miltefosine (HePC) and HePC-PM against HeLa cervical carcinoma cells and healthy L929 fibroblastic cells.*

Treatment	***IC_{50} (µg/mL)****		***Selective index (SI)******
	L929	***HeLa***	
Free-HePC	*18.3*	*2.7*	*6.8*
HePC-PM	*29.3*	*1.2*	*24.4*

**The IC_{50} values were calculated from the dose-response plots. Each value represents the mean of three experiments.*
***The degree of selectivity (i.e. selective index, SI) were expressed using the following ratio: IC_{50} of the treatment in normal cell line / IC_{50} of the same treatment in cancer cell line.*
Cell viability was determined by the neutral red uptake assay as described previously

For free HePC we found an IC_{50} of 18.3 µg/mL against L929 cells in comparison to 2.7 µg/mL against HeLa cells. The IC_{50} value of free HePC found for HeLa cells agrees of previously reports, *i.e.* 2.6 µg/mL (Valenzuela-Oses, García, Feitosa, *et al*., 2017, **Appendix A**), 2.8 µg/mL (Rybczynska *et al* 2001b), 3.3 µg/mL (Ruiter *et al*., 2003), and 5.6 µg/mL (Gontijo *et al*., 2014), however is below that 13.1 µg/mL (Papazafiri *et al*., 2005) and 52.5 µg/mL (Lukáč *et al*.,

2009). Other studies showed an IC_{50} around 50 µg/mL for L929 cell (Morais *et al.,* 2014; Grecco *et al.*, 2018), contrarily, HePC 65 µg/mL did not show any cytotoxic impact on these cells, cultured in medium with 10% FBS (Polat *et al*., 2014). In fact, these discrepancies may be due to experimental differences between the studies, such as cell origin, cell density, drug contact time, composition of the culture medium, concentration of FBS, method to verify cell viability, among others.

Interestingly, incorporation of HePC into PM seems to protect L929 from HePC cytotoxicity by increasing the IC_{50} value from 18.3 to 29.3 µg/mL **(Figure 2 and Table 1)**. In contrast, for the same drug concentration, HePC-PM displayed cytotoxicity against HeLa tumor cells (**Figure 2B and Table 1)**, by decreasing IC_{50} value from 2.7 to 1.2 µg/mL. The results indicate that HePC-PM exhibit potent and selective anticancer activity. Additionally, the cytotoxicity of empty PM was also investigated **(data not shown)** and no toxic effects were observed up to 1% (w/v) Pluronic F127.

Therefore, based on IC_{50} values in tumor and non-tumor cell lines, we calculated the selectivity, expressed by its selective-index (SI) value, of free HePC and HePC-PM treatments **(Table 1)**. As expected, free HePC displayed selective cytotoxicity, presenting SI~6.8. In general, an SI value higher than 2.0 indicates a differential drug selectivity. In fact, HePC, as other APLs, preferentially accumulates in tumor cells displaying in *vitro* and *in vivo* antineoplastic activities in a selective way (Kostadinova *et al*., 2015). This selectivity of APLs can be attributed to a higher uptake capacity of neoplastic cells as compared to normal cells due to deferentially lipid composition of the membranes (Mollinedo *et al*., 2004).

Interestingly, HePC-PM treatment enhanced 3.6-folds the drug selectivity (SI = 24.4). As the SI demonstrates the differential activity of a drug, the higher the SI value, the more selective it is. This result suggests that these nanostructures are preferentially captured by tumor cells.

HePC interacts with living cells by instantaneous partition between the surrounding medium and the plasmatic membrane, and thus this drug can act on targets localized in the plasma membrane or cytosol (Rybczynska *et al*., 2001a). Indeed, considering that HePC incorporation into PM reduce the interaction between the drug and plasmatic membrane (**Chapter 1)**, at the same time; it enhances cytotoxicity to HeLa tumor cells and decrease for normal L929 cells. HePC exhibits high affinity for the plasma membrane, once incorporated it follows consecutive internal traffic until anchoring intracellular membranes of organelles (Geilen *et al*., 1994). Furthermore, the intracellular concentration of HePC is not directly related to the cell sensitivity, differential susceptibility to apoptosis could explain the drug uptake-independent sensitivity to HePC (Rybczynska *et al*., 2001a).

Previous studies show that HePC, eldefosine and perifosine induced time- and dose-dependent, apoptosis in HeLa cells (Rybczynska *et al*., 2001a; Ruiter *et al*., 2003). In fact, McShane *et al*. (2015) demonstrated that HePC inhibited both Akt/PKB and ERK phosphorylation in HeLa cells in a dose-dependent manner. The inhibition of Akt/PKB phosphorylation with APLs is in agreement with an earlier report performed in HeLa cells (Ruiter *et al*., 2003) Additionally, in HeLa cells, HePC antagonizes the process of cytidylyltransferase translocation from cytosol (inactive form) to membrane (active form), this is a key-enzyme of

phosphatidylcholine biosynthesis (Wieder *et al*., 1993) and thus alterations in this pathway can lead to apoptosis.

In this way, HePC incorporation into PM seems to drive an intracellular delivery of this drug inside HeLa cells, improving it cytotoxicity specifically against this tumor cell, thus enhancing the selectivity of the treatment.

4. Conclusion

Polymeric micelles are well-known colloidal drug delivery systems and the amphiphilic nature of HePC favors its incorporation into theses micelles. Altogether, our study supports that the Pluronic F127 polymeric micelles might be used as a safe vehicle for the administration of HePC since these nanostructures were able to modify the partition of HePC and reduced its toxicity on vascularized membranes, evidencing the protective effect that polymeric micelles provides over the administration of free HePC. Besides, cytotoxicity studies demonstrated that polymeric micelles provided a selective effect while increased its efficacy against tumor cells toxicity. Given the importance of HePC, our colloidal system developed can be effective applied to reduce HePC toxicity, allowing its further use for anticancer therapy.

Acknowledgements

This study was financed in part by the Coordination of Superior Level Staff Improvement (CAPES/Brazil, finance code 001), the State of São Paulo Research Foundation (FAPESP/Brazil, processes 2014/01983-0) and the National Council for Scientific and Technological Development (CNPq/Brazil). The authors wish to thank Basf Company (Brazil) for kindly supplying all Pluronic copolymers. VAF also acknowledges to IPT Foundation for the “Novos Talentos” fellowship. The authors are also in debt with Antonio Fernando Montemor for his excellent technical support.

References

ABDELKADER et al. Critical appraisal of alternative irritation models: three decades of testing ophthalmic pharmaceuticals. Br. Med. Bull., 113 (2015), pp. 59-71 doi.org/10.1093/bmb/ldv002.

BARRATT at el. Cellular Transport and Lipid Interactions of Miltefosine. Current Drug Metabolism, 2009, 10, 247-255.

BHATTACHARYA et al. Phase 4 trial of miltefosine for the treatment of Indian visceral leishmaniasis J Infect Dis, 196 (2007), pp. 591-598.

BLITTERSWIJK and VERHEIJ. Anticancer mechanisms and clinical application of alkylphospholipids. Biochimica et Biophysica Acta 1831 (2013) 663–674.

DARIO et al. Stability and safety of quercetin-loaded cationic nanoemulsion: In vitro and in vivo assessments. Colloids and Surfaces A: Physicochem. Eng. Aspects 506 (2016) 591–599.

GEILEN et al. Uptake, subcellular distribution and metabolism of the phospholipid analogue hexadecylphosphocholine in MDCK cells. Biochim Biophys Acta, 1211 (1994), pp. 14-22.

GONTIJO et al. Long-chain alkyltriazoles as antitumor agents: synthesis, physicochemical properties, and biological and computational evaluation. Med Chem Res (2015) 24:430–441 DOI 10.1007/s00044-014-1137-3.

GRECCO et al. Neolignans isolated from twigs of Nectandra leucantha Ness & Mart (Lauraceae) displayed in vitro antileishmanial activity. J. Venom. Anim. Toxins incl. Trop. Dis vol.24 Botucatu 2018 Epub Oct 18, 2018.

GRIMAUDO et al. Poloxamer 407/TPGS Mixed Micelles as Promising Carriers for Cyclosporine Ocular Delivery. Mol. Pharmaceutics 2018, 15, 2, 571-584.

GRIMAUDO et al. Poloxamer 407/TPGS Mixed Micelles as Promising Carriers for Cyclosporine Ocular Delivery. Mol. Pharmaceutics, 2018, 15 (2), pp 571–584 DOI: 10.1021/acs.molpharmaceut.7b00939.

GUPTA et al. Sustained Ocular Drug Delivery from a Temperature and pH Triggered Novel In Situ Gel System. Drug Delivery, 14:507–515, 2007.

IOS, ISO 10993-5: Biological evaluation of medical devices (Tests for in vitro cytotoxicity). (International Organization for Standardization, 2009), pp. 34.

KANOUJIA et al. Evaluation of gatifloxacin pluronic micelles and development of its formulation for ocular delivery. Drug Deliv. and Transl. Res. (2014) 4:334–343 DOI 10.1007/s13346-014-0194-y

KOSTADINOVA et al. Antitumor Lipids--Structure, Functions, and Medical Applications. Adv Protein Chem Struct Biol. 2015;101:27-66. doi: 10.1016/bs.apcsb.2015.08.001.

LASA-SARACÍBAR et al. Lipid nanoparticles protect from edelfosine toxicity in vivo. Int J Pharm. 2014 Oct 20;474(1-2):1-5. doi: 10.1016/j.ijpharm.2014.07.053.

LIEBSCH and SPIELMANN, INVITTOX Protocol No. 47: The HET-CAM Test, (2002).

LUKÁČ et al. Synthesis and biological activity of dialkylphosphocholines. Bioorg. Med. Chem. Lett. 19 (2009) 6346–6349.

MAURER et al. Miltefosine: a novel treatment option for mast cell-mediated diseases. Journal of Dermatological Treatment, 24:4, 244-249, DOI: 10.3109/09546634.2012.671909.

McSHANE et al. A Combination of Screening and Computational Approaches for the Identification of Novel Compounds That Decrease Mast Cell Degranulation. 2015, Vol. 20(6) 720–728.

MENEZ et al. Inward translocation of the phospholipid analogue miltefosine across Caco-2 cell membranes exhibits characteristics of a carrier-mediated process. Lipids. 2007;42:229–240.

MORAIS et al. Antiparasitic Activity of Natural and Semi-Synthetic Tirucallane Triterpenoids from Schinus terebinthifolius (Anacardiaceae): Structure/Activity Relationships. Molecules 2014, 19, 5761-5776; doi:10.3390/molecules19055761

PAPAZAFIRI et al. Structure-activity relationships of antineoplastic ring-substituted ether phospholipid derivatives. Cancer Chemother Pharmacol (2005) 56: 261–270 DOI 10.1007/s00280-004-0935-6.

POLAT et al. Miltefosine and polyhexamethylene biguanide: a new drug combination for the treatment of Acanthamoeba keratitis. Clinical and Experimental Ophthalmology 2014; 42: 151–158 doi: 10.1111/ceo.12120.

PRÊTRE and WICKI. Inhibition of Akt and other AGC kinases: A target for clinical cancertherapy? Seminars in Cancer Biology 48 (2018) 70–77.

RAHMAN et al. Phase IV trial of miltefosine in adults and children for treatment of visceral leishmaniasis (kala-azar) in Bangladesh Am J Trop Med Hyg, 85 (2011), pp. 66-69.

RÍOS-MARCO et al., Alkylphospholipids: An update on molecular mechanisms and clinical relevance. Biochimica et Biophysica Acta, 1859, (2017) 1657-1667.

RUITER et al. Anti-cancer alkyl-lysophospholipids inhibit the phosphatidylinositol 3-kinase–Akt/PKB survival pathway. Cancer Drugs 14:167–173, 2003.

RYBCZYNSKA et al MDR1 causes resistance to the antitumour drug miltefosine. British Journal of Cancer (2001b) 84(10), 1405–1411.

RYBCZYNSKA et al. Effects of miltefosine on various biochemical parameters in a panel of tumor cell lines with different sensitivities. Biochemical Pharmacology 62 (2001a) 765–772.

SÁ et al. Alkylphosphocholines as Promising Antitumor Agents: Exploring the Role of Structural Features on the Hemolytic Potential. Mol. Inf.2014, 33, 53 – 64.

SILVA et al. Miltefosine-induced acute interstitial pneumonitis in a patient with renal dysfunction. InternationalJournalofInfectiousDiseases17(2013)e660–e661.

SUNDAR and SINGH. Chemotherapeutics of visceral leishmaniasis: present and future developments. Parasitology (2018), 145, 481–489.

WIEDER et al. Antagonism of phorbol-ester-stimulated phosphatidylcholine biosynthesis by the phospholipid analogue hexadecylphosphocholine. Biochem J, 291 (1993), pp. 561-571.

WIEDER et al. Antagonism of phorbol-ester-stimulated phosphatidylcholine biosynthesis by the phospholipid analogue hexadecylphosphocholine. Biochem. J. (1993) 291, 561-567.

Chapter III

This third chapter describes the main results achieved during my internship at the Centre for Craniofacial Development & Stem Cell Biology, King's College London (UK), under supervision of Dr. Paul Long and Prof. Agamemnon Grigoriadis.

Miltefosine-loaded polymeric micelles present cytotoxicity to osteosarcoma cells

Valker Araujo Feitosa[1,2,3], Daniel Doro[3], Paul Long[1,4], Agamemnon Grigoriadis[3], Carlota de Oliveira Rangel-Yagui[1]

[1]Department of Biochemical and Pharmaceutical Technology, School of Pharmaceutical Sciences, University of São Paulo, Brazil
[2]Bionanomanufacturing Center, Institute for Technological Research, Brazil
[3]Centre for Craniofacial Development & Stem Cell Biology, King's College London, UK
[4]Institute of Pharmaceutical Science, King's College London, UK

Abstract

Osteosarcoma is a common neoplastic bone disease with high morbidity and mortality, occurring primarily in children and young adults. Here we report that miltefosine induces in vitro cytotoxicity and decrease cell survival, migration and proliferation in murine and human osteosarcoma cells. We have shown that cytotoxicity by miltefosine is associated with caspase-3 activation, DNA fragmentation, apoptotic-like body's formation and inhibition of both constitutive and cytokine-stimulated Akt (PKB) phosphorylation. These signaling changes together can be responsible for apoptosis induction in osteosarcoma cells. We also show that miltefosine incorporation into polymeric micelles of Pluronic F127 clearly reduces the drug cytotoxic effects evidenced by increase in cell viability, as well as prolongs cell survival, migration and proliferation. Finally, we demonstrate that Pluronic F127 polymeric micelles are efficient for cargo delivering the encapsulated drug preferentially within tumor cells rather than healthy cells. These findings together suggest that miltefosine loaded into polymeric micelles provide a potential alternative for osteosarcoma therapy.

***Keywords**: Pluronic; poloxamer; alkylphospholipids; alkylphosphocholines; hexadecilphosphocholine; HePC; caspase-3; Akt; PKB.*

1. Background

Neoplastic bone disorders include both primary bone tumors and metastasis. Osteosarcoma (OS) is the most common type of primary malignant bone tumor (36% of total), followed by chondrosarcoma (20–25%) and Ewing sarcoma (16%) (Evola *et al.*, 2017). OS is extremely heterogeneous in etiology, genetics, molecular pathogenesis as well as clinical manifestations, and is not well understood yet (Lindsey *et al.*, 2017). In spite of recent research advances, patients with OS still have very poor outcomes. The current standard treatment includes neoadjuvant chemotherapy, surgery and post-operative adjuvant chemotherapy. The main chemotherapeutic schemes include cisplatin, doxorubicin, high-dose methotrexate with leucovorin rescue, and isofosfamide with or without etoposide (Lindsey *et al.*, 2017). However, most of these therapeutic regimens remain essentially unchanged since the 1970s. Multiple efforts have been taken to improve therapeutic efficacy but unfortunately more effective or less toxic schemes have not yet been described (Saraf *et al.*, 2018).

Among the new generation of chemotherapeutics with potential application in OS treatment, we highlight the synthetic antitumor lipids (ATLs) (Yao *et al.*, 2013; Bonilla *et al.*, 2015; Gonzalez-Fernandez *et al.*, 2017), which are analogs of endogenous lysophosphatidylcholine (LysoPC) and include alkylphospholipids (APLs) and alkylphosphocholines (APCs). Miltefosine (hexadecyl phosphocholine, HePC), the prototype of APCs, was the first ATL to be used clinically to treat cutaneous metastases of breast cancer (Leonard *et al*., 2001).

HePC is an amphiphilic molecule composed of a hydrophobic tail and a polar phosphocholine head group (Dorlo *et al*., 2012). Unlike conventional DNA-

targeting chemotherapeutic agents, this drug acts on lipid-linked signaling pathways (*i.e.* lipid rafts), interfering with lipid metabolism (e.g. phospholipid biosynthesis, non-vesicular cholesterol transport and homeostasis), biochemical survival pathways (e.g. Akt-mTOR inactivation), lipid-dependent signal transduction (e.g. phospholipase C, phospholipase D, protein kinase C), as well as stress pathways leading to apoptosis (Van Blitterswijk and Verheij, 2008; 2013; Sá and Rangel-Yagui 2015; Sá *et al*., 2015; Alonso and Alonso, 2016).

Additionally, HePC is more effective in metabolically active, proliferating cells, such as cancer cells, but not in quiescent normal cells, reducing, in this way, side effects on healthy cells (Van Blitterswijk and Verheij, 2013). So far, the precise mechanism of action has not been fully elucidated.

HePC exhibits antitumor effects in different cell lines including human hepatoma (Jimenez-Lopez *et al.*, 2006; Marco *et al.*, 2009; Jimenez-Lopez *et al.*, 2010; Rios-Marco *et al.*, 2011; Rios-Marco *et al.*, 2013; Rios-Marco *et al.*, 2016) and glioblastoma cells (Tewari *et al.*, 2008; Thakur *et al.*, 2013). HePC displays potent antitumor activity *in vitro* and *in vivo;* it is clinically approved by the FDA for topical treatment of skin metastases of breast cancer, as well as cutaneous lymphoma. HePC is widely used as an effective peroral treatment for visceral leishmaniasis and it has been reported to possess similar modes of action in *Leishmania* and human cancer cells (Alonso and Alonso, 2016). It also exhibits antibacterial, anti-trypanosomal and broad-spectrum antifungal activities (Pachioni *et al.*, 2013).

HePC has been extensively tested in preclinical models (reviewed by Pachioni *et al*., 2013). However, it presents significant irritancy profile involving gastrointestinal symptoms (e.g. nausea, vomiting and diarrhea) as well as

hemolytic effects (e.g. hemolysis and thrombophlebitis), owing to its surfactant structure. Due to its hemolytic effect, HEPC cannot be administered intravenously, but only orally (Impavido®) for leishmaniasis or topically (Miltex®) for cutaneous metastasis of breast cancer (Dorlo *et al*., 2012). Therefore, the development of a drug delivery system allowing the controlled release of HePC would be useful to overcome these limitations.

The first application of nanocarriers for HePC delivery dates back to 1991 when it was incorporated into liposomes (Zeisig *et al*., 1991). Thereafter, a series of formulations based on liposomes, with or without pegylation, were developed Thakur *et al*., 2013; Momeni *et al*., 2013; Zhukova *et al*. 2010; Lindner *et al*., 2008; Papagiannaros *et al*., 2005a; Papagiannaros *et al*., 2005b; Mravljak *et al*., 2005; Zeisig *et al*., 2003; Ratz *et al*., 2001; Arndt *et al*., 2001; Arndt *et al*., 1999; Arndt *et al*. 1998; Kaufmann-Kolle *et al*. 1998; Eue *et al*., 1998; Arndt *et al*., 1997; Zeisig *et al*. 1996a; Zeisig *et al*. 1996b; Fichtner *et al*., 1994; Zeisig *et al*., 1994; Kaufmannkolle *et al*., 1994; Zeisig *et al*., 1993).

In some cases, miltefosine was co-administered with other antitumor agents (e.g. doxorubicin, paclitaxel, mitoxantrone, etc). Other lipid-based formulations reported were nanoemulsions (Bock *et al*., 1994) and nanocochelates (Pham *et al*., 2013). Recent studies have also been conducted for HePC encapsulation into albumin-microparticles (Das *et al*., 2011), polycaprolactone (PCL) nanofibers (Wang *et al*., 2013) and poly(lactic-co-glycolic acid)-poly(ethylene oxide) (PLGA-PEG) nanoparticles (Kumar *et al*., 2016). All of these studies aimed at delivering the drug to specific targets and reducing side effects.

In nanomedicine, special attention has been given to polymeric micelles (Rangel-Yagui et al., 2005), which are colloidal nanostructures (~10-100 nm)

formed by the spontaneously self-aggregation of amphiphilic block copolymers (consisting of both hydrophilic and hydrophobic monomer units) in aqueous environments. These amphiphilic block copolymers self-assemble to form a hydrophobic core, amenable to the loading of hydrophobic drugs, and a hydrophilic shell or corona (Rangel-Yagui et al., 2005; Sirsi and Borden, 2014). They are widely considered as convenient nanocarriers for multiple pharmaceutical applications such as therapeutic agents' delivery (*e.g.* drugs, genes, peptides and proteins), diagnostic imaging (*e.g. in vivo* biodistribution studies), and theranostics (Movassaghian, Merkel and Torchilin, 2015).

The Pluronics (also called Poloxamers) are amphiphilic triblock copolymers of poly(ethylene oxide)-poly(propylene oxide)-poly(ethylene oxide) (PEO-PPO-PEO). They are biocompatible, FDA-approved and commonly described to its self-assembly into polymeric micelles nanostructures (Talelli and Hennink, 2011). Recently, we proved that HePC-loaded polymeric micelles of Pluronic F127 significantly lower the hemolytic effect of HePC while preserving the *in vitro* cytotoxicity against the HeLa cancer cell line (Valenzuela-Oses, García, Feitosa, *et al*., 2017, **Appendix A**). Here, we investigated HEPC and HEPC-loaded polymeric micelles (HePC-PM) cytotoxicity against osteosarcoma cell lines. We show that incorporation into PM reduces drug cytotoxicity *in vitro*, but increases selectivity for tumor cells. Additionally, we show that HePC-PM promote intracellular drug delivery.

2. Materials and methods

2.1. Chemicals and reagents

Miltefosine (HePC) was purchased from Avanti Polar Lipids, Inc. (Alabama, USA). Pluronic F127 (12.6 kDa) with the formula $(PEO)_{100}$-$(PPO)_{65}$-$(PEO)_{100}$ was donated by BASF (São Paulo, Brazil). All other chemicals were of analytical grade (Sigma-Aldrich, Dorset, UK) unless otherwise stated.

2.2. Preparation of drug-loaded polymeric micelles (PM)

Drug-loaded PM were prepared using a previously described hydration method (Valenzuela-Oses, García, Feitosa, *et al*., 2017, **Appendix A**) with minor modifications. Briefly, a 1 % (w/v) Pluronic F127 dispersion was prepared using α-Minimum Essential Medium (α-MEM, Lonza Biologics, Slough, UK) as the diluent. HePC or tetramethylrhodamine(TRITC)-phalloidin was added to the dispersion and then incorporated into the micelles by smooth homogenization for 1 h at 37 ºC. The drug-loaded micelles were then sterilized by filtration through a 0.22 µm pore size membrane.

2.3. Cell culture

The source and a description of the cell lines used in this study are shown in **Table 1**. Cells were grown in α-MEM containing GlutaMAX and supplemented with 50 U/mL penicillin, 50 µg/mL streptomycin, and different concentrations of fetal bovine serum (FBS) (Thermo Scientific Gibco, UK) as indicated. Cells were grown at 37 °C in 5 % (v/v) CO_2.

Table 1. Source and a description of the cell lines used in this study.

Cell line	*Cell type*	*Species*
MG-63	*Osteosarcoma*	*Human*
U2OS	*Osteosarcoma*	*Human*
SAOS-2	*Osteosarcoma*	*Human*
K7M2	*Osteosarcoma*	*Murine*
P1.15	*Osteosarcoma*	*Murine*
HCC1	*Osteoblast*	*Human*
HFF1	*Fibroblast*	*Human*
MC3T3-E1	*Osteoblast*	*Murine*

2.4. Cytotoxicity assays

Cells were sub-cultured into 96-well plates (Falcon®) at a density of $1x10^4$ cells/well in α-MEM and incubated for at least 3 h at 37 °C in 5% (v/v) CO_2. The medium was then replaced with fresh medium supplemented with varying concentrations of either HePC or HePC-PM from 4 to 245 µM. Unloaded PMs were tested as negative controls. Untreated cells were included as positive controls. After 24 h of incubation, the total metabolic activity of the cells was quantified by reduction of fluorescent Alamar blue® dye.

2.5. Time-lapse live-cell imaging assays

Human (MG-63) and murine (K7M2) osteosarcoma cells were cultured to confluence in a 96-well ImageLockTM plate (IncuCyteTM) in α-MEM. For the scratch, a 96-pin mechanical device (WoundMaker™) was used to create homogeneous 700-800 µm wounds in the confluent monolayers according to the manufacturer's instructions (IncuCyte® Cell Migration Kit; Essen Bioscience). The following treatments were applied to the cells prior to the scratch making: HePC, HePC-PM and α-MEM as control. For observation of cell growth, migration and proliferation, the plates were then incubated and scanned in the IncuCyte®

Zoom system at the rate of one scan/h, up to 48 h. Image processing and all the analyses were made using the IncuCyte® ZOOM Software.

2.6. Immunoblotting

Cells lysates containing equal amounts of protein were heated at 95 °C for 5 min and separated by sodium dodecyl sulfate polyacrylamide gel electrophoresis (SDS-PAGE). The separated proteins were transferred onto polyvinylidene fluoride (PVDF) membranes and nonspecific binding was blocked with 5% (v/v) bovine serum albumin (BSA) solution for 1 h at room temperature. The PVDF membranes were incubated overnight with primary antibodies against phosphorylated protein kinase B (pAKT, 1:5000), cleaved caspase-3 (1:5000) or rabbit glyceraldehyde 3-phosphate dehydrogenase-GAPDH (1:5000) antibodies followed by the horseradish peroxidase–conjugated secondary antibodies. All antibodies were purchased from Abcam (Cambridge UK) except GAPDH from Sigma, UK. The membranes were imaged using ECL (Bio-Rad) in a ChemiDoc Imager (Bio-Rad) and scanned using ImageLab TM software (Bio-Rad).

3. Results

3.1. Miltefosine inhibits cell viability in osteosarcoma cells

We first investigated the effects of free HePC on the viability of a panel of human and murine OS cell lines. The cells were incubated with HePC ranging from 15 to 245 μM, in α-MEM containing 5% FBS as show **Figure 1A.** Treatment with HePC for 24h in standard medium (*i.e.* containing 5% FBS) caused a dose-dependent reduction in viability of all five osteosarcoma cell lines. Under these conditions, K7M2 cells appeared to be the most sensitive and P1.15 cells relatively more resistant **(Figure 1A)**.

As it is well-established that APLs can bind to serum proteins around 97% (Dorlo *et al*. 2012) we next investigated the cytotoxic effects of HePC in reduced FBS conditions **(Figure 1B).** Accordingly, all cell lines tested were more sensitive to HePC treatment in media containing 1% FBS**.**

3.2. Selective induction of cytotoxicity by miltefosine in osteosarcoma cells

We next investigated whether HePC cytotoxicity differed between non-tumor osteoblast cells (MC3T3-E1) and fibroblast cells (HFF1), and osteoblastic osteosarcoma cells (K7M2 and MG-63), as well as whether cytotoxicity could be modulated by HePC incorporation into polymeric micelles (PM) as presented in **Figure 2.**

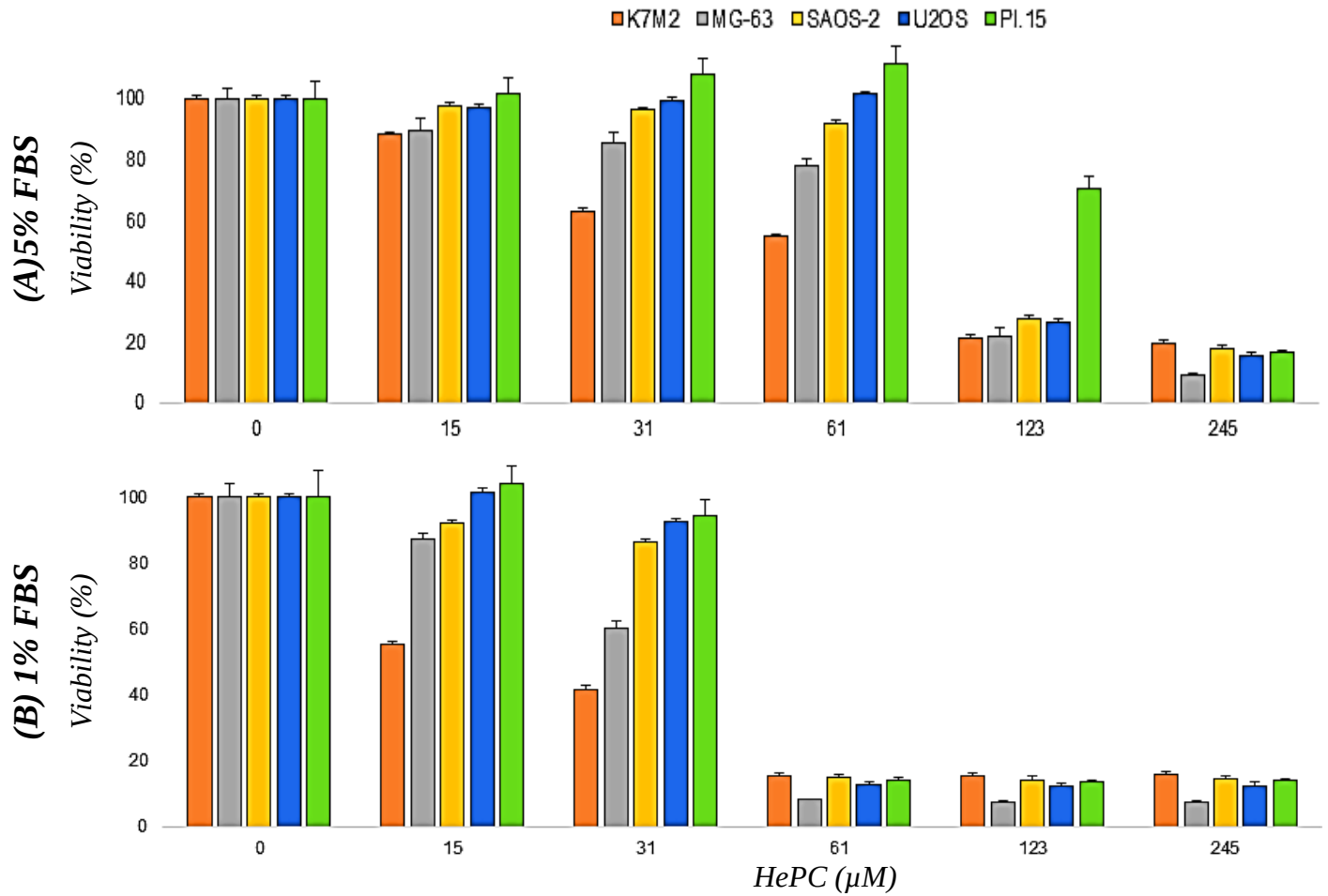

Figure 1. Cytotoxity of HePC against human and murine osteosarcoma cells. *Cell lines were cultured in α-MEM supplemented with 5%* ***(A)*** *or 1%* ***(B)*** *FBS.*

1

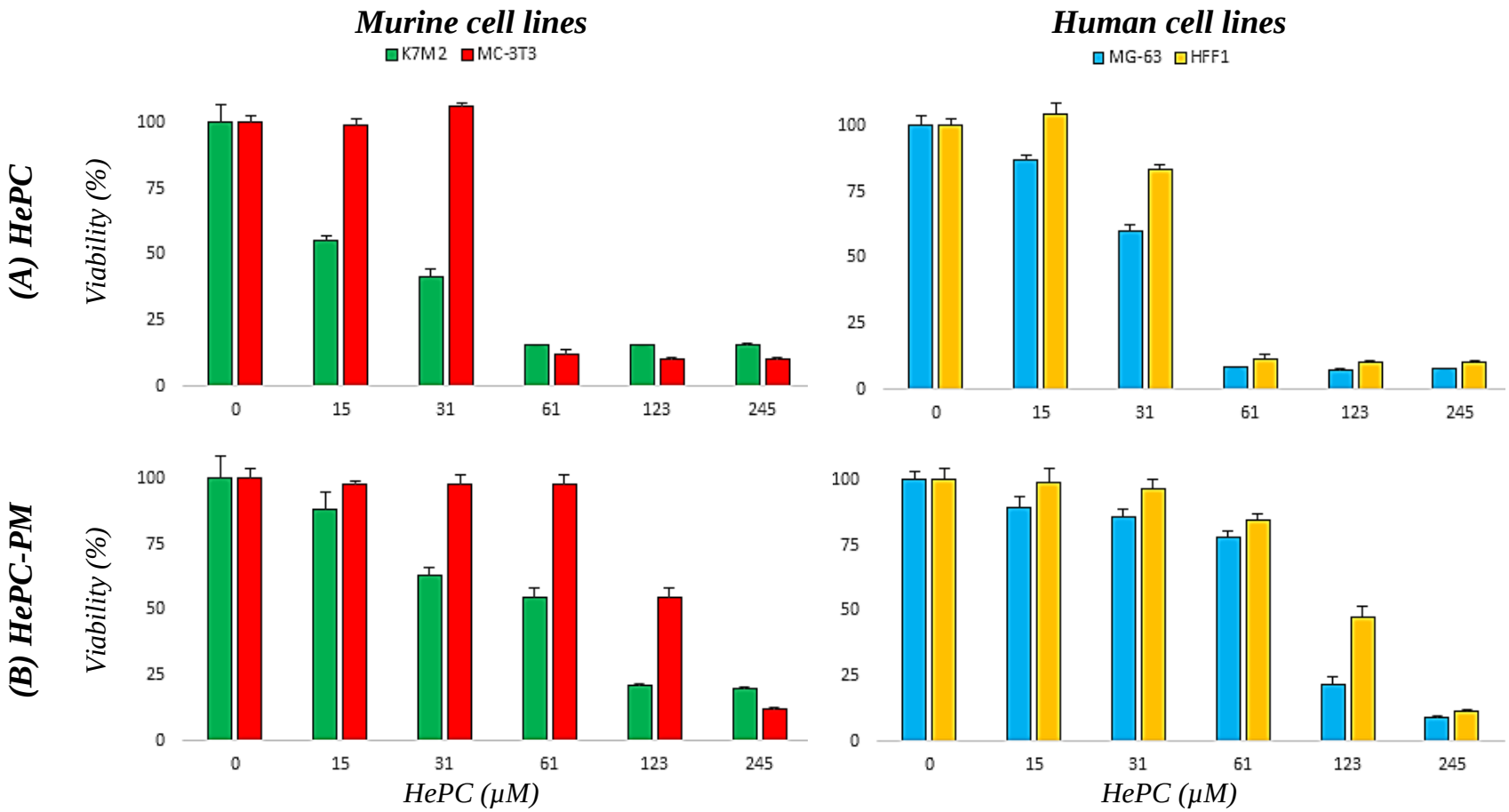

Figure 2. Selective cytotoxicity of HePC-PM in osteosarcoma cells. *Cytotoxity effect after HePC treatment, free* ***(A)*** *or loaded into polymeric micelles* ***(B)****, against osteosarcoma (MG-63 and K7M2) and non-tumoral cell lines (HFF1 and MC-3T3). Cell lines were cultured in α-MEM supplemented with 5% FBS.*

1

Whereas the tumor cells were very sensitive to the drug, the non-tumor cells were less sensitive when treated with equimolar concentrations of HePC **(Figure 2).** However, the drug was also active against human stromal osteoblast cells (HCC1) **(Data not shown)**. Interestingly, incorporation of HePC into PM seems to protect cell lines against HePC cytotoxicity. For example, at 61 µM free HePC was very toxic against both murine tumor (K7M2) and healthy (MC3T3-E1) cells **(Figure 2A)**, but for the same drug concentration in HePC-PM we observed selective cytotoxicity to tumor cells (**Figure 2B)**. The same profile of selective toxicity was observed for human cells but at a higher drug concentration (123 µM) **(Figure 2A and 2B)**. Therefore, HePC encapsulation protects cells from cytotoxicity and this protective effect is more pronounced in the non-transformed cell lines.

3.3. Miltefosine inhibits osteosarcoma cell proliferation

In vitro antitumor activity was evaluated by *IncuCyte* live-cell imaging. Anti-proliferation and cytotoxicity of HePC against K7M2 and MG-63 cells were confirmed. HePC exhibited significant anti-proliferative effects against MG-63 and K7M2 cells cultured in α-MEM supplemented with 5% FBS as shown in **Figure 3**.

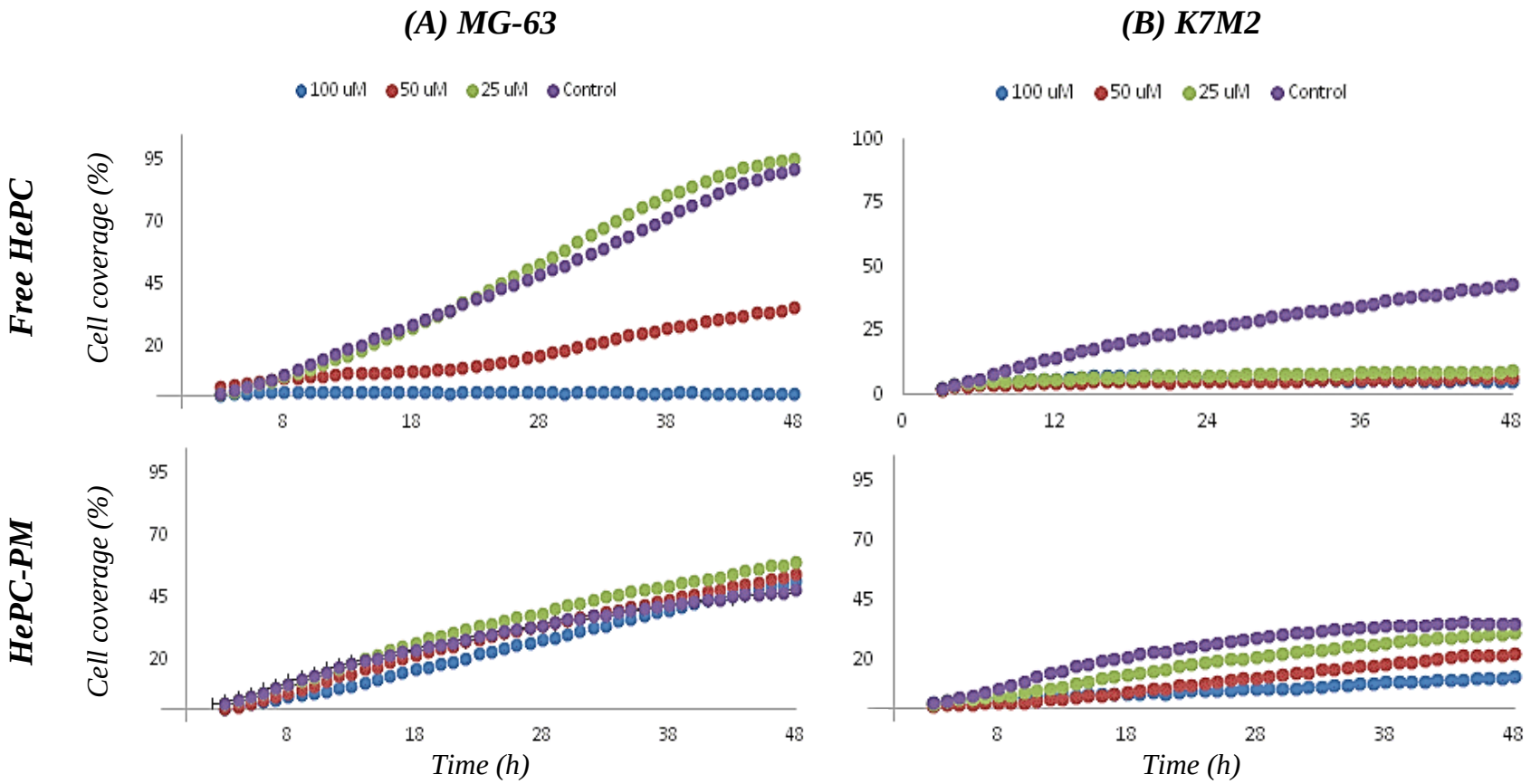

Figure 3. HePC affects proliferation of osteosarcoma cells. *Proliferation of human MG-G3* ***(A)*** *and murine K7M2* ***(B)*** *cell lines after HePC treatment, free* ***(upper panel)*** *or loaded into polymeric micelles* ***(lower panel)****. Dot graphs represent the percentage of wound coverage of over time. Cell were cultured in α-MEM supplemented with 5% FBS.*

1

Time-lapse imaging of untreated cells (control) showed standard growth kinetics that reached approximately 100% cell confluence by 48 h **(Figure 3A)**. The same profile was observed with 25 µM HePC, whereas treatment with 50 µM efficiently suppressed cell proliferation, with a 70% reduction in confluence by 48 h. HePC at 100 µM completely inhibited cell growth **(Figure 3A).**

Proliferation of the K7M2 cells cultured in α-MEM with 5% FBS was reduced, reaching only 50% of confluence within 48 h **(Figure 3B)**. Nonetheless, these cells were more sensitive to HePC than MG-63 cells, with significantly suppressed cell proliferation even at the lowest concentration of 25 µM HePC **(Figure 3B)**. For all cell lines, the HePC incorporation into PM seems to play a protective effect, since the cells show a proliferation even at high concentrations as 100 µM (**Figure 3A and 3B)**.

3.4. Miltefosine inhibits osteosarcoma cell migration

To check the effect of HePC over cell migration, real-time cytotoxicity experiments were carried out against both MG-63 and K7M2 cells cultured in α-MEM without FBS supplementation as presented in **Figure 4.**

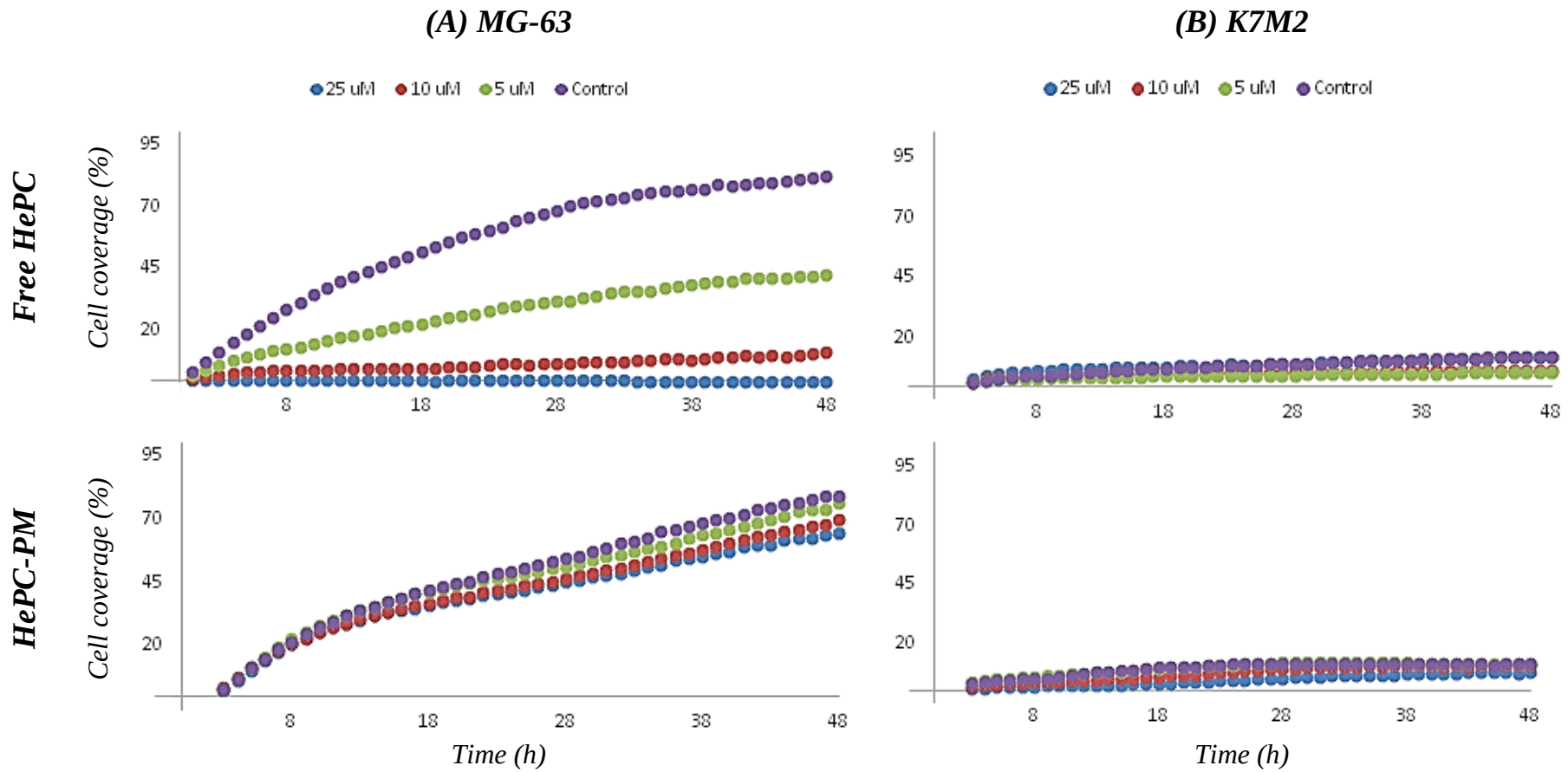

Figure. 4. HePC affects migration of osteosarcoma cells. *Migration of human MG-G3* ***(A)*** *and murine K7M2* ***(B)*** *cell lines after HePC treatment, free* ***(upper panel)*** *or loaded into polymeric micelles* ***(lower panel)****. Dot graphs represent the percentage of wound coverage of over time. Cell were cultured in α-MEM without FBS supplementation.*

1

Interesting e for our surprise, K7M2 cells did not migrate in the culture medium without FBS supplementation, not even in the control condition **(Figure 4B)**. In contrast, MG-63 cells reached a plateau of 70% confluence up to 48 h **(Figure 4A)**. HePC performed excellent dose-dependent inhibition of cell migration even at the lowest concentration of 5 µM **(Figure 4A)**. On the other hand, data for HePC-PM shows that the drug incorporation into PM prevented it effect on MG-63 cell migration.

Comparatively, both proliferation **(Figure 3)** and migration **(Figure 4)** assays, at the same HePC concentration (25 µM), clearly show that MG-63 cells were more affected by HePC in the medium without FBS **(Figure 4)** than when supplemented with 5% FBS **(Figure 3).**

3.5. Miltefosine promotes apoptosis in osteosarcoma cells

To investigate whether the effects of HePC on viability could also be caused by independent effects on cell death, multiple markers for cell apoptosis were tested including Hoechst staining of nuclear DNA and Western blots to detect cleaved caspase-3 as shown in **Figure 5.**

Phase-contrast images indicated that HePC increased the appearance of apoptotic-like cell bodies **(Figure 5A)**, and this was confirmed by nuclear staining showing increased DNA condensation and fragmentation **(Figure 5B).** Western blot analysis of cleaved caspase-3 which is a marker of apoptosis also demonstrated that HePC induced apoptosis in OS cells **(Figure 5C)**. Taken together, the results strongly suggest that the mechanism of action of HePC on viability is likely due to effects on both proliferation and cell apoptosis in a dose-dependent manner.

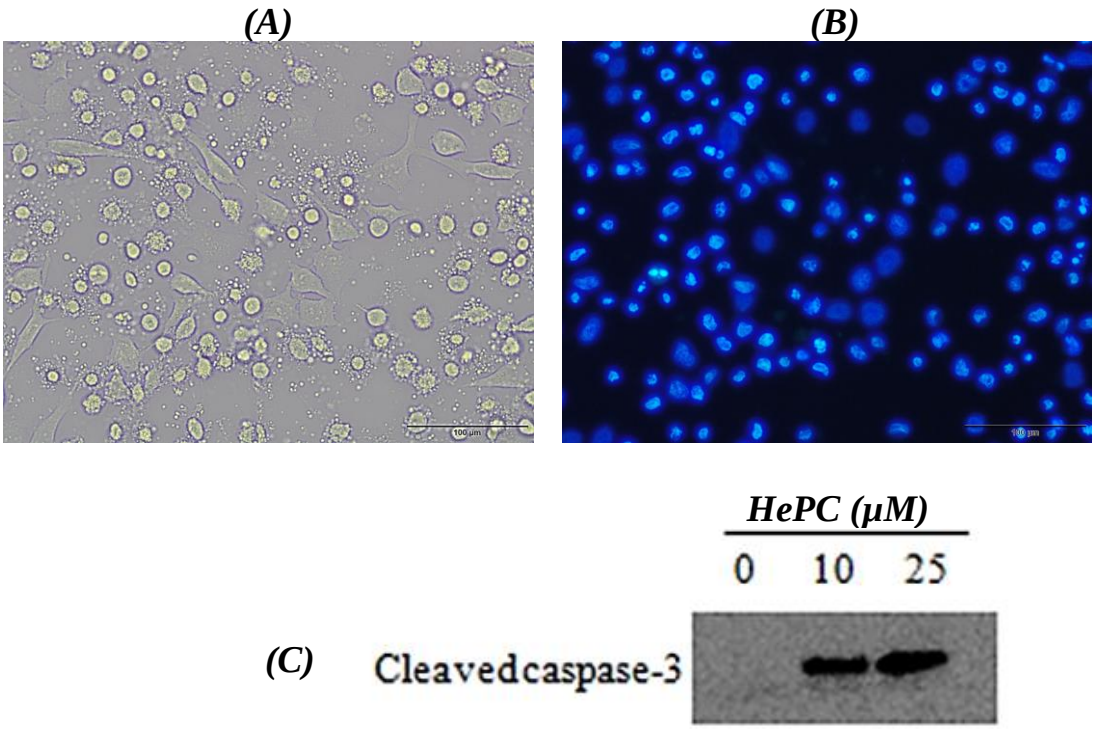

Figure. 5. HePC promotes apoptosis in osteosarcoma cells. *Representative images of phase contrast* ***(A)*** *and nuclear DNA staining by Hoechst dye* ***(B)*** *showing K7M2 cells treated with 10 μM miltefosine. Notice the apoptotic bodies' formation and DNA condensation and fragmentation. Scale bar, 100 μm.* ***(C)*** *Western blotting of K7M2 cells lysates showing that miltefosine induce cleavage of caspase-3 after 3 h treatment.*

1

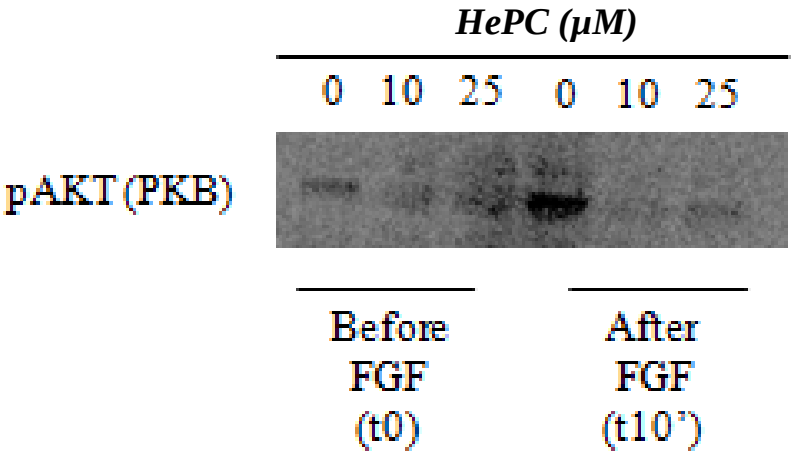

Figure. 6. HePC blocks Akt/PKB activation in K7M2 osteosarcoma cells*. Western blotting of K7M2 cells lysates showing that HePC blocks Akt/PKB phosphorylation after 10 min of FGF2 induction.*

2

3.6. Miltefosine blocks Akt/PKB activation in K7M2 osteosarcoma cells

Since the Akt/PKB pathway is known to promote cell survival, we next examined the effect of HePC on basal and cytokine-induced Akt/PKB activation in cultured K7M2 cells. These cells were cultured with or without HePC (10-25 μM) followed by FGF2 (10 ng/mL) stimulation for 10 min. Total cell lysates were prepared and subjected to immunoblotting using specific antibodies and the results are presented in **Figure 6.**

Western blot analysis demonstrated that HePC as low as 10 μM clearly blocked basal Akt/PKB phosphorylation in K7M2 osteosarcoma cells, as well as following exogenous growth factor (FGF2) stimulation **(Figure 6)**. These results suggest that HePC reduces cell viability via blocking this pro-survival signaling pathway.

3.7. Pluronic polymeric micelles promote intracellular drug delivery

The encapsulation of HePC in Pluronic F127 polymeric micelles (PM) showed marked effects on cell viability, proliferation and migration. To confirm that PM are incorporating efficiently into cells, we incorporated TRITC-phalloidin into PM and investigated their ability to penetrate inside both MG-63 and HCC1 cells as seen in **Figure 7.**

As shown in **Figure 7B**, significant uptake of the TRITC probe was observed when incorporated into PM, whereas the free probe did not significantly penetrate into the cells **(Figure 7A)**. Interestingly, it also appeared that tumor cells (MG-63) were able to incorporate greater levels of TRITC-phalloidin than non-transformed cells (HCC1), showing promise at being able to deliver drug compounds specifically to cancer cells.

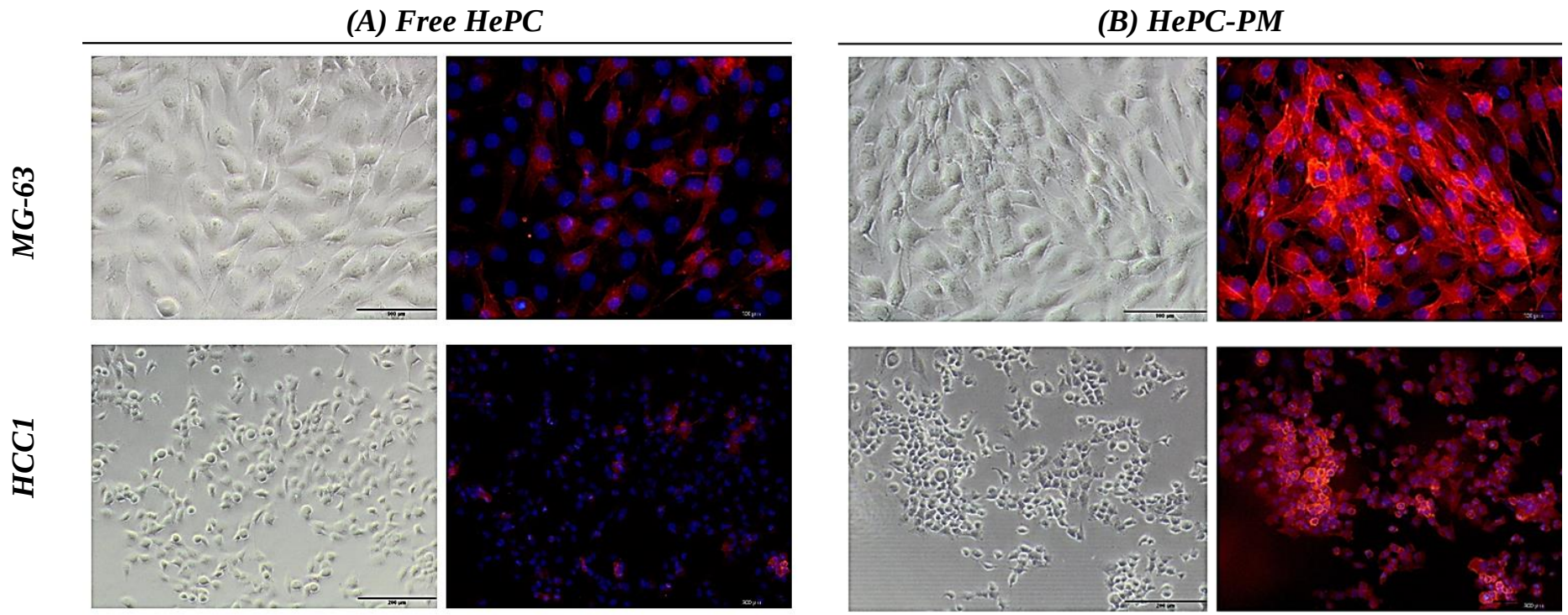

Figure. 7. Pluronic F127 polymeric micelles show efficient intracellular drug delivery. *Representative images of phase contrast, nuclear DNA staining (Hoechst, blue) and actin staining (TRITC-phalloidin, red) of MG-63 osteosarcoma and HCC1 osteoblastic cells treated for 18 h with free TRITC-phalloidin* ***(A)*** *or TRITC-phalloidin loaded into polymeric micelles (****B****). Scale bar, 100 μm.*

1

4. Discussion

Given our results findings, HePC holds promise for the OS treatment. In cultured OS cells, we demonstrate that HePC decrease cell viability, reduce both cell migration and proliferation, blocks Akt/PKB phosphorylation while inducing pro-apoptotic caspase-3 activation, probably inducing the cell to apoptotic death.

Here, for the first time we show the cytotoxic effect of HePC against human (MG-G3, U2OS and SAOS-2) and murine (K7M2 and PI.15) OS cells. HePC induced a remarkable cytotoxic activity in OS cells when used at the micromolar range (15-50 µM), which is low than median plasma concentration (~75 µM) of patients treated orally with 50 mg HePC/day for 28 days (Dorlo *et al*., 2008). Moreover, OS cancer cells seem to be more sensitive to HePC than the non-transformed cells probably due to their higher content in lipid rafts that mediate the APLs uptake (González-Fernándeza *et al*., 2015; González-Fernándeza *et al*., 2018).

Interesting, the drug was also active against healthy human osteoblastic cells (HCC1), however these cells were immortalized with Simian virus 40 (SV40 T-antigen). This result is in agreement with Mollinedo *et al*. (1997), according to which no-transformed 3T3 cells were resistant to the apoptotic action of edelfosine and incorporated only small amounts of this drug, while upon transformation with SV40 T-antigen, these cells became sensitive and incorporated significant amounts of this drug. These data indicate that this class of drugs is more specific for tumor cells and that both cellular uptake and apoptosis are dependent on the malignant state of the cells (Kostadinova *et al*., 2015).

HePC is a member of a new class of antitumor drugs, which potently inhibits protein kinases. The protein kinase B (PKB) better known as Akt is a serine/threonine-specific protein kinase which acts as mediator via PI3K/Akt/mTOR pathway in many biological processes, *e.g.* transcription, glucose metabolism, cell growth and differentiation, neo-angiogenesis and apoptosis (Bhutani, Sheikh and Niazi, 2013; Nitulescu *et al*., 2016). Targeting PI3K/Akt/mTOR signalling may be a promising therapeutic approach for treating OS (Ding *et al*., 2016). Akt plays a central role in many types of cancer and has been validated as a therapeutic target (Nitulescu *et al*., 2016). This pathway is frequently over-expressed or over-activated in osteosarcoma, providing a strong rationale to target it in cancer therapy. Fewer Akt-targeting agents have entered in clinical development, among these Akt-inhibiting compounds we highlight the ones from APL class including HePC, edelfosine (1-O-octadecyl-2-O-methyl-rac-glycero-3-phosphocholine, ET-18-OCH3) ilmofosine (BM 41.440), perifosine (D-21266), erucylphosphocholine (ErPC) and erufosine (ErPC3, erucylphosphohomocholine) (Bhutani, Sheikh and Niazi, 2013; Nitulescu *et al*., 2016). Nonetheless, only HePC has already completed a phase III trial and so far is the first Akt-inhibitor approved by the FDA (Porta, Paglino and Mosca 2014).

Inhibition of the Akt/PKB pathway at several levels using Akt inhibitors, such as HePC, triggers both *in vitro* and *in vivo* cell cytotoxicity. Therefore, the Akt/PKB pathway represents an important target for novel treatments in OS cells. In this way, a number of recent studies have confirmed the antitumor activity of APLs for treatment of bone tumours. Yao *et al*., 2013 reported that perifosine induces cell apoptosis and growth inhibition in OS cells, blocking Akt/mTOR complex 1 (mTORC1) signaling, while promoting caspase-3, c-Jun N-terminal

kinases (JNK), and p53 activation. Perifosine also inhibits survivin expression probably by disrupting its association with heat shock protein-90 (HSP90).

Clinically relevant APLs were tested against Ewing's sarcoma (ES). Bonilla *et al*., 2015 demonstrate the *in vitro* capacity of edelfosine, perifosine, erucylphosphocholine and miltefosine to promote apoptosis in ES cells. The most active edelfosine accumulated in the endoplasmic reticulum and triggered a stress response leading to caspase-dependent apoptosis. This apoptotic response involved mitochondrial-mediated processes with cytochrome c release, caspase-9 activation and generation of reactive oxygen species. Edelfosine-induced apoptosis was also dependent on sustained c-Jun NH2-terminal kinase activation. Peroral administration of edelfosine also showed a potent *in vivo* antitumor activity in an ES xenograft animal model.

Edelfosine showed higher efficacy treating both primary and metastatic OS cells. This efficacy was improved when edelfosine was administered in lipid based nanoparticles (González-Fernándeza *et al*., 2015). Recently, the same group demonstrated the efficacy of edelfosine, whether free or encapsulated into lipid nanoparticles, against MNNG-HOS (HOS) and 143B OS cells. Both treatments decreased the growth of OS cells *in vitro* and slowed down the primary tumor growth in two orthotopic OS murine models (González-Fernándeza *et al*., 2018). Additionally, co-treatment of doxorubicin edelfosine-lipid nanoparticles was effective acting synergistically against drug-resistant OS cells (González-Fernándeza *et al*., 2017).

In fact, APLs emerge as a new antitumor class that could be potential agents against OS. HePC has already been evaluated as a peroral therapy in clinical trials against soft tissue sarcomas (Verweij *et al*., 1993) and advanced

colorectal cancer (Rieche and Sindermann, 1993); however, the doses required for the antitumor effects were too toxic, hampering the clinical utilization of HePC due to hemolytic potential as well gastrointestinal toxicity. Thus, their use in cancer therapy is restricted to topical application for cutaneous breast cancer (Leonard *et al*, 2001; Nitulescu *et al*., 2016).

In this sense, our research group has been combining efforts to reduce the toxic effects of HePC by incorporating into polymeric micelles (PM) composed by Pluronic F127. Previously, we demonstrated a significant reduction in the hemolytic potential of HePC when loaded into PM **(Chapter 1)**, preserving its *in vitro* cytotoxicity against cervical tumor HeLa cells (Valenzuela-Oses, García, Feitosa, *et al*., 2017, **Appendix A**).

Here we have expanded the application of HePC-PM under several normal bone cell lines and OS cell lines and observed that incorporation of HePC into PM protect non-specifically the cells from drug toxicity, probably reducing the interaction between HePC and cell membrane. These results are in agreement with previous findings that demonstrate that encapsulation of edelfosine into lipid-nanoparticles provide a potent protective effect against APL toxicity (Lasa-Saracíbar *et al*., 2014). Additionally, we also note that the PM is able to intracellular drug delivery, preferably to tumor cells rather than healthy cells. This opens up an opportunity for the use of HePC for the treatment of OS with reduced collateral effects associated with non-specific lysis of cell membranes.

5. Conclusion

These results together support that HePC, as well as other alkylphospholipids, loaded into Pluronic F127-based polymeric micelles provide a potential alternative for selectively intracellular anti-osteosarcoma therapy.

Acknowledgements

This study was financed in part by the Coordination of Superior Level Staff Improvement (CAPES/Brazil, finance code 001), the State of São Paulo Research Foundation (FAPESP/Brazil, processes 2014/01983-0) and the National Council for Scientific and Technological Development (CNPq/Brazil). The authors wish to thank Basf Company (Brazil) for kindly supplying all Pluronic copolymers. V.A.F is grateful to the PDSE/CAPES for his internship at King's College London (KCL). The authors are also in debt with Susmitha Rao for her excellent technical advice.

References

ARNDT et al. Alkylphospholipid liposomes: Preparation, properties and use in cancer research. Drugs of Today 34, 83-96 (1998).

ARNDT et al. Antineoplastic activity of sterically stabilized alkylphosphocholine liposomes in human breast carcinomas. Breast Cancer Research and Treatment 43, 237-246 (1997).

ARNDT et al. Liposomal bleomycin: Increased therapeutic activity and decreased pulmonary toxicity in mice. Drug Delivery 8, 1-7 (2001).

ARNDT et al. Pharmacokinetics of sterically stabilized hexadecylphosphocholine liposomes versus conventional liposomes and free hexadecylphosphocholine in tumor-free and human breast carcinoma bearing mice. Breast Cancer Research and Treatment 58, 71-80 (1999).

BHUTANI, SHEIKH and NIAZI. Akt inhibitors: mechanism of action and implications for anticancer therapeutics. Infectious Agents and Cancer20138:49

BOCK et al. A novel assay to determine the hemolytic-activity of drugs incorporated in colloidal carrier systems. Pharmaceutical Research 11, 589-591 (1994).

BONILLA, X. et al. Endoplasmic reticulum targeting in Ewing's sarcoma by the alkylphospholipid analog edelfosine. Oncotarget, v. 6, n. 16, p. 14596-14613, Jun 2015. ISSN 1949-2553. Available at: < <Go to ISI>://WOS:000359010000060 >.

DAS et al., Miltefosine loaded albumin microparticles for treatment of visceral leishmaniasis: formulation development and in vitro evaluation. Polymers for Advanced Technologies 22, 172-179 (2011).

DING et al., mTOR: An attractive therapeutic target for osteosarcoma? Oncotarget. 2016 Aug 2; 7(31): 50805–50813.

DORLO et al., Pharmacokinetics of Miltefosine in Old World Cutaneous Leishmaniasis Patients. ANTIMICROBIAL AGENTS AND CHEMOTHERAPY, Aug. 2008, p. 2855–2860.

EUE et al. Differential uptake of conventional and polyethylene glycol modified-alkylphosphocholine-liposomes by J 774A.1 murine macrophages. Drug Delivery 5, 265-273 (1998).

EVOLA, F. R. et al. Biomarkers of Osteosarcoma, Chondrosarcoma, and Ewing Sarcoma. Frontiers in Pharmacology, v. 8, p. 14, Apr 2017. ISSN 1663-9812. Available at: < <Go to ISI>://WOS:000398655100001 >.

FICHTNER et al., Antineoplastic activity of allkylphosphocholines (apc) in human breast carcinomas in-vivo and in-vitro - use of liposomes. Breast Cancer Research and Treatment 32, 269-279 (1994).

GONZALEZ-FERNANDEZ, Y. et al. Doxorubicin and edelfosine lipid nanoparticles are effective acting synergistically against drug-resistant osteosarcoma cancer cells. Cancer Letters, v. 388, p. 262-268, Mar 2017. ISSN 0304-3835. Available at: < <Go to ISI>://WOS:000395959800026 >.

KAUFMANN-KOLLE et al. Liposomal alkylphosphocholines. Drugs of Today 34, 107-115 (1998).

KAUFMANNKOLLE et al., Pharmacokinetic behavior and antineoplastic activity of liposomalhexadecylphosphocholine. Cancer Chemotherapy and Pharmacology 34, 393-398 (1994).

KOSTADINOVA et al. Antitumor Lipids-Structure, Functions, and Medical Applications. Adv Protein Chem Struct Biol. 2015;101:27-66. doi: 10. 1016/bs.apcsb.2015.08.001

KUMAR et al., Development of PLGA-PEG encapsulated miltefosine based drug delivery system against visceral leishmaniasis. Materials Science & Engineering C-Materials for Biological Applications 59, 748-753 (2016).

LASA-SARACÍBAR et al. Lipid nanoparticles protect from edelfosine toxicity in vivo. International Journal of Pharmaceutics 474 (2014) 1–5

LINDNER et al., Dual role of hexadecylphosphocholine (miltefosine) in thermosensitive liposomes: Active ingredient and mediator of drug release. Journal of Controlled Release 125, 112-120 (2008).

LINDSEY, B. A.; MARKEL, J. E.; KLEINERMAN, E. S. Osteosarcoma Overview. Rheumatology and Therapy, v. 4, n. 1, p. 25-43, Jun 2017. ISSN 2198-6584. Available at: < <Go to ISI>://WOS:000406302300002 >.

MOLLINEDO et al. (1997). Selective induction of apoptosis in cancer cells by the ether lipid ET-18-OCH3 (Edelfosine): Molecular structure requirements, cellular uptake, and protection by Bcl-2 and Bcl-X(L). Cancer Research, 57(7), 1320–1328.

MOMENI et al., Development of liposomes loaded with anti-leishmanial drugs for the treatment of cutaneous leishmaniasis. Journal of Liposome Research 23, 134-144 (2013).

MOVASSAGHIAN, MERKEL, TORCHILIN, Applications of polymer micelles for imaging and drug delivery. Wiley Interdisciplinary Reviews-Nanomedicine and Nanobiotechnology 7, 691-707 (2015).

MRAVLJAK et al. Synthesis and biological evaluation of spin-labeled alkylphospholipid analogs. Journal of Medicinal Chemistry 48, 6393-6399 (2005).

NITULESCU et al. Akt inhibitors in cancer treatment: The long journey from drug discovery to clinical use (Review). INTERNATIONAL JOURNAL OF ONCOLOGY 48: 869-885, 2016.

NITULESCU et al., 2016 Akt inhibitors in cancer treatment: The long journey from drug discovery to clinical use. Int J Oncol. 2016 Mar; 48(3): 869–885.

PACHIONI, J.G. et al. Alkylphospholipids—a promising class of chemotherapeutic agents with a broad pharmacological spectrum J. Pharm. Pharm. Sci., 16, 2013, pp. 742-759

PAPAGIANNAROS et al. Antileishmanial and trypanocidal activities of new miltefosine liposomal formulations. Biomedicine & Pharmacotherapy 59, 545-550 (2005a).

PAPAGIANNAROS et al. Doxorubicin-PAMAM dendrimer complex attached to liposomes: Cytotoxic studies against human cancer cell lines. International Journal of Pharmaceutics 302, 29-38 (2005b).

PHAM et al. Interactions of antileishmanial drugs with monolayers of lipids used in the development of amphotericin B-miltefosine-loaded nanocochleates. Colloids and Surfaces B-Biointerfaces 106, 224-233 (2013).

PORTA, PAGLINO and MOSCA. Targeting PI3K/Akt/mTOR signaling in cancer. Front. Oncol., 14 April 2014 | https://doi.org/10.3389/fonc.2014.00064

RATZ et al. Separation and quantitation of alkylphosphocholines and analogues of different liposome formulations by HPTLC. Journal of Aoac International 84, 1277-1282 (2001).

SÁ and RANGEL-YAGUI. Molecular Determinants for the Binding Mode of Alkylphosphocholines in the C2 Domain of PKCα. Molecular Informatics, v. 34, p. 84-96, 2015.

SÁ et al., Understanding Miltefosine-Membrane Interactions Using Molecular Dynamics Simulations. Langmuir, v. 31, p. 4503-4512, 2015.

SARAF, A. J.; FENGER, J. M.; ROBERTS, R. D. Osteosarcoma: Accelerating Progress Makes for a Hopeful Future. Frontiers in Oncology, v. 8, Jan 2018. ISSN 2234-943X. Available at: < <Go to ISI>://WOS:000423359000001 >.

THAKUR et al. Proapoptotic miltefosine nanovesicles show synergism with paclitaxel: Implications for glioblastoma multiforme therapy. Cancer Letters 334, 274-283 (2013).

VALENZUELA-OSES JK, GARCÍA MC, FEITOSA VA, PACHIONI-VASCONCELOS JA, GOMES-FILHO SM, LOURENÇO FR, CERIZE NNP, BASSÈRES DS, RANGEL-YAGUI CO. Development and characterization of miltefosine-loaded polymeric micelles for cancer treatment. Mater Sci Eng C Mater Biol Appl. 2017 Dec 1;81:327-333. doi: 10.1016/j.msec.2017.07.040. Epub 2017 Jul 29.

VERWEIJ J, et al. Phase II study of miltefosine (hexadecylphosphocholine) in advanced soft tissue sarcomas of the adult - an EORTC Soft Tissue and Bone Sarcoma Group Study. Eur J Cancer. 1993;29A:208–209. doi: 10.1016/0959-8049(93)90177-H.

WANG et al. Vesicle-formation of hexadecyl phosphatidyl choline released from epsilon-caprolactone electrospun fibrous mats: preparation and characterization. Colloid and Polymer Science 291, 2475-2479 (2013).

YAO et al., Perifosine Induces Cell Apoptosis in Human Osteosarcoma Cells: New Implication for Osteosarcoma Therapy? Cell Biochem Biophys (2013) 65:217–227 DOI 10.1007/s12013-012-9423-5.

YAO, C. et al. Perifosine Induces Cell Apoptosis in Human Osteosarcoma Cells: New Implication for Osteosarcoma Therapy? Cell Biochemistry and Biophysics, v. 65, n. 2, p. 217-227, Mar 2013. ISSN 1085-9195. Available at: < <Go to ISI>://WOS:000315161000016 >.

ZEISIG et al. Cytotoxic effects of alkylphosphocholines or alkylphosphocholine-liposomes and macrophages on tumor-cells. Anticancer Research 14, 1785-1789 (1994).

ZEISIG et al. Effect of sterical stabilization on macrophage uptake in vitro and on thickness of the fixed aqueous layer of liposomes made from alkylphosphocholines. Biochimica et Biophysica Acta-Biomembranes 1285, 237-245 (1996a).

ZEISIG et al. Lipoplexes with alkylphospholipid as new helper lipid for efficient in vitro and in vivo gene transfer in tumor therapy. Cancer Gene Therapy 10, 302-311 (2003).

ZEISIG et al. Preparation and properties of sterically stabilized hexadecylphosphocholine (miltefosine)-liposomes and influence of this modification on macrophage activation. Biochimica et Biophysica Acta-Biomembranes 1283, 177-184 (1996b).

ZEISIG et al., Antineoplastic activity invitro of free and liposomal alkylphosphocholines. Anti-Cancer Drugs 4, 57-64 (1993).

ZEISIG, R et al. Antitumor effects of alkylphosphocholines in different murine tumor-models - use of liposomal preparations. Anti-Cancer Drugs 2, 411-417 (1991).

ZHUKOVA et al. Hemolytic properties of miltefosine in liposomes of various lipid compositions. Pharmaceutical Chemistry Journal 44, 507-509 (2010).

.

Final considerations

We have studied the incorporation of the miltefosine (HePC), amphiphilic antitumor drug, into Pluronic F127 polymeric micelles (PM). Our data support that the composition of Pluronic copolymers influence the aggregation state of amphiphilic drugs; also Pluronic F127 concentration has a pronounced effect on the HePC hemolytic profile and that the amount of HePC-loaded into polymeric micelles might be adjusted by varying the concentration of Pluronic F127. Moreover, SAXS data indicated that Pluronic F127 concentration plays an important role on the micelle structure. *In vitro* hemolysis results indicated that these colloidal nanostructures can protect the erythrocytes from HePC toxicity and, by achieving this level of hemolysis protection, a promising application is on the view for the intravenously use of HePC. We also showed that HePC encapsulation into PM prevented mucosal irritancy, opening the possibility of its peroral administration in higher doses. In addition, HePC-PM presented preferential cytotoxicity against HeLa carcinoma and osteosarcomas cell lines in comparison to normal cell lines, suggesting a differential uptake of these nanostructures by malignant cells following by intracellular delivery of cargo drug and inducing apoptosis cell death. Taken together, the results presented in this thesis, demonstrate that HePC encapsulation into PM reduces drug side effects and increases selective cytotoxicity against tumor cells providing a potential alternative for cancer therapy.

Appendix A: Full paper: "Development and characterization of miltefosine-loaded polymeric micelles for cancer treatment", published at Journal of Materials Science and Engineering: C

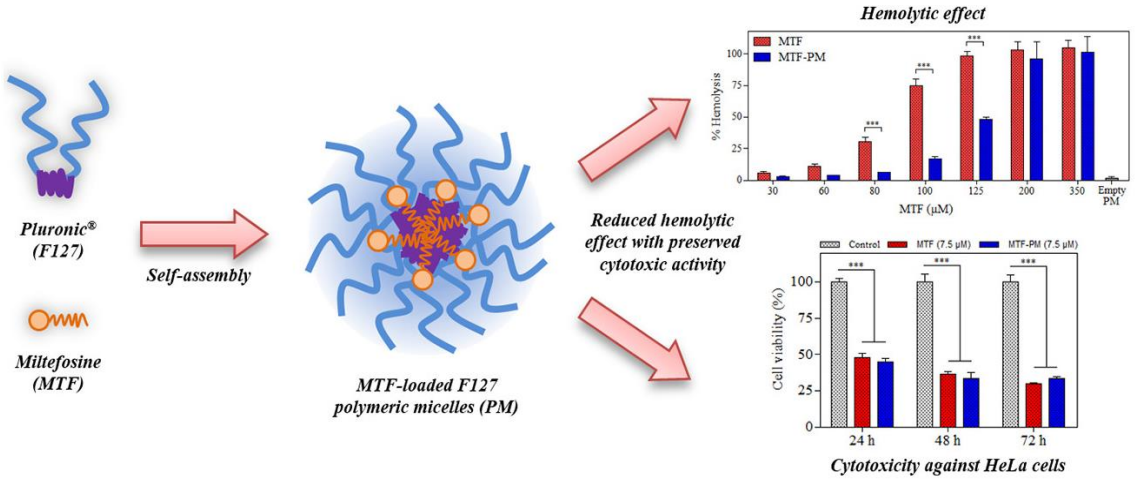

Highlights

- We developed a formulation of miltefosine-loaded Pluronic F127 polymeric micelles.
- Miltefosine-loaded polymeric micelles significantly reduce drug hemolytic effect.
- Miltefosine-loaded polymeric micelles preserve the drug cytotoxic activity against cancer cell lines.

Materials Science & Engineering C 81 (2017) 327–333

Contents lists available at ScienceDirect

Materials Science & Engineering C

journal homepage: www.elsevier.com/locate/msec

Development and characterization of miltefosine-loaded polymeric micelles for cancer treatment

Johanna K. Valenzuela-Oses[a,1], Mónica C. García[b,1], Valker A. Feitosa[a,c,1], Juliana A. Pachioni-Vasconcelos[a], Sandro M. Gomes-Filho[c], Felipe R. Lourenço[d], Natalia N.P. Cerize[e], Daniela S. Bassères[c], Carlota O. Rangel-Yagui[a,*]

[a] Department of Biochemical and Pharmaceutical Technology, School of Pharmaceutical Sciences, University of São Paulo, Brazil
[b] Unidad de Investigación y Desarrollo en Tecnología Farmacéutica (UNITEFA), CONICET and Departamento de Farmacia, Facultad de Ciencias Químicas, Universidad Nacional de Córdoba, Ciudad Universitaria, X5000HUA Córdoba, Argentina
[c] Department of Biochemistry, Chemistry Institute, University of São Paulo, Brazil
[d] Department of Pharmacy, School of Pharmaceutical Sciences, University of São Paulo, Brazil
[e] Bionanomanufacturing Center, Institute for Technological Research (IPT), São Paulo, Brazil

ARTICLE INFO

Keywords:
Alkylphosphocholines
Miltefosine
Block-copolymer
Polymeric micelles
Cancer therapy
Hemolytic potential

ABSTRACT

Miltefosine presents antineoplastic activity but high hemolytic potential. Its use in cancer has been limited to treating cutaneous metastasis of breast cancer. To decrease hemolytic potential, we developed a formulation of miltefosine-loaded polymeric micelles (PM) of the copolymer Pluronic-F127. A central composite design was applied and the analysis of variance showed that the optimum level of hydrodynamic diameter and polydispersity index predicted by the model and experimentally confirmed were 29 nm and 0.105, respectively. Thermal analyses confirmed that miltefosine was molecularly dispersed within PM. Pluronic-F127 PM with miltefosine 80 μM presented a significant reduction of hemolytic effect (80%, $p < 0.05$) in comparison to free drug. *In vitro* assays against HeLa carcinoma cells demonstrated similar cytotoxicity to free miltefosine and PM. Our results suggest that, by lowering hemolytic potential, miltefosine-loaded Pluronic-F127 PM a promising alternative to broaden this drug use in cancer therapy, as well as of other alkylphosphocholines.

1. Introduction

Miltefosine (MTF) is an alkylphospholipid drug (APL) used orally for the treatment of leishmaniasis and topically to treat skin metastases of breast cancer [1]. This drug class also has potential to treat fungal and bacterial infections, as well as Chagas' disease [2]. Unlike other DNA-targeting anticancer agents, APL drugs are involved in phospholipid metabolism, non-vesicular cholesterol transport and homeostasis, biochemical survival pathways (for example, Akt-mTOR pathway), and interaction with membrane signal transduction proteins, such as phospholipase C, phospholipase D and protein kinase C. However, the precise mechanism of action has not been fully elucidated yet [3].

Miltefosine presents potent antitumor activity *in vitro* [4] and in experimental animal models. Nevertheless, clinical use is limited due to side effects associated with its amphiphilic nature [5–7]. More specifically, MTF is highly hemolytic when administered intravenously and orally it was associated with cumulative gastrointestinal toxicity. These side effects, correlated to the drug aggregation into micelles, have limited the maximum daily dose by these routes (maximum tolerated dose: 200 mg/day), preventing *in vivo* observation of antiproliferative effects [6–8]. One strategy to improve the efficacy and safety of oral and/or intravenous cancer treatment with MTF refers to nanotechnology. More specifically, MTF incorporation in nanocarriers may prevent its self-aggregation into micelles and, therefore, the above-mentioned side effects.

In the last decade, nanocarriers have been widely used in anticancer systems/formulations to avoid drug contact with healthy tissues and allow drug accumulation in tumor cells [8]. The incorporation of drugs in nanocarriers enhances solubility and blood half-life, promoting controlled and site-specific release. In addition, combined therapy can be achieved by incorporation of more than one drug [9–11]. The first application of nanocarriers for MTF delivery dates back to 1991 when it

* Corresponding author.
E-mail addresses: jkvalenzuelao@gmail.com (J.K. Valenzuela-Oses), mgarcia@fcq.unc.edu.ar (M.C. García), valker@usp.br (V.A. Feitosa), julianapachioni@yahoo.com.br (J.A. Pachioni-Vasconcelos), sandromascena@gmail.com (S.M. Gomes-Filho), feliperl@usp.br (F.R. Lourenço), ncerize@ipt.br (N.N.P. Cerize), basseres@iq.usp.br (D.S. Bassères), corangel@usp.br (C.O. Rangel-Yagui).
[1] Authors contributed equally to this work.

http://dx.doi.org/10.1016/j.msec.2017.07.040
Received 2 June 2017; Received in revised form 13 July 2017; Accepted 27 July 2017
Available online 29 July 2017

was incorporated in liposomes [12]. Thereafter, a series of formulations based on liposomes, pegylated or not, were developed with phospholipids and MTF as bilayer forming constituents [7,13–15]. However, poor stability of liposomal delivery systems limits their use in drug delivery; few liposome-based marketed products are available regardless of extensive and long research in this area [2]. On the other hand, polymeric micelles are an interesting alternative to prevent MTF side effects and, to the best of our knowledge, there are no previous reports using polymeric micelles for the delivery of MTF.

Polymeric micelles (PM) are unique core-shell nanostructures formed by amphiphilic copolymers aggregation that can incorporate poorly soluble drugs [16–20]. Amphiphilic block copolymers have the ability to self-assemble into PM in aqueous media and they have been widely studied in the field of nanomedicine, biomedicine and pharmacy [20–22]. The PM represent thermodynamic aggregations of multi amphiphilic macromolecules above their critical micelle concentration (CMC) [23].

An important property of PM is their size, which usually ranges from 10 to 80 nm, thereby closing the gap between individual macromolecule drug carriers (albumin, dextran, and antibodies) with sizes bellow 10 nm; and nanocarriers such as liposomes and nanocapsules with sizes of 100–200 nm [24]. Closing this gap is relevant for selected drug administration routes, such as percutaneous lymphatic delivery, or extravasation into solid tumors. Comparing to surfactant micelles (such as MTF micelles), PM are much less hemolytic and kinetically stable. They present slow dissociation that allows them to retain integrity and perhaps drug content in blood circulation above or even below the critical micelle concentration for some time, increasing the chances of reaching the target site before decaying into monomers [20].

One of the most commonly employed polymer class to prepare PM is the Pluronics [25], triblock copolymers of poly(ethylene oxide)–poly (propylene oxide)–poly(ethylene oxide) (PEO-PPO-PEO) with very low CMC values and a solution-gel transition behavior depending on the temperature [26]. Pluronic-based nanocarriers are safe, Food and Drug Administration (FDA) approved and undergo less opsonization than other nanocarriers (since they are sterically stabilized), preventing the subsequent recognition and uptake by macrophages of the reticuloendothelial system (RES). As a consequence, PM of Pluronics may have a reasonably longer half-life in circulation and may deliver the payload to desired sites of action more efficiently [27,28].

Considering the advantages of PM as drug carriers and the potential of MTF as a chemotherapeutic agent for cancer therapy, we developed MTF-loaded PM of Pluronic F127 that showed to be significantly less hemolytic than the free drug. To develop the formulation, a factorial design was employed to evaluate the effect of hydration temperature, stirring speed and stirring time on nanostructure mean size (D_h) and polydispersity index (PI). Our results of *in vitro* activity show that MTF-loaded PM are less hemolytic than the free drug while preserving the antiproliferative activity against tumor cell lines.

2. Materials and methods

2.1. Materials

The miltefosine (MTF) was purchased from Avanti® Polar Lipids, Inc. (Alabama, USA). Pluronic® F127 ($(PEO)_{100}$-$(PPO)_{65}$-$(PEO)_{100}$; Mw: 12,600 Da), 3-(4,5-dimethyl-thiazol-2-yl)-2,5-diphenyl-tetrazolium bromide (MTT) and phosphotungstic acid were supplied by Sigma-Aldrich® (St. Louis, MO, USA). Dulbecco's modified Eagle's medium (DMEM) was supplied by Gibco® Laboratories (USA). Defibrinated sheep blood was obtained from New Prov® (Pinhais, Brazil). The human cervical carcinoma cell line (HeLa) and the human bronchioalveolar carcinoma cell line (H-358) were obtained from ATCC® (Manassas, VA, USA). All other chemicals were of analytical grade and used without further purification. All experiments were carried out with ultra-purified water (Milli-Q, Millipore®, Bedford, MA, USA).

2.2. Preparation of miltefosine-loaded polymeric micelles

MTF-loaded PM were prepared by thin-film hydration method [29]. Briefly, 3.6 mg of MTF and 90.7 mg of Pluronic F127 were dissolved in 5 mL of chloroform in a round-bottom flask. The solvent was extracted by rotary evaporation (Buchi Rotavapor R-210/215, Buchi®, Switzerland) at 50 °C, 150 rpm, and 100 mBar for 30 min to obtain MTF:polymer matrix forming a thin film. Then, the film was hydrated with phosphate buffer saline (PBS), 10 mM, pH 7.4, at different temperatures, stirring rates and stirring times according to the experimental design detailed in the following section. The micellar dispersions were filtered through a 0.22 μm membrane to remove aggregates. After defining the optimal micellar dispersion, prepared according to the experimental design, the system was freeze-dried (24 h at 0.120 mBar, after freezing at −70 °C overnight) in a Liotop® L101 equipment (Liobras, Brazil).

2.3. Central composite design (CCD)

Preliminary experiments at a fixed Pluronic F127 concentration (7.2 mM) and varying MTF concentration were conducted to define the maximum drug concentration to be incorporated in the polymeric micelles. Then, a central composite design (CCD) was used for the optimization of three independent variables, namely hydration temperature (X_1), stirring speed (X_2) and stirring time (X_3). The micelles mean hydrodynamic diameter (D_h) and polydispersity index (PI) were selected as dependent variables, according to a 2^3 full factorial design matrix generated by Minitab® software (Trial version 17). Response surface methodology (RSM) was used in the optimization of response variables of D_h and PI. For the estimation of the significance and validity of the model, analysis of variance (ANOVA) was applied with 5% significance level, and regression coefficients were calculated. Fisher's *F*-test was performed to test the adequacy of the model.

The D_h and PI values were measured by dynamic light scattering (DLS) in a Zetasizer® Nano ZS (Malvern Instruments, Worcestershire, UK). Analyses were performed at a scattering angle of 90° at 25 °C. Previous to measurement, each freshly prepared sample was diluted two times in PBS to avoid multi-scattering phenomena. The results were expressed as a mean size ± SD for three separate experiments.

2.4. Surface morphology by transmission electronic microscopy (TEM)

The morphology of the MTF-loaded PM obtained from the optimized formulation was evaluated by TEM (JEM-2100, Jeol® Tokyo, Japan). Samples were dropped onto copper coated carbon grids, then stained with phosphotungstic acid solution 2% (w/v) and the excess was wiped by filter paper [30].

2.5. Thermal analysis

Differential scanning calorimetry (DSC) and thermogravimetric analysis (TGA) were carried out using TA-Instruments® (New Castle, DE, USA) calibrated with indium. Freeze-dried MTF-loaded PM were weighed to place 4 mg for DSC and 3 mg for TGA, and the samples were retained in hermetically sealed aluminum pans. As a control, a pan containing the same amount of free MTF was prepared. Thermal analysis of isolated copolymer Pluronic F127 and the physical mixture of MT and Pluronic F127 (a blend of both solids without interaction media) were also carried out. The dynamic scans were taken in N_2 atmosphere at the heating rate of 10 °C/min.

2.6. Hemolytic potential

The effect of the MTF-loaded PM on erythrocyte membranes integrity was investigated by *in vitro* hemolysis assay [31]. The systems were prepared with MTF-loaded PM and free MT at different drug

concentrations, in a range of 30 to 350 μM in PBS with 5% (v/v) of defibrinated sheep blood. The samples were incubated at 37 °C for 1 h under gentle agitation and after that were centrifuged at 25 °C, 1788 × *g* for 5 min. The percent of hemolysis (HP %) in the supernatant was spectrophotometrically (Molecular Devices®) measured at 540 nm, according to Eq. (1). Distilled water and PBS were used as positive and negative control of hemolysis, respectively.

$$HP\% = \frac{\text{Abs sample}}{\text{Abs distilled water}} \times 100 \quad (1)$$

Statistical analysis by comparison of different experimental conditions according to the evaluation of mean values assessed by analysis of variance (two-way ANOVA) with the Bonferroni's *post hoc* test using Graph Pad® software. A p-value < 0.05 or less was considered significant.

2.7. Cell toxicity assays

Human epithelial cervix carcinoma (HeLa) and human bronchioalveolar carcinoma (H358) cell lines were used to perform cytotoxicity assays according to ISO standards (Third ed., 2009). Cells were cultured in DMEM supplemented with fetal bovine serum to a final concentration of 10%, pH 7.2. Cells were placed on 96-well plates at a density of 6×10^3 cells/well in 100 μL of complete media and incubated for 24 h at 37 °C in a humidified atmosphere with 5% CO_2. Next, the cells were treated with 100 μL of complete medium containing free MTF or MTF-loaded PM with a gradient at specific concentrations. Unloaded PM was also tested at 6 μM (equivalent to the concentration of polymer present in the MTF-loaded PM evaluated). Untreated cells were used as controls.

After 24, 48 and 72 h, the mitochondrial metabolic activity of cells was quantitatively determined by the 3-(4,5-dimethyl-thiazol-2-yl)-2,5-diphenyl-tetrazolium bromide (MTT) assay [32]. Briefly, cells were washed with PBS at pH 7.4, and complete fresh medium with 5 mg/mL MTT was added, followed by incubation for 1 h at 37 °C. Then, dimethylsulfoxide (DMSO) was added to dissolve the MTT formazan crystals. Finally, MTT reduction to formazan was measured colorimetrically at 570 nm in a spectrophotometer (Biotek®). At each time point, the absorbance of treated samples was normalized by the absorbance of control samples (which was considered as 100% viability). Assays were performed in quadruplicate and statistical significance was assessed by analysis of variance (two-way ANOVA) with the Bonferroni's *post hoc* test using Graph Pad® software. A p-value < 0.05 or less was considered significant.

3. Results

3.1. Development of miltefosine-loaded polymeric micelles

To prepare the PM, we employed 7.2 mM of Pluronic F127 what is about 60 times above the copolymer CMC estimated by us based on the pyrene solubilization method (CMC ~0.118 mM, data not shown). For this fixed concentration of copolymer, we investigated the incorporation of increasing amounts of MTF up to a maximum where pure MTF micelles were still not detected (see MTF DLS at Supplementary material, Fig. S1) and PM characteristics (size, polydispersity) were preserved. The MTF-loaded PM were evaluated by DLS and the scattering profiles are presented as Supplementary material (Fig. S2) and summarized in Table 1.

As can be seen, Pluronic F127 micelles of approximately 30 nm of D_h were obtained in the absence of MTF. At increasing drug concentrations, the D_h of PM was ~25 nm, and at 12 mM of MTF, a second peak corresponding to nanostructures of D_h ~4.9 nm was observed. We believe these smaller structures could be pure MTF micelles formed by unloaded drug aggregation. Since the drug is amphiphilic, we assumed it behaved as a co-surfactant aggregating with the Pluronic F127 into PM. However, at high concentrations (above 9 mM) part of the MTF molecules was not able to accommodate in the PM and aggregated as pure MTF micelles. Therefore, we considered 9 mM as the maximum concentration of MTF to be incorporated in 7.2 mM of Pluronic F127 PM without resulting in drug aggregation in pure MTF micelles. In other words, for systems with a copolymer:drug molar ratio up to 1:1.3, MTF monomer concentration was considered to be the drug CMC, reported in the literature as approximately 0.05 mM [33]. Considering the co-micellization process and free MTF concentration approximately the drug CMC, we assumed that 99.4% of miltefosine was in aggregates with Pluronic F127.

Table 1
Hydrodynamic diameter (D_h) and polydispersity index (PI) of F127 polymeric micelles (7.2 mM) with different concentrations of miltefosine.

Miltefosine (mM)	Peak 1 D_h (nm)	Intensity peak 1 (%)	Peak 2 D_h (nm)	Intensity peak 2 (%)	PI ± SD
0	30.96	100	–	–	0.109 ± 0.01
1	30.30	100	–	–	0.093 ± 0.01
3	25.25	100	–	–	0.169 ± 0.01
6	25.92	100	–	–	0.121 ± 0.01
9	36.46	98	–	–	0.245 ± 0.02
12	26.17	94.1	4.9	2.6	0.253 ± 0.02

The effects of hydration temperature (X_1), stirring speed (X_2) and stirring time (X_3) on D_h and PI of PM were studied by a 2^3 full factorial design, and the results are presented in Table 2.

Response surface plots were obtained according to regression equations with Minitab™ 17, and the three factors were found to influence 1/PI ($p < 0.05$), while they did not significantly affect D_h. Lower temperatures led to a very slight and statistically insignificant average size increase (21 nm to 24 nm). Considering that only the 1/PI was influenced by the factors under study, in Fig. 1 we present the surface plot for 1/PI as a function of temperature (X_1), stirring speed (X_2), and stirring time (X_3). As can be seen, the surface plotted indicates an optimal region (red color) where the factors evaluated allow obtaining higher 1/PI values, corresponding to lower PI.

A summary of ANOVA results is shown in Table S1 (Supplementary material), and the mathematical model for PI was well fitted (R-Sq of 0.9753 (adj) and 0.9472 (pred)). Taking higher values of inverse PI (1/PI), the optimal formulation was selected as follows: hydration temperature of 30 °C, stirring speed of 550 rpm, and stirring time of 30 min, according to Eq. (2):

Table 2
Independent variables of the 2^3 full factorial design for miltefosine-loaded Pluronic F127 polymeric micelles preparation with the coded values expressed in brackets and response variables hydrodynamic diameter (D_h) and the inverse of polydispersity index (1/PI).

Experiment number	X_1 Hydration temperature (oC)	X_2 Stirring speed (rpm)	X_3 Stirring time (min)	D_h [nm]	1/PI
1	30 (−1)	550 (−1)	30 (−1)	24	8.8
	30 (−1)	550 (−1)	30 (−1)	24	9.0
2	30 (−1)	550 (−1)	60 (+1)	22	4.5
	30 (−1)	550 (−1)	60 (+1)	21	4.2
3	30 (−1)	750 (+1)	30 (−1)	23	5.2
	30 (−1)	750 (+1)	30 (−1)	22	4.9
4	30 (−1)	750 (+1)	60 (+1)	24	7.2
	30 (−1)	750 (+1)	60 (+1)	23	6.4
5	50 (+1)	550 (−1)	30 (−1)	23	4.4
	50 (+1)	550 (−1)	30 (−1)	23	4.5
6	50 (+1)	550 (−1)	60 (+1)	22	4.0
	50 (+1)	550 (−1)	60 (+1)	22	4.1
7	50 (+1)	750 (+1)	30 (−1)	22	5.0
	50 (+1)	750 (+1)	30 (−1)	23	5.2
8	50 (+1)	750 (+1)	60 (+1)	24	6.6
	50 (+1)	750 (+1)	60 (+1)	22	6.3

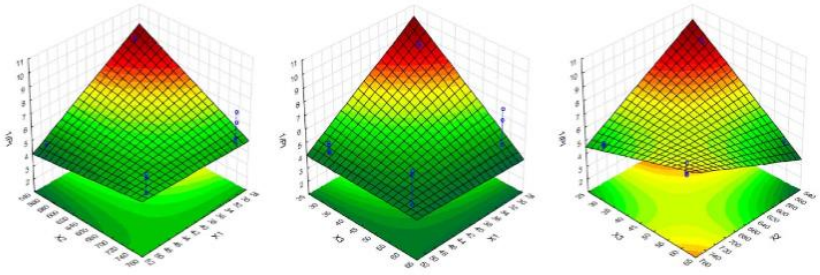

Fig. 1. Response surfaces of the polydispersity index inverse (1/PI) for miltefosine-loaded Pluronic F127 polymeric micelles as a function of temperature (X_1), stirring speed (X_2) and stirring time (X_3). Graphs were plotted using the program Statistica™; higher 1/PI results are represented in red and lower values in darker green. (For interpretation of the references to color in this figure legend, the reader is referred to the web version of this article.)

$$\frac{1}{PI} = 91.59 - 1.674 \times X_1 - 0.11863 \times X_2 - 1.562 \times X_3 + 0.002263 \times X_1 \times X_2 + 0.02777 \times X_1 \times X_3 + 0.002188 \times X_2 \times X_3 - 0.000038 \times X_1 \times X_2 \times X_3 \quad (2)$$

The average D_h and PI of experimentally obtained optimized MTF-loaded PM were 24 ± 0.2 nm and 0.112 ± 0.005, respectively. Optimized formulation was submitted to freeze-drying, and both D_h and PI were preserved after this process. The D_h presented minimal variations from 24 nm to 22 nm, and PI slightly increased to 0.181.

3.2. Transmission electron microscopy

The morphology of the optimal formulation under TEM presented in Fig. 2 revealed spherical structures that we attributed to the MTF-loaded PM. Based on previous work, we believe that gray spots represent the PPO core of micelles. According to TEM images, the spherical nanostructures presented a mean diameter of about 40 nm, which is slightly higher than the results obtained by DLS (29 nm). The size difference may be due to some degree of nanostructures aggregation on the grids by the absence of solvent.

3.3. Thermal analysis

Fig. 3 shows the DSC curves of free MTF, isolated Pluronic F127, the physical mixture of MTF and Pluronic F127 and the MTF-loaded PM. The DSC curve of MTF presented different endothermic events, and the melting temperature was about 225 °C (ΔH 30.20 J/g), whereas freeze-dried MTF-loaded PM did not present the drug melting endotherm. The Pluronic F127 presented an endothermic event at 48 °C (ΔH 143 J/g); similar results were obtained by other authors [34,35]. The physical mixture exhibited an endothermic event at a lower temperature than free MTF, which could be attributed to the solid free drug in the blend.

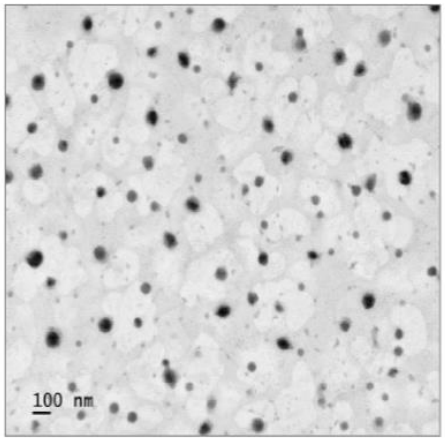

Fig. 2. TEM image of miltefosine-loaded Pluronic F127 polymeric micelles.

Complimentary to DSC, thermogravimetric analysis (Supplementary material, Fig. S3) showed that Pluronic F127 presents high thermal stability, with decomposition temperatures in the range of 330–430 °C. The TGA of MT-loaded PM showed a weight loss of 89% at temperatures higher than 300 °C. Free MT presented a weight loss of 24% at decomposition temperature of 253 °C. The TGA curves of physical mixture exhibited weight loss of 95% in the range of 245–417 °C.

3.4. Hemolytic potential

Fig. 4 shows the hemolytic potential of free MTF and MTF-loaded PM at different concentrations of the drug. For MTF concentrations up to 125 μM the HP% of MTF-loaded PM was significantly lower than free drug ($p < 0.001$). Above this concentration, no significant differences were observed between free drug and MTF-loaded PM. The triblock copolymer Pluronic F127 had no hemolytic effect on red blood cells (empty PM on Fig. 4). In addition, the hemolytic effect was dose-dependent for MTF.

3.5. In vitro cytotoxicity assay

Initially, we determined the drug IC_{50} in human HeLa (Fig. 5A) and H358 (Fig. 5B) cell lines based on MTT assay at 24 h and found an IC_{50} of 6.4 μM HeLa in comparison to 52.4 μM in H358. Giving the higher effect of the drug against HeLa cells, we compared IC_{50} in this cell line for the free MTF and MTF incorporated in PM (Fig. 5C) and found no significant differences in the drug cytotoxic effect. The IC_{50} for MTF-loaded PM was 8.1 μM. We also compared the cytotoxicity of free MTF and MTF-loaded PM at different times, 24, 48 and 72 h (Fig. 5D). For both formulations, cell viability was significantly lower at each time evaluated when compared to the control group ($p < 0.01$). The cytotoxicity of empty Pluronic F127 micelles was also investigated (Supplementary material, Fig. S5) and no significant differences were observed between the empty micelles at 6 μM of Pluronic F127 and the control ($p > 0.05$).

4. Discussion

We developed a Pluronic F127 micellar formulation incorporating the antitumor agent MTF, aiming at lowering its hemolytic potential and improving drug safety. For the pure copolymer, PM with D_h of about 30 nm were obtained. For Pluronic:MTF molar ratios up to 1:1.3, the D_h of MTF-loaded PM was ~25 nm, which is still large enough to avoid first-pass renal clearance that faces particles smaller than 10 nm, thus maintaining their longevity in the bloodstream [36]. As mentioned before, we assumed that MTF co-micellized with Pluronic F127 and free drug concentration was considered approximately the CMC (0.05 mM). Nevertheless, at 1:1.7 Pluronic:MTF molar ratio (12 mM of MTF), a secondary peak corresponding to structures of 4.9 nm diameter was observed. If we consider that pure MTF micelles have a diameter of

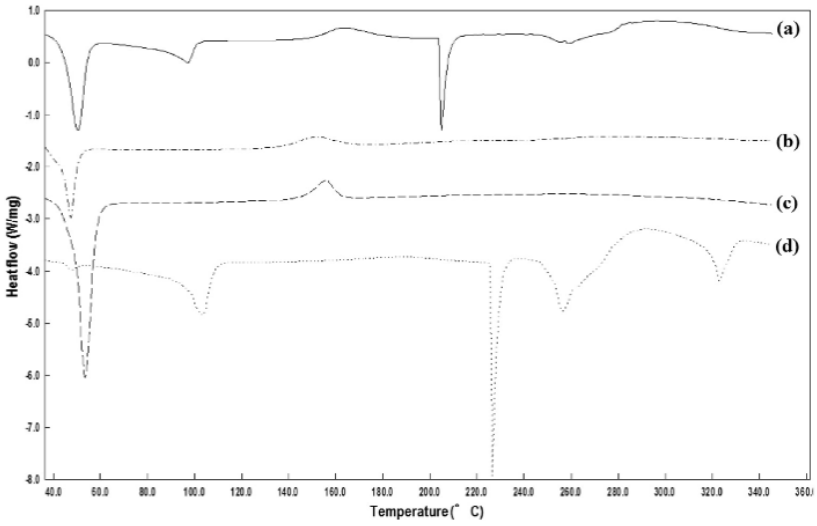

Fig. 3. DSC curves of the physical mixture (a), miltefosine-loaded Pluronic F127 polymeric micelles (b), isolated copolymer Pluronic F127 (c) and free miltefosine (d).

6 nm (Supplementary files, Fig. S1), we can assume that an excess of the drug is aggregating in pure micelles, what is not desirable in terms of drug delivery. Pure MTF micelles are known to be very hemolytic and disaggregate easily under oral or intravenous administration [37]. Therefore, we considered 9 mM as the maximum drug load in 7.2 mM Pluronic F127 PM.

The PEO:PPO ratio of the Pluronic, its concentration and formulation parameters such as temperature and ionic strength, are important determinants for drug encapsulation [38,39]. A CCD study allowed us to evaluate the influence of hydration temperature (X_1), stirring speed (X_2) and stirring time (X_3) on D_h (Y_1) and PI (Y_2). Nanostructured formulations for intravenous pharmaceutical applications should present good control of particle size since large particles may result in capillaries obstruction. Our results show that lower temperatures lead to narrower size distribution for MTF-loaded PM, in agreement with previous reports for Pluronic F127 [40]. This may be attributed to the dehydration of the Pluronics PEO heads at higher temperatures, resulting in interactions among the polymeric micelles and, therefore, higher polydispersity.

Regarding MTF incorporation, the effect of temperature on the solubility of drugs depends on its location in the micelle (within the PPO core or in the PEO corona). Drugs that are located preferably in the PEO corona are affected by temperature due to dehydration of PEO groups with increasing temperatures, which reduces the available space for drug incorporation [24]. Since we assumed that MTF behaved as a cosurfactant, its solubility should not change drastically with temperature.

Additionally, lower PI values were observed when higher stirring speed was used to prepare MTF-loaded PM. We believe this is related to an increased probability of micellar aggregation and decrease in bulky polymer at this condition. Regarding stirring time, higher values did not result in lower PI values indicating that kinetics of aggregation is relatively fast for Pluronic 127.

The TEM microscopy analysis showed spherical structures, an important feature to provide long circulation times in the bloodstream and prevent nanotoxicity. Studies reported that spiky nanoparticles could stimulate macrophages within the tissue and nanostructures without roughness or sharp edges avoid the uptake by RES [41,42]. The particle size range observed for MTF-loaded PM (Dh ~25–40 nm) allows incorporation into endocytic vesicles or cellular access to endocytosis pathways [29].

The thermal analysis of the pure polymer, free MTF, physical mixture and MTF-loaded PM by DSC indicated the thermic events and the differences between the curves in presence or absence of MTF. The DSC analysis of MTF-loaded PM showed that MTF melting peak was not present, suggesting the drug dispersion in the micellar formulations. It appears that PEO and PPO groups interact with MTF avoiding phase separation. The DSC curves for physical mixture showed an endothermic event at lower temperatures in comparison to free MTF, confirming the presence of free drug and polymer. As mentioned above, for the MTF-loaded PM this event was not observed suggesting the interaction between the polymeric matrix and the drug. The DSC analysis

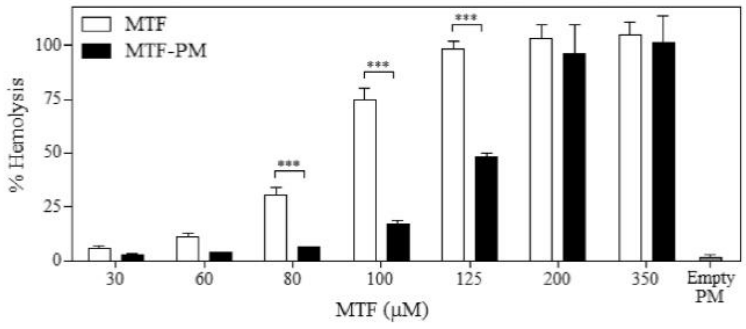

Fig. 4. Hemolytic potential (HP%) of free miltefosine (MTF), MTF-loaded Pluronic F127 polymeric micelles (PM) at different MTF concentrations, and empty PM (7.2 mM of Pluronic F127). Asterisks indicate a significant difference between the indicated groups ($p < 0.001$).

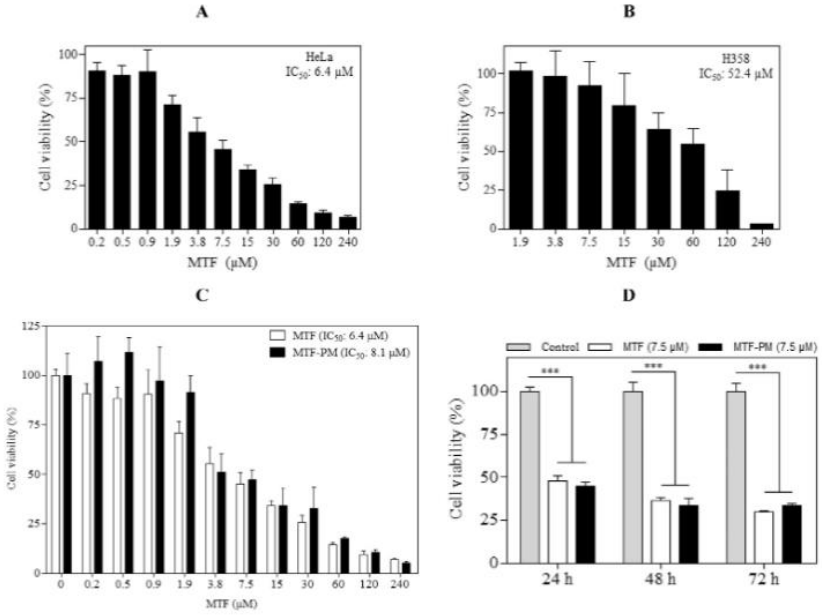

Fig. 5. Cytotoxicity results by MMT assay: (A) cytotoxicity against HeLa epithelioid cervix carcinoma cell line of free miltefosine (MTF) after 24 h; (B) cytotoxicity against H358 bronchioalveolar carcinoma cell line of free MTF after 24 h; (C) comparison between free MTF and MTF-loaded polymeric micelles (PM) cytotoxicity against HeLa cell line at several MTF concentrations after 24 h; (D) comparison between free MTF and MTF-loaded PM cytotoxicity against HeLa cell line at a fixed MTF concentration (7.5 μM) and different times (24, 48 and 72 h). Asterisks indicate a significant difference between the groups relative to the control (***$p < 0.001$).

also showed miscibility between the polymer and drug, since a decrease in melting point was observed [43,44]. Pluronic F127 has a lower melting temperature than MTF and, therefore, the decrease in melting temperature suggests miscibility of MTF and the polymer chains [45].

The TGA of Pluronic F127, free MTF, physical mixture and MTF-loaded PM were performed, and the curves obtained for the pure polymer, and free MTF showed a weight loss of 94% and 25%, respectively, with a decomposition temperature above 254 °C for MTF [46]. Physical mixture showed thermal degradation at 245 °C with a weight loss of 95.5%. The decomposition temperature of MTF-loaded PM (359–392 °C) was higher than the one for the drug alone (254 °C), indicating an increase in MTF stability upon co-aggregation with Pluronic F127.

Blood compatibility of nanomaterials is an important feature for intravenous administration [47,48]. The hemolytic effect of MTF can be explained by the fact that this molecule presents a classic surfactant structure and aggregates in micelles in aqueous solutions. Micelles are related to cell lysis by a mechanism involving micellar dissolution and partition into the membrane followed by a phase transition between lamellae and micelles with membrane solubilization. In general, it is accepted that the amount of surfactant required for membrane solubilization increases with the ease of forming micelles, *i.e.*, with the CMC [24]. We found that MTF causes 100% hemolysis at 200 μM while MTF-loaded PM at 80 μM MTF presents a relatively low hemolytic potential, around 6.1% (the free drug exhibited 30% hemolysis at the same concentration). Unloaded PM of Pluronic F127 had no hemolytic effect at 7.2 mM, which is the concentration of polymer in the PM. Our results show that significant differences in hemolytic potential are found between the free drug and MTF-loaded PM at MTF concentrations up to 125 μM ($p < 0.001$). There is one previous report of MTF incorporation in emulsions, but for 100 μM of MTF, the hemolytic potential was reduced from 100% (free drug) to 80% (MTF in the emulsion) [49]. We found 60% of hemolysis reduction with 100 μM of MTF incorporated in Pluronic F127 PM. Therefore, MTF incorporation into PM may enable the drug transport in the bloodstream significantly reducing hemolysis and consequently improving drug safety.

Regarding MTF release, data from the literature shows that *in vitro* release of drugs from Pluronic F127 micelles is characterized by a first stage with relatively rapid release followed by a slow and sustained release according to Higuchi and Power law, indicating a diffusional kinetic mechanism [45]. Since Pluronic micelles are self-aggregated nanostructures and miltefosine does not present specific interactions with the Pluronic molecules, the same diffusional kinetic mechanism should take place for MTF-loaded PM.

The cytotoxicity of MTF was evaluated in human epithelioid cervix carcinoma (HeLa), and bronchioalveolar carcinoma (H358) cell lines after 24 h of incubation and HeLa cells were found to be eight times more sensitive to MTF, with IC_{50} of 6.4 μM. To confirm that MTF cytotoxicity would be retained when incorporated in PM, cytotoxicity assays were also performed with MTF-loaded PM and the same cytotoxic profile was observed, with an IC_{50} of 8.1 μM for the drug incorporated in the PM. Regarding the effect of Pluronic F127 on HeLa cells (Fig. S4) a slight decrease in cell viability (< 25%) is noticed, but no significant cytotoxicity was detected ($p > 0.05$). This effect might result from the surfactant nature of Pluronic F127 that may have limited cell adhesion to the surface of the culture plate. The MTF-loaded PM and free MTF at the same drug concentrations exhibited similar cytotoxicity in HeLa cells after 24, 48 and 72 h of incubation (Fig. 5D), indicating the potential of the developed formulation to treat human epithelioid cervix carcinoma.

Since our main concern here was to prove that MTF activity would be preserved in PM, we chose a sensitive cell line (HeLa) for proof of concept. Nonetheless, MTF is cytotoxic for several cancer cell lines, such as soft tissue sarcoma, metastatic colorectal cancer, and head and neck squamous cell carcinoma [2], suggesting that our MTF-loaded F127 formulation may be used as a therapeutic strategy to deliver MTF safely to other cancer types.

5. Conclusions

The MTF-loaded PM are a promising alternative to treat cancers by the intravenous administration since they preserve the drug antitumoral activity and lower hemolytic effect. In other words, the therapeutic formulation developed take advantage of MTF potential for

cancer treatment and improve the pharmacotherapy by reducing side effects. Additionally, our results show that PM are promising for the delivery of other surfactant-like drugs, bringing new possibilities for drugs once put aside due to surfactant-related toxicity.

Acknowledgements

This work was supported by grants from the Coordination for Higher Level Graduate Improvements (CAPES/Brazil) (23536007864 and 01095849379), State of São Paulo Research Foundation (FAPESP/Brazil, processes #2014/01983-0 and #2010/52685-9). MCG thanks to CONICET for postdoctoral fellowship and to the *Red de Macro Universidades de América Latina y el Caribe* for the scholarship received. VAF also acknowledges to IPT Foundation for the "*Novos Talentos*" scholarship received.

Appendix A. Supplementary data

Supplementary data to this article can be found online at http://dx.doi.org/10.1016/j.msec.2017.07.040.

References

[1] S. Sundar, P.L. Olliaro, Miltefosine in the treatment of leishmaniasis: clinical evidence for informed clinical risk management, Ther. Clin. Risk Manag. 3 (2007) 733.
[2] J.A. Pachioni-Vasconcelos, A.M. Lopes, A.C. Apolinário, J.K. Valenzuela-Oses, J. Costa, L.O. Nascimento, A. Pessoa, L. Barbosa, C.O. Rangel-Yagui, Nanostructures for protein drug delivery, Biomater. Sci. 4 (2016) 205.
[3] M. Malta de Sá, V. Sresht, C.O. Rangel-Yagui, D. Blankschtein, Understanding miltefosine–membrane interactions using molecular dynamics simulations, Langmuir 31 (2015) 4503–4512.
[4] P. Hilgard, T. Klenner, J. Stekar, C. Unger, Alkylphosphocholines: a new class of membrane-active anticancer agents, Cancer Chemother. Pharmacol. 32 (1993) 90–95.
[5] C. Munoz, K. Alzoubi, J. Jacobi, M. Abed, F. Lang, Effect of miltefosine on erythrocytes, Toxicol. in Vitro 27 (2013) 1913–1919.
[6] H. Sindermann, J. Engel, Development of miltefosine as an oral treatment for leishmaniasis, Trans. R. Soc. Trop. Med. Hyg. 100 (2006) S17–S20.
[7] M. Zhukova, O. Romanenko, V. Nikolaevich, Hemolytic properties of miltefosine in liposomes of various lipid compositions, Pharm. Chem. J. 44 (2010) 507–509.
[8] F. Danhier, O. Feron, V. Préat, To exploit the tumor microenvironment: passive and active tumor targeting of nanocarriers for anti-cancer drug delivery, J. Control. Release 148 (2010) 135–146.
[9] O.C. Farokhzad, R. Langer, Nanomedicine: developing smarter therapeutic and diagnostic modalities, Adv. Drug Deliv. Rev. 58 (2006) 1456–1459.
[10] D.A. Groneberg, M. Giersig, T. Welte, U. Pison, Nanoparticle-based diagnosis and therapy, Curr. Drug Targets 7 (2006) 643–648.
[11] A.S. Thakor, S.S. Gambhir, Nanooncology: the future of cancer diagnosis and therapy, CA Cancer J. Clin. 63 (2013) 395–418.
[12] R. Zeisig, I. Fichtner, D. Arndt, S. Jungmann, Antitumor effects of alkylphosphocholines in different murine tumor models: use of liposomal preparations, Anti-Cancer Drugs 2 (1991) 411–418.
[13] L.H. Lindner, M. Hossann, M. Vogeser, N. Teichert, K. Wachholz, H. Eibl, W. Hiddemann, R.D. Issels, Dual role of hexadecylphosphocholine (miltefosine) in thermosensitive liposomes: active ingredient and mediator of drug release, J. Control. Release 125 (2008) 112–120.
[14] A. Papagiannaros, S. Hatziantoniou, K. Dimas, G.T. Papaioannou, C. Demetzos, A liposomal formulation of doxorubicin, composed of hexadecylphosphocholine (HePC): physicochemical characterization and cytotoxic activity against human cancer cell lines, Biomed Pharmacother 60 (2006) 36–42.
[15] M. Teymouri, H. Farzaneh, A. Badiee, S. Golmohammadzadeh, K. Sadri, M.R. Jaafari, Investigation of hexadecylphosphocholine (miltefosine) usage in pegylated liposomal doxorubicin as a synergistic ingredient: in vitro and in vivo evaluation in mice bearing C26 colon carcinoma and B16F0 melanoma, Eur. J. Pharm. Sci. 80 (2015) 66–73.
[16] Z. Luo, J. Jiang, pH-sensitive drug loading/releasing in amphiphilic copolymer PAE–PEG: integrating molecular dynamics and dissipative particle dynamics simulations, J. Control. Release 162 (2012) 185–193.
[17] G.P. Mishra, D. Nguyen, A.W. Alani, Inhibitory effect of paclitaxel and rapamycin individual and dual drug-loaded polymeric micelles in the angiogenic cascade, Mol. Pharm. 10 (2013) 2071–2078.
[18] T. Wang, V.A. Petrenko, V.P. Torchilin, Paclitaxel-loaded polymeric micelles modified with MCF-7 cell-specific phage protein: enhanced binding to target cancer cells and increased cytotoxicity, Mol. Pharm. 7 (2010) 1007–1014.
[19] X.J. Loh, J.S. del Barrio, P.P.C. Toh, T.-C. Lee, D. Jiao, U. Rauwald, E.A. Appel, O.A. Scherman, Triply triggered doxorubicin release from supramolecular nanocontainers, Biomacromolecules 13 (2011) 84–91.
[20] X.J. Loh, Z.-X. Zhang, Y.-L. Wu, T.S. Lee, J. Li, Synthesis of novel biodegradable thermoresponsive triblock copolymers based on poly[(R)-3-hydroxybutyrate] and poly(*N*-isopropylacrylamide) and their formation of thermoresponsive micelles, Macromolecules 42 (2008) 194–202.
[21] X.J. Loh, S.J. Ong, Y.T. Tung, H.T. Choo, Dual responsive micelles based on poly [(R)-3-hydroxybutyrate] and poly(2-(di-methylamino) ethyl methacrylate) for effective doxorubicin delivery, Polym. Chem. 4 (2013) 2564–2574.
[22] C.K. Liu, Q. Dou, S.S. Liow, J.N. Kumar, X.J. Loh, Cationic micelles based on polyhedral oligomeric silsesquioxanes for enhanced gene transfection, Aust. J. Chem. 69 (2016) 363–371.
[23] X. Fan, Z. Li, X.J. Loh, Recent development of unimolecular micelles as functional materials and applications, Polym. Chem. 7 (2016) 5898–5919.
[24] C.O. Rangel-Yagui, A. Pessoa Jr., L.C. Tavares, Micellar solubilization of drugs, J. Pharm. Pharm. Sci. 8 (2005) 147–163.
[25] X.J. Loh, S.H. Goh, J. Li, Biodegradable thermogelling poly[(R)-3-hydroxybutyrate]-based block copolymers: micellization, gelation, and cytotoxicity and cell culture studies, J. Phys. Chem. B 113 (2009) 11822–11830.
[26] N.A.K. Meznarich, Effect of Ternary Solutes on the Evolution of Structure and Gel Formation in Amphiphilic Copolymer Solutions, The University of Michigan, 2012.
[27] S.R.M. Grallert, C.D.O. Rangel-Yagui, K.F.M. Pasqualoto, L.C. Tavares, Polymeric micelles and molecular modeling applied to the development of radiopharmaceuticals, Braz. J. Pharm. Sci. 48 (2012) 1–16.
[28] X. He, X. Wu, C. Gao, K. Wang, S. Lin, W. Huang, M. Xie, D. Yan, Synthesis and self-assembly of a hydrophilic, thermo-responsive poly(ethylene oxide) monomethyl ether-block-poly(acrylic acid)-block-poly(*N*-isopropylacrylamide) copolymer to form micelles for drug delivery, React. Funct. Polym. 71 (2011) 544–552.
[29] A.V. Kabanov, V.Y. Alakhov, Pluronic® block copolymers in drug delivery: from micellar nanocontainers to biological response modifiers, Crit. Rev. Ther. Drug Carrier Syst. 19 (2002).
[30] W. Zhu, A. Yu, W. Wang, R. Dong, J. Wu, G. Zhai, Formulation design of microemulsion for dermal delivery of penciclovir, Int. J. Pharm. 360 (2008) 184–190.
[31] C.O. Rangel-Yagui, H.W. Hsu, L.R. Barbosa, W. Caetano, A. Pessoa Jr., L.C. Tavares, R. Itri, Novel potential drug against *T. cruzi* and its interaction with surfactant micelles, Pharm. Dev. Technol. 12 (2007) 183–192.
[32] G. Ciapetti, E. Cenni, L. Pratelli, A. Pizzoferrato, In vitro evaluation of cell/biomaterial interaction by MTT assay, Biomaterials 14 (1993) 359–364.
[33] B. de Castro, P. Gameiro, J.L. Lima, C. Matos, S. Reis, Interaction of drugs with hexadecylphosphocholine micelles. Derivative spectroscopy, acid–base and solubility studies, Mater. Sci. Eng. C 18 (2001) 71–78.
[34] R.A. Fule, T.S. Meer, A.R. Sav, P.D. Amin, Artemether-soluplus hot-melt extrudate solid dispersion systems for solubility and dissolution rate enhancement with amorphous state characteristics, J. Pharm. 2013 (2013).
[35] R.C. Rowe, P.J. Sheskey, M.E. Quinn, Handbook of Pharmaceutical Excipients, 6° ed., Pharmaceutical Press, 2009.
[36] M.E. Davis, D.M. Shin, Nanoparticle therapeutics: an emerging treatment modality for cancer, Nat. Rev. Drug Discov. 7 (2008) 771–782.
[37] T. Calogeropoulou, P. Angelou, A. Detsi, I. Fragiadaki, E. Scoulica, Design and synthesis of potent antileishmanial cycloalkylidene-substituted ether phospholipid derivatives, J. Med. Chem. 51 (2008) 897–908.
[38] D.A. Chiappetta, A. Sosnik, Poly(ethylene oxide)–poly(propylene oxide) block copolymer micelles as drug delivery agents: improved hydrosolubility, stability and bioavailability of drugs, Eur. J. Pharm. Biopharm. 66 (2007) 303–317.
[39] Y. Wang, L. Yu, L. Han, X. Sha, X. Fang, Difunctional pluronic copolymer micelles for paclitaxel delivery: synergistic effect of folate-mediated targeting and Pluronic-mediated overcoming multidrug resistance in tumor cell lines, Int. J. Pharm. 337 (2007) 63–73.
[40] M. Nilsson, B. Håkansson, O. Söderman, D. Topgaard, Influence of polydispersity on the micellization of triblock copolymers investigated by pulsed field gradient nuclear magnetic resonance, Macromolecules 40 (2007) 8250–8258.
[41] A. Albanese, E.A. Sykes, W.C. Chan, Rough around the edges: the inflammatory response of microglial cells to spiky nanoparticles, ACS Nano 4 (2010) 2490–2493.
[42] G.S. Kwon, K. Kataoka, Block copolymer micelles as long-circulating drug vehicles, Adv. Drug Deliv. Rev. 16 (1995) 295–309.
[43] M. Bragagni, C. Beneitez, C. Martín, D.H.P. de la Ossa, P.A. Mura, M.E. Gil-Alegre, Selection of PLA polymers for the development of injectable prilocaine controlled release microparticles: usefulness of thermal analysis, Int. J. Pharm. 441 (2013) 468–475.
[44] C. Rouzes, M. Leonard, A. Durand, E. Dellacherie, Influence of polymeric surfactants on the properties of drug-loaded PLA nanospheres, Colloids Surf. B: Biointerfaces 32 (2003) 125–135.
[45] A. Sahu, N. Kasoju, P. Goswami, U. Bora, Encapsulation of curcumin in Pluronic block copolymer micelles for drug delivery applications, J. Biomater. Appl. 25 (2011) 619–639.
[46] P. Mishra, D. Javia, Development and Performance Evaluation of Miltefosine Loaded Nanostructured Lipid Carriers for Managements of Viceral Leishmaniasis, National Institute of Pharmaceutical Education and Research, India, 2015.
[47] A. Yildirim, G.B. Demirel, R. Erdem, B. Senturk, T. Tekinay, M. Bayindir, Pluronic polymer capped biocompatible mesoporous silica nanocarriers, Chem. Commun. 49 (2013) 9782–9784.
[48] T. Yu, A. Malugin, H. Ghandehari, Impact of silica nanoparticle design on cellular toxicity and hemolytic activity, ACS Nano 5 (2011) 5717–5728.
[49] M.M. Eissa, R.M. El-Moslemany, A.A. Ramadan, E.I. Amer, M.Z. El-Azzouni, L.K. El-Khordagui, Miltefosine lipid nanocapsules for single dose oral treatment of *Schistosomiasis mansoni*: a preclinical study, PLoS One 10 (2015) e0141788.

Supplementary material

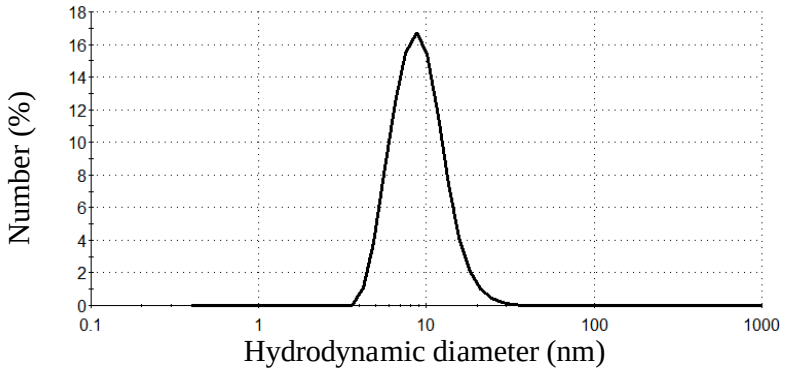

Figure S1. Size distribution by number of miltefosine micelles (3 mM) in phosphate buffer solution at pH 7.4.

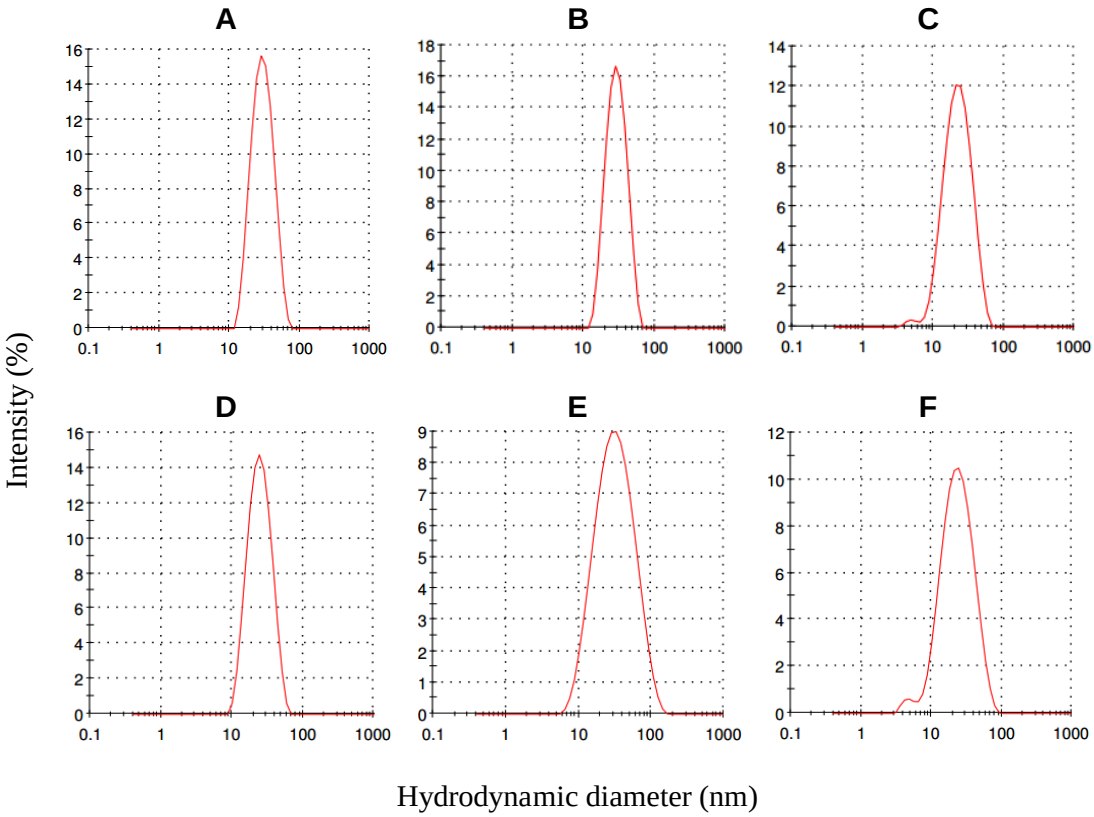

Figure S2. Size distribution by intensity of F127 polymeric micelles (7.2 mM) with different miltefosine concentrations: **(A)** 0 mM, **(B)** 1 mM, **(C)** 3 mM, **(D)** 6 mM, **(E)** 9 mM and **(F)** 12 mM.

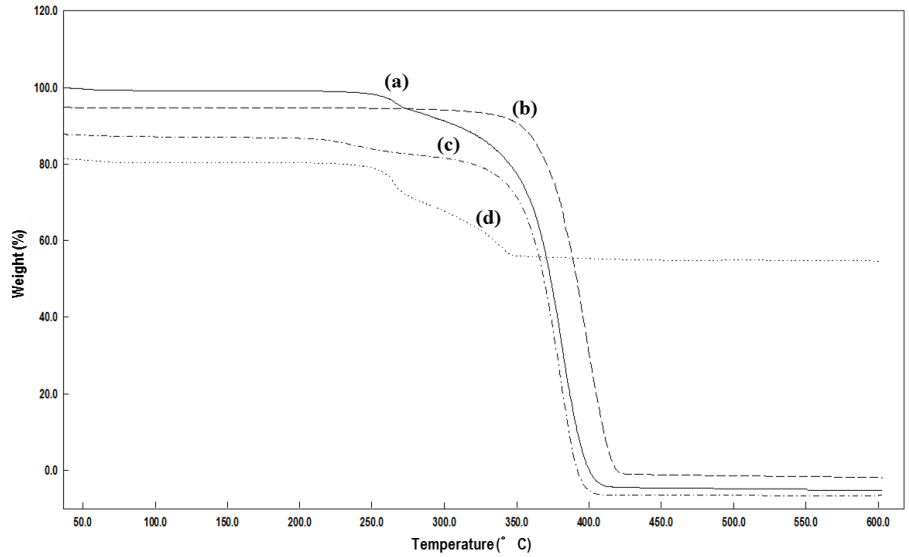

Figure S3. TGA curves of physical mixture **(a)**, isolated copolymer Pluronic F127 **(b)**, miltefosine- loaded Pluronic F127 polymeric micelle **(c)** and free miltefosine **(d)**.

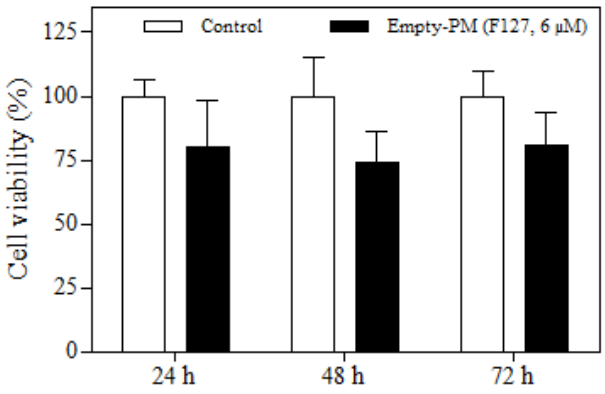

Figure S4. Cytotoxicity against HeLa epithelioid cervix carcinoma cell line of Pluronic F127 polymeric micelles without any drug incorporated (Empty-PM) employing the MTT assay. The concentration of Pluronic F127 was 6 □M, which is the maximum concentration employed to test the miltefosine-loaded PM.

Table S1. ANOVA for response surface regression of the inverse of polydispersity index (1/PI) as a function of hydration temperature (X_1 - ºC), stirring speed (X_2 - rpm) and stirring time (X_3 - min) for miltefosine-loaded Pluronic F127 polymeric micelles preparation.

Source	D.F.	SS	MS	F-value	*p*-value
Model	7	37.7544	5.3935	85.44	0.000
Linear	3	7.9119	2.6373	41.78	0.000
X_1	1	6.3756	6.3756	101.00	0.000
X_2	1	0.6806	0.6806	10.78	0.011
X_3	1	0.8556	0.8556	13.55	0.006
2 order interactions	3	24.6669	8.2223	130.25	0.000
X_1 x X_2	1	4.9506	4.9506	78.43	0.000
X_1 x X_3	1	3.5156	3.5156	55.69	0.000
X_2 x X_3	1	16.2006	16.2006	256.64	0.000
3 order interactions	1	5.1756	5.1756	81.99	0.000
X_1 x X_2 x X_3	1	5.1756	5.1756	81.99	0.000
Error	8	0.5050	0.0631		
Total	15	38.2594			

Appendix B: Deposited patent "BR1020170200" at Brazilian Institute of Industrial Property (INPI)

TIPO	MICELAS POLIMÉRICAS CARREGADAS DO FÁRMACO MILTEFOSINA E PRODUTO PARA O TRATAMENTO DO CANCER E DOENÇAS INFECCIOSAS
NÚMERO DE REGISTRO / PUBLICAÇÃO NA RPI	BR1020170200
DOCENTE RESPONSÁVEL	Profa. Carlota de Oliveira Rangel Yagui
DATA DE DEPÓSITO	19/09/2017

Carlota O. Rangel-Yagui, Johanna Valenzuela-Oses, Valker A. Feitosa, Mónica C. García, Natália N. P. Cerize

Resumo

"MICELAS POLIMÉRICAS CARREGADAS DO FÁRMACO MILTEFOSINA E PRODUTO PARA O TRATAMENTO DO CANCER E DOENÇAS INFECCIOSAS", pertencente ao setor de preparações medicinais caracterizadas por método de produção de formas físicas especiais contendo ingredientes ativos orgânicos e ingredientes não ativos de compostos macromoleculares insaturados carbono-carbono formando agentes antineoplásticos, refere-se a produto de micelas poliméricas de um copolímero de polióxido de etileno (PEO) e polióxido de propileno (PPO), com tamanho de partículas reduzido de aproximadamente 30 nm, contendo o ativo miltefosina ou outra alquilfosfocolina para tratamentos para os quais a miltefosina ou outra alquilfosfocolina apresente ação terapêutica, permitindo sua administração intravenosa para tratamento de cânceres, como câncer bronquioalveolar e câncer de colo de útero, e doenças infecciosas, como leishmaniose, aumentando a eficacia do tratamento devido a diminuição do efeito hemolítico da miltefosina ou alquilfosfocolina.

Appendix C: Academic Transcripts

Janus - Sistema Administrativo da Pós-Graduação

Universidade de São Paulo
Faculdade de Ciências Farmacêuticas
FICHA DO ALUNO

9135 - 6763594/2 - Valker Araujo Feitosa

Email:	valker@usp.br
Data de Nascimento:	27/01/1986
Cédula de Identidade:	RG - 2001097084947 - CE
Local de Nascimento:	Estado do Ceará
Nacionalidade:	Brasileira
Graduação:	Farmacêutico - Universidade Estadual da Paraíba - Paraíba - Brasil - 2011
Mestrado:	Mestre em Ciências - Área: Tecnologia de Fermentações - Faculdade de Ciências Farmacêuticas - Universidade de São Paulo - São Paulo - Brasil - 2014

Curso:	Doutorado
Programa:	Tecnologia Bioquímico-Farmacêutica
Área:	Tecnologia Químico-Farmacêutica
Data de Matrícula:	10/07/2014
Início da Contagem de Prazo:	10/07/2014
Data Limite para o Depósito:	07/01/2019
Orientador:	Prof(a). Dr(a). Carlota de Oliveira Rangel Yagui - 08/04/2015 até o presente. Email: corangel@usp.br
Co-orientador:	Prof(a). Dr(a). Natália Neto Pereira Cerize - 12/11/2015 até o presente. Email: ncerize@ipt.br
Proficiência em Línguas:	Inglês, Aprovado em 10/07/2014
Trancamento(s):	60 dias Período de 04/08/2016 até 02/09/2016 Período de 05/07/2016 até 03/08/2016
Prorrogação(ões):	120 dias Período de 08/09/2018 até 06/01/2019
Data de Aprovação no Exame de Qualificação:	Aprovado em 27/10/2016
Estágio no Exterior:	King's College London, Inglaterra - Período de 13/05/2017 até 12/11/2017
Data do Depósito do Trabalho:	
Título do Trabalho:	
Data Máxima para Aprovação da Banca:	
Data de Aprovação da Banca:	
Data Máxima para Defesa:	
Data da Defesa:	
Resultado da Defesa:	

Aluno matriculado no Regimento da Pós-Graduação USP (Resolução nº 6542 em vigor de 20/04/2013 até 28/03/2018).
Última ocorrência: Prorrogação em 28/08/2018
Impresso em: 04/01/2019 12:55:36

Sandra Lara
Chefe do Serviço de Pós-Graduação
Nº USP 3054695
FCF/USP

Janus - Sistema Administrativo da Pós-Graduação

Universidade de São Paulo
Faculdade de Ciências Farmacêuticas
FICHA DO ALUNO

9135 - 6763594/2 - Valker Araujo Feitosa

Sigla	Nome da Disciplina	Início	Término	Carga Horária	Cred.	Freq.	Conc.	Exc.	Situação
Crédito Externo	Biotecnologia Industrial (1)	19/05/2014	29/08/2014	-	4	100	T	-	-
FBC5766-4/1	Tópicos em Análises Clínicas IV	05/08/2014	17/11/2014	15	1	100	A	N	Concluída
BMP5784-1/1	Workshop em Modelos Experimentais para Pesquisa em Malária (Instituto de Ciências Biomédicas - Universidade de São Paulo)	06/11/2014	19/11/2014	60	4	75	A	N	Concluída
FBT5738-1/2	Tópicos Especiais em Tecnologia Bioquímico-Farmacêutica III	03/08/2015	19/10/2015	30	2	80	A	N	Concluída
FBF5805-2/1	Delineamento de Experimentos e Ferramentas Estatísticas Aplicadas às Ciências Farmacêuticas	05/08/2015	13/10/2015	90	6	75	A	N	Concluída
ICB5723-1/3	Metodologias de Microscopia Eletrônica de Varredura de Alta Resolução Empregadas para Material Biológico (Instituto de Ciências Biomédicas - Universidade de São Paulo)	07/10/2015	10/11/2015	75	5	100	A	N	Concluída
FBA5758-1/1	Fundamentos do Planejamento Experimental e Otimização Simplex	26/01/2016	01/02/2016	30	2	80	A	N	Concluída
BTC5739-3/1	Biopolímeros de Interesse Industrial (Curso Interunidades: Biotecnologia - Universidade de São Paulo)	29/03/2016	18/04/2016	60	4	100	A	N	Concluída
FBT5776-5/3	Tópicos Especiais de Tecnologia Bioquímico-Farmacêutica II	17/10/2016	30/10/2016	30	2	100	A	N	Concluída

	Créditos mínimos exigidos		Créditos obtidos
	Para exame de qualificação	Para depósito de tese	
Disciplinas:	0	20	30
Estágios:			
Total:	0	20	30

Créditos Atribuídos à Tese: 167

Observações:
1) Disciplinas(s) cursada(s) na(o) Instituto de Pesquisas Tecnológicas. Atribuição de créditos aprovada pelo(a) Comissão Coordenadora de Programa em Sessão de 31/08/2015.

Conceito a partir de 02/01/1997:
A - Excelente, com direito a crédito; B - Bom, com direito a crédito; C - Regular, com direito a crédito; R - Reprovado; T - Transferência.
Um(1) crédito equivale a 15 horas de atividade programada.

Última ocorrência: Prorrogação em 28/08/2018
Impresso em: 04/01/2019 12:55:36

Sandra Lara
Chefe do Serviço de Pós-Graduação
Nº USP 3054695
FCF/USP

Appendix C: Scientific publications

Skin permeation of hydrophobic drugs loaded into polymeric nanoparticles

V.A. Feitosa; T.S. Balogh; K.L. Guimarães; M.H.A. Zanin; A.M. Oliveira; N.N.P. Cerize

Laboratory of Chemical Processes and Particle Technology, BioNanoManufacturing Center, Institute for Technological Rescarch (LPP/Bionano/IPT), São Paulo, Brazil
ncerize@ipt.br

ABSTRACT

Polymeric nanoparticles have been employed for topical pharmaceutical applications due to its capacity to carry drugs across the skin. Biocompatible polymers are extensively applied as coating nanoparticles allowing them to present controlled physical and chemical characteristics. The proposal of this work was to evaluate the skin permeation of polymeric nanoparticles loading hydrophobic drugs. The emulsion/diffusion process was applied to produce nanocapsules composed by poly(ε-caprolactone, PCL) and PEO-PPO-PEO triblock copolymers (Pluronic®), this process promotes the nanoencapsulation of drugs into oil core from pre-formed polymer precipitation. The organic phase was comprised of polymers (Pluronic F127 and PCL), oil, Nile red fluorophore, and hydrocortisone acetate as hydrophobic drug model, solubilized in ethyl acetate. The aqueous phase was comprised of distilled water saturated with ethyl acetate and Tween 20 surfactant. The organic phase was transferred into the aqueous phase under ultrahigh agitation (7,000 rpm), the emulsion formed was immediately transferred to a stirred reactor, the dilution phase (water and Tween® 20) was added and then the solvent was extracted under vacuum pressure. The *in vitro* skin permeation of nanoparticles containing the fluorophore Nile red was evaluated by a vertical diffusion cell employing pig ear skin. The study covered the steps of preparation of animal membrane; monitoring the permeation into vertical diffusion vessel (Franz cell) up to 8 hours; preparation of histological sections into cryomicrotome; and visualization of fluorescence by confocal laser microscopy. It was possible to verify the location of polymeric nanoparticles containing the Nile red fluorophore encapsulated in presence or absence of hydrocortisone drug. It was observed that after two hours, the permeation of the particles was very low. However, for a more prolonged exposure (8 hours) was observed the deposition of the particles in the outer layers of the skin (stratum corneum and epidermis) as well as in hair follicles. These data show that the produced nanoparticles perform the delivery of the drug in the superficial skin layers, fulfilling the role of topical application.

Keywords: Nanotechnology, drug delivery, nanocapsules, topical administration.

1 BACKGROUND

The skin is an alternative route for delivering drugs [1]. Topical and transdermal drug delivery systems are gaining increasing popularity and several drugs have been successfully delivered into skin for local and/or systemic action. [2]. The skin drug delivery is advantageous in that it can not only concentrate drug molecules in a specific skin area but also can reduce unexpected side effects [1].

However, one the major limitations of skin drug administration is the penetration barrier provided by the protective stratum corneum, composed of keratin-rich corneocytes and an intercellular matrix of a unique composition of lipids [3].

The increasing progress of nanotechnology in cosmetic and pharmaceutical fields allow the development of several formulations designed to overcome stratum corneum barrier [4]. Nanocarrier systems can improve dermal penetration, including vesicular delivery systems (*e.g.* liposomes, polymersomes, transfersomes, ethosomes, and niosomes), nanostructured lipid carriers (*e.g.* solid lipid nanoparticles, lipid nanocapsules, nanoemulsions, and solid lipid nanoparticles), and polymeric-based particles (*e.g.* nanospheres and nanocapsules) [1,3,5].

Synthetic, semi-synthetic and natural polymers have been explored for nanoparticle production. Increased attention has been paid to biocompatible and biodegradable polymers, including poly(lactide acid, PLA, poly(lactide-co-glycolide acid, PLGA), poly(ε-caprolactone, PCL) as well as biocompatible amphiphilic triblock copolymers poloxamers, composed of poly(ethylene oxide, PEO) and poly(propylene oxide, PPO), PEO-PPO-PEO, commercially available under the trade name Pluronic®.

In order to determine the drug delivery of polymeric nanostructures into skin, we investigate the skin penetration of hydrophobics molecules loaded with colloidal nanoparticles based on PCL and Pluronic polymers. Employing confocal laser scanning microscopy, we demonstrated that a colloidal polymeric nanocarrier system can significantly improve the specific topical delivery of hydrophobic compounds only through the stratum corneum and epidermis, but not into dermal skin layer.

Integrated System to produce Nano/Microparticles for drug delivery using LTCC Microfluidics devices

Liz Katherine Rincón Ardila; Mario Ricardo Gongora-Rubio; Luciana Wasnievski da Silva Ramos; Adriano Marim de Oliveira; Tatiana Santana Balogh; Valker Araujo Feitosa; Natalia Neto Pereira Cerize.
Bionanomanufacture
Institute for Technological Research of State of São Paulo
São Paulo, Brazil
liz@ipt.br; gongoram@ipt.br; swluciana@ipt.br; amarim@ipt.br; tatibalogh@ipt.br; valker@ipt.br; ncerize@ipt.br

Houari Cobas Gomez
Laboratory of Integrated Systems
University of São Paulo
São Paulo, Brazil
hcobas@ipt.br

***Abstract*—Encapsulated nano/micro particles are highly used for biological, chemical, pharmaceutical and medical applications. The polymeric particles show potential capacity to release drugs and compatibility in biological environments. The emulsion/diffusion process is applied to produce these particles, and technologies based on microfluidic provide miniaturization of such process allowing particles with physical and chemical controlled characteristics. Nevertheless, the integrated system of technological devices like sensors, microactuators and controllers is crucial to improve the performance and efficiency of particles production with automatic cycles. The proposal of this work is to develop the integrated system to produce nano/microparticles for drug encapsulation, using microfluidics devices with control and automatic actions in continuous scale. The system is developed through devices integration, system characterization and control loops, using sensors, pumps, microfluidics devices, communication drivers, data acquisition, and control programs. The result of this work is the integrated system to produce particles of size 499-1500 nm with polydispersity index of 0.3 to 0.5 with potential to be used as drug delivery systems. The experimental results were validated by size measurement and polydispersity distribution with optical microscopy, scanning electron microscopy and dynamic light scattering.**

Keywords—Integrated System; Microfluidic Devices ; Nano and Microparticles; Drug Delivery; Automatic Control.

I. INTRODUCTION

The fabrication of encapsulated micro and nano particles is widely used for biological and biomedical applications [1]. These particles are defined as solid colloidal particles, which have different kind of structure, such as: liquid or solid core with polymeric membrane or polymeric matrix and active substance that can be the liquid core or dispersed into the matrix [2]. These nano/microparticles are used for Drug Delivery Systems (DDS). The particles can be prepared with polymerization methods and synthesis with preformed polymers. In this work is used the emulsion/diffusion process for microparticles fabrication [3]. This process is based on the theory that each emulsion produces several nanocapsules and these are formed by combination of polymer precipitation and interfacial phenomena during solvent diffusion which produces particles for drug encapsulation with delivery control [2]. Technologies based on microfluidic devices [4, 5, 6] provide miniaturization of such process. This work uses mixers that offering an alternative and versatile solution to produce emulsions with low dispersion in mL/min range. However, the automation and integration of technological devices like sensors, microactuators [7], and control systems [8] are essential to increase the performance of particles production with automatic actions. The purpose of this work is to develop the integrated system to produce polymeric nano/microparticles in continuous scale for drug delivery, using LTCC (Low Temperature Co-Fired Ceramic) microfluidics devices [9, 10] with control and supervision of automatic cycles.

II. PROPOSED INTEGRATED SYSTEM FOR FABRICATION OF NANO/MICROPARTICLES

The integrated system (Fig. 1) is composed by the following modules: 1) microfluidic devices; 2) actuators, controllers, hydraulic and electrical connections; 3) electronic instrumentation, peripheral devices, signal acquisition and monitoring and controlling programs; 4) power and supply system; and 5) fluidic inputs (chemical solutions). The modules are integrated for nano/microparticles fabrication.

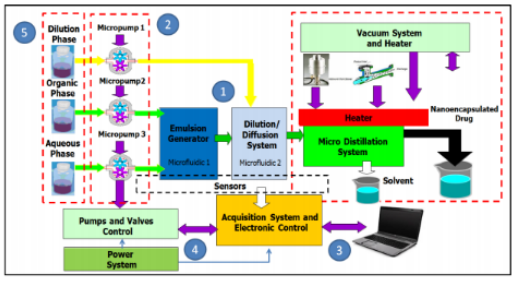

Fig. 1. Integrated System for polymeric nano/microparticles fabrication.

The system applies three chemical solution phases as input materials: organic, aqueous and dilution. For emulsion step, organic and aqueous phases are applied to the inlet of microfluidic emulsion generator. In this stage, polymers,

Financiadora de Estudos e Projetos, FINEP
Conselho Nacional de Desenvolvimento Científico e Tecnológico, CNPQ
Coordenação de Aperfeiçoamento de Pessoal de Nível Superior, CAPES

978-1-4799-6836-7/14/$31.00 ©2014 IEEE

Development of a LTCC Micro Spray Dryer

Houari Cobas Gomez[a], Antonio Carlos Seabra
Laboratório de Sistemas Integráveis
Universidade de São Paulo, USP
São Paulo, Brazil
hcobas_gomez@yahoo.com.br[a]

Valker Araujo Feitosa, Juliana de Novais Schianti, Adriano Marim de Oliveira, Luciana Wasnievski da Silva de Luca Ramos, Mario Ricardo Góngora-Rubio[b]
Núcleo de Bionanomanufatura
Instituto de Pesquisas Tecnológicas, IPT
São Paulo, Brazil
gongoram@ipt.br[b]

***Abstract*—Low Temperature Co-fired Ceramic (LTCC) Microsystem technology have a relevant role in the miniaturization of Chemical Processes area. Microfluidic devices have been applied to carry out several chemical processes operations, including mixing, separation, chemical reactions, heterogeneous catalysis, heat exchange and so on. More recently, LTCC microfluidic systems are employed to produce micro and nanoparticles with excellent control of size distribution, morphology and constitution. The present work reports the development of a LTCC Micro Spray Dryer for Micro and Nanoparticle fabrication showing simulation results and experimental work.**

Keywords—LTCC, Microfluidic Devices, Chemical Process Intensification, Miniaturization, Nano /Microparticle fabrication

I. INTRODUCTION

There are several techniques for fabricating microfluidic reactors [1], among them is the Low Temperature Co-fired Ceramic (LTCC) technology. LTCC displays interesting advantages such as the possibility to microfabricate 3D geometries, is chemically inert to most solvents, it has a low contact angle, presents low thermal coefficient of expansion, can hold out high operational temperatures, can withstand high internal pressures, allowing implementation of several chemical process with applications in stringent environments [2]. Applications of LTCC microfluidic devices to implement several chemical processes unitary operations are reported in the literature, including bioreactors [3], enzymatic reactors [4], combustors [5], microthrusters [6], mixers [7], chemical reactions [8], heat exchange [9] and gold nanoparticles [10], among others.

Spray dryer is a standard technique for pharmaceutical fabrication. It allows instantaneous drying of solutions, emulsions and suspensions in one step, producing a fine powder. Typical spray dryers require large quantities of sample. For drug formulation, it is interesting to miniaturize the process using microfluidics.

Recently, a successful attempt to make a micro spray dryer using microfluidic techniques was done, but the device suffer some problems because it was implemented using PDMS [11]. This material is hydrophobic and is subject to channel deformation with applied pressure.

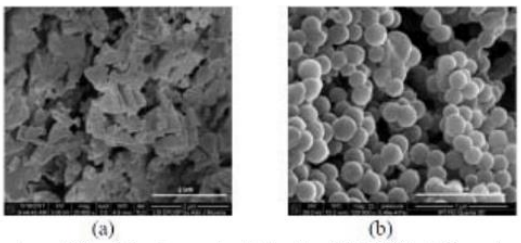

Fig. 1. Rifampicin micrographs obtained by SEM-FEG technique: a) raw Rifampicin without microfluidic process and b) the Rifampicin nanoparticles obtained in the reservoir device, using a flow rate of 2000 µL/min [12, 13].

Lately, Schianti et al. reported their experience using a microfluidic nano precipitation process to generate Rifampicin nanoparticles [12, 13]. Fig. 1 shows the obtained nanoparticles morphology. In Fig. 1a we show raw Rifampicin, without microfluidic process. As we can see in Fig. 1b the particles have a round profile. This profile, together with particle size reduction, can improve the drug dissolution rate.

The present work describes the development of a LTCC microfluidic device Spray Dryer aimed to produce Rifampicin powder that can overcome problems presented by other devices. The proposed device can be applied to any particulate material. At this time we used raw Rifampicin to test our device.

II. DEVICE DESIGN AND OPERATING PRINCIPLE

The designed device has two 3D focalization structures as shown in Fig. 2. The first focalization channel has a hydraulic diameter (D_H) and length of 676 µm and 7.12 mm respectively. The second focalization channel, also named atomization channel, has a D_H and length of 1.66 mm and 9.85 mm respectively. The Rifampicin channel outlet has a D_H of 211µm. By design, the Rifampicin channel outlet is centered in the first focalization channel, and those are centered in the atomization channel.

3D flow focusing is dependent on flow ratio between drug and DI water.

Coordenação de Aperfeiçoamento de Pessoal de Nível Superior, CAPES
Instituto de Pesquisas Tecnológicas do Estado de São Paulo, IPT
Departamento de Engenharia Elétrica da Universidade de São Paulo

978-1-4799-6836-7/14/$31.00 ©2014 IEEE

frontiers in Microbiology

REVIEW
published: 10 April 2015
doi: 10.3389/fmicb.2015.00269

Marine-derived fungi: diversity of enzymes and biotechnological applications

*Rafaella C. Bonugli-Santos[1], Maria R. dos Santos Vasconcelos[2], Michel R. Z. Passarini[2], Gabriela A. L. Vieira[3], Viviane C. P. Lopes[3], Pedro H. Mainardi[3], Juliana A. dos Santos[3], Lidia de Azevedo Duarte[3], Igor V. R. Otero[3], Aline M. da Silva Yoshida[3], Valker A. Feitosa[4], Adalberto Pessoa Jr[4] and Lara D. Sette[2,3]**

[1] Instituto Latino Americano de Ciências da Vida e da Natureza, Centro Interdisciplinar de Ciências da Vida, Universidade Federal da Integração Latino-Americana, Paraná, Brazil, [2] Divisão de Recursos Microbianos, Centro Pluridisciplinar de Pesquisas Químicas, Biológicas e Agrícolas, Universidade Estadual de Campinas, Paulínia, Brazil, [3] Laboratório de Micologia Ambiental e Industrial, Departamento de Bioquímica e Microbiologia, Instituto de Biociências, Universidade Estadual Paulista Júlio de Mesquita Filho, Rio Claro, Brazil, [4] Departamento de Tecnologia Bioquímico-Farmacêutica, Faculdade de Ciências Farmacêuticas, Universidade de São Paulo, São Paulo, Brazil

OPEN ACCESS

Edited by:
Gavin J. Collins, National University of Ireland, Ireland

Reviewed by:
Oded Yarden, The Hebrew University of Jerusalem, Israel
Ka-Lai Pang, National Taiwan Ocean University, Taiwan

***Correspondence:**
Lara D. Sette, Laboratório de Micologia Ambiental e Industrial, Departamento de Bioquímica e Microbiologia, Instituto de Biociências, Universidade Estadual Paulista Júlio de Mesquita Filho, Avenida 24A, 1515 Bela Vista, Rio Claro, SP 13506-900, Brazil
larasette@rc.unesp.br

Specialty section:
This article was submitted to Microbiotechnology, Ecotoxicology and Bioremediation, a section of the journal Frontiers in Microbiology

Received: *27 November 2014*
Accepted: *18 March 2015*
Published: *10 April 2015*

Citation:
Bonugli-Santos RC, dos Santos Vasconcelos MR, Passarini MRZ, Vieira GAL, Lopes VCP, Mainardi PH, dos Santos JA, de Azevedo Duarte L, Otero IVR, da Silva Yoshida AM, Feitosa VA, Pessoa A Jr and Sette LD (2015) Marine-derived fungi: diversity of enzymes and biotechnological applications. Front. Microbiol. 6:269. doi: 10.3389/fmicb.2015.00269

The ocean is considered to be a great reservoir of biodiversity. Microbial communities in marine environments are ecologically relevant as intermediaries of energy, and play an important role in nutrient regeneration cycles as decomposers of dead and decaying organic matter. In this sense, marine-derived fungi can be considered as a source of enzymes of industrial and/or environmental interest. Fungal strains isolated from different substrates, such as invertebrates, decaying wood, seawater, sediments, and mangrove detritus, have been reported to be producers of hydrolytic and/or oxidative enzymes, with alginate lyase, amylase, cellulase, chitinase, glucosidase, inulinase, keratinase, ligninase, lipase, nuclease, phytase, protease, and xylanase being among the enzymes produced by fungi of marine origin. These enzymes present temperature and pH optima ranging from 35 to 70°C, and 3.0 to 11.0, respectively. High-level production in bioreactors is mainly performed using submerged-state fermentation. Certain marine-derived fungal strains present enzymes with alkaline and cold-activity characteristics, and salinity is considered an important condition in screening and production processes. The adaptability of marine-derived fungi to oceanic conditions can be considered an attractive point in the field of fungal marine biotechnology. In this review, we focus on the advances in discovering enzymes from marine-derived fungi and their biotechnological relevance.

Keywords: marine-derived fungi, enzymes, marine mycology, culture-dependent methods, culture-independent methods, environmental pollutants, industrial microbiology

Introduction

Marine microbial communities (bacteria, fungi, algae, plankton, and viruses) are considered important ecological components in marine environments due to their performance in biogeochemical processes (Sowell et al., 2008). Marine fungi have been classified as obligate or facultative: obligate marine fungi are those that grow and sporulate exclusively in a marine or estuarine habitat, whereas facultative marine fungi are those from freshwater or

BRAZILIAN JOURNAL OF MICROBIOLOGY 47S (2016) 51–63

BRAZILIAN JOURNAL OF MICROBIOLOGY

http://www.bjmicrobiol.com.br/

Biotechnology and Industry Microbiology

Biopharmaceuticals from microorganisms: from production to purification

Angela Faustino Jozala[a], *Danilo Costa Geraldes*[b], *Louise Lacalendola Tundisi*[b], *Valker de Araújo Feitosa*[c], *Carlos Alexandre Breyer*[d], *Samuel Leite Cardoso*[e], *Priscila Gava Mazzola*[f], *Laura de Oliveira-Nascimento*[f,g], *Carlota de Oliveira Rangel-Yagui*[c], *Pérola de Oliveira Magalhães*[h], *Marcos Antonio de Oliveira*[d], *Adalberto Pessoa Jr*[c,*]

[a] *Universidade de Sorocaba (UNISO), Departamento de Tecnologia e Processo Ambiental, Sorocaba, SP, Brazil*
[b] *Universidade de Campinas (UNICAMP), Instituto de Biologia, Programa de Pós-Graduação em Biociências e Tecnologia de produtos bioativos, Campinas, SP, Brazil*
[c] *Universidade de São Paulo, Departamento de Bioquímica e Tecnologia Farmacêutica, São Paulo, SP, Brazil*
[d] *Universidade Estadual de São Paulo (UNESP), Instituto de Biociências, Campus do Litoral Paulista, SP, Brazil*
[e] *Universidade de Brasília, Faculdade de Ciências da Saúde, Programa de Pós-Graduação em Ciências Farmacêuticas, Brasília, DF, Brazil*
[f] *Universidade Estadual de Campinas, Faculdade de Ciências Farmacêuticas, Campinas, SP, Brazil*
[g] *Universidade Estadual de Campinas, Instituto de Biologia, Departamento de Bioquímica e Biologia Tecidual, Campinas, SP, Brazil*
[h] *Universidade de Brasília, Faculdade de Ciências da Saúde, Departamento de Farmácia, Brasília, DF, Brazil*

ARTICLE INFO

Article history:
Received 6 September 2016
Accepted 22 September 2016
Available online 26 October 2016

Associate Editor: Nelson Durán

Keywords:
Biopharmaceuticals
Fermentation process
Biotechnology
Upstream process
Downstream process

ABSTRACT

The use of biopharmaceuticals dates from the 19th century and within 5–10 years, up to 50% of all drugs in development will be biopharmaceuticals. In the 1980s, the biopharmaceutical industry experienced a significant growth in the production and approval of recombinant proteins such as interferons (IFN α, β, and γ) and growth hormones. The production of biopharmaceuticals, known as bioprocess, involves a wide range of techniques. In this review, we discuss the technology involved in the bioprocess and describe the available strategies and main advances in microbial fermentation and purification process to obtain biopharmaceuticals.

* Corresponding author.
E-mail: pessoajr@usp.br (A. Pessoa Jr).
http://dx.doi.org/10.1016/j.bjm.2016.10.007

Fungal Biology 122 (2018) 302–309

Contents lists available at ScienceDirect

Fungal Biology

journal homepage: www.elsevier.com/locate/funbio

Laccase production in bioreactor scale under saline condition by the marine-derived basidiomycete *Peniophora* sp. CBMAI 1063

Pedro H. Mainardi [a], Valker A. Feitosa [b], Livia B. Brenelli de Paiva [c], Rafaella C. Bonugli-Santos [d], Fabio M. Squina [e], Adalberto Pessoa Jr. [b], Lara D. Sette [a, *]

[a] Universidade Estadual Paulista Júlio de Mesquita Filho (UNESP), Departamento de Bioquímica e Microbiologia, Rio Claro, SP, Brazil
[b] Universidade de São Paulo (USP), Faculdade de Ciências Farmacêuticas (FCF), São Paulo, SP, Brazil
[c] Centro Nacional de Pesquisa em Energia e Materiais (CNPEM), Laboratório Nacional de Ciência e Tecnologia do Bioetanol (CTBE), Campinas, SP, Brazil
[d] Universidade Federal da Integração Latino-Americana (UNILA), Instituto Latino Americano de Ciências da Vida, Paraná, PR, Brazil
[e] Programa de Processos Tecnológicos e Ambientais, Universidade de Sorocaba, Sorocaba, Brazil

ARTICLE INFO

Article history:
Received 22 November 2017
Received in revised form
25 January 2018
Accepted 31 January 2018
Available online 9 February 2018

Corresponding Editor: Simon Avery

Keywords:
Aerobic fermentation
Filamentous fungi
Green chemistry
Laccases
Multi-cooper oxidases
Salinity

ABSTRACT

Laccase production in saline conditions is still poorly studied. The aim of the present study was to investigate the production of laccase in two different types of bioreactors by the marine-derived basidiomycete *Peniophora* sp. CBMAI 1063. The highest laccase activity and productivity were obtained in the Stirred Tank (ST) bioreactor, while the highest biomass concentration in Air-lift (AL) bioreactor. The main laccase produced was purified by ion exchange and size exclusion chromatography and appeared to be monomeric with molecular weight of approximately 55 kDa. The optimum oxidation activity was obtained at pH 5.0. The thermal stability of the enzyme ranged from 30 to 50 °C (120 min). The Far-UV Circular Dichroism revealed the presence of high β-sheet and low α-helical conformation in the protein structure. Additional experiments carried out in flask scale showed that the marine-derived fungus was able to produce laccase only in the presence of artificial seawater and copper sulfate. Results from the present study confirmed the fungal adaptation to marine conditions and its potential for being used in saline environments and/or processes.

1. Introduction

Laccases (EC 1.10.3.2) are enzymes that belong to the group of polyphenol oxidases and catalyze the oxidation of various organic substances, typically phenolic compounds, with the simultaneous reduction of oxygen to water through a radical-catalyzed reaction mechanism (Baldrian, 2006). Laccases can be found in many different species of organisms, like plants, fungi, prokaryotes, and insects (Yoshida, 1883; Claus, 2004; Dwivedi et al., 2011). They are referred as "moonlight" enzymes due to their multiple physiologic functions, which includes vegetal lignification and delignification, wound healing, pigment synthesis, anti-stress regulation, and fungal morphogenesis (Sharma and Kuhad, 2008).

The use of chemical mediators in the enzymatic reaction of the laccases greatly expanded their oxidation capacities (Bourbonnais and Paice, 1990). The mediators act as electron "shuttle" between the enzyme and the substrate, enabling the oxidization of complex substrates that could not be oxidized by the enzyme itself (Kunamneni et al., 2008; Cañas and Camarero, 2010). Laccases and their mediators (Laccase-Mediator System) are used to degrade and remove a series of recalcitrant pollutants, such as industrial dyes, pesticides, insecticides, endocrine disrupters, and polycyclic aromatic hydrocarbons (Strong and Claus, 2011; Viswanath et al., 2014). Moreover, laccases are also used in the formulation of biofuels and biosensors, medical analyses, and synthesis of new hybrid molecules (Mikolasch and Schauer, 2009; Senthivelan et al., 2016).

The successful application of laccase requires the production of high amounts of enzyme at low costs (Brijwani et al., 2010). Many strategies were already reported in the literature, such as the isolation of new strains for production, development of optimized culture medium, use of agro-industrial residues as carbon source, and heterologous expression of laccase genes (Osma et al., 2011).

* Corresponding author. Departamento de Bioquímica e Microbiologia-IB, Universidade Estadual Paulista-UNESP, Av. 24A, 1515–Bela Vista, Rio Claro, SP, 13506-900, Brazil. Fax: +55 19 3534 0009.
E-mail address: larasette@rc.unesp.br (L.D. Sette).

https://doi.org/10.1016/j.funbio.2018.01.009
1878-6146/

World J Microbiol Biotechnol (2017) 33:201
DOI 10.1007/s11274-017-2373-8

ORIGINAL PAPER

Bioconversion of α-chitin into *N*-acetyl-glucosamine using chitinases produced by marine-derived *Aeromonas caviae* isolates

Flávio Augusto Cardozo[1] · Juan Miguel Gonzalez[2] · Valker Araujo Feitosa[3] · Adalberto Pessoa[3] · Irma Nelly Gutierrez Rivera[1]

Received: 14 October 2016 / Accepted: 24 October 2017 / Published online: 27 October 2017

Abstract *N*-Acetyl-D-glucosamine (GlcNAc) is a monosaccharide with great application potential in the food, cosmetic, pharmaceutical, and biomaterial areas. GlcNAc is currently produced by chemical hydrolysis of chitin, but the current processes are environmentally unfriendly, have low yield and high cost. This study demonstrates the potential to produce GlcNAc from α-chitin using chitinases of ten marine-derived *Aeromonas* isolates as a sustainable alternative to the current chemical process. The isolates were characterized as *Aeromonas caviae* by multilocus sequence analysis (MLSA) using six housekeeping genes (*gltA, groL, gyrB, metG, ppsA*, and *recA*), not presented the virulence genes verified (*alt, act, ast, ahh1, aer, aerA, hlyA, ascV* and *ascF*G), but showed hemolytic activity on blood agar. GlcNAc was produced at 37 °C, pH 5.0, 2% (w/v) colloidal chitin and crude chitinase extracts (0.5 U mL^{-1}) by all the isolates with yields from 14 to 85% at 6 h, 17–89% at 12 h and 19–93% after 24 h. The highest yield of GlcNAc was observed by *A. caviae* CH129 (93%). This study demonstrates one of the most efficient chitin enzymatic hydrolysis procedures and *A. caviae* isolates with great potential for chitinases expression and GlcNAc production.

✉ Flávio Augusto Cardozo
flavio.cardozo@usp.br; flavio.acardozo@gmail.com

[1] Department of Microbiology, Biomedical Sciences Institute, University of São Paulo, 1374 Professor Lineu Prestes Ave., São Paulo 05508-000, Brazil

[2] Institute of Natural Resources and Agrobiology of Seville, Spanish National Research Council, 10 Reina Mercedes Ave., 41012 Seville, Spain

[3] Department of Biochemical and Pharmaceutical Technology, School of Pharmaceutical Sciences, University of São Paulo, 580 Professor Lineu Prestes Ave., São Paulo 05508-000, Brazil

CHAPTER 6

Recent Biotechnological Advances in Food Additives

Valker A. Feitosa[1,2], Daniela A.V. Marques[3], Angela F. Jozala[4], Jorge F. B. Pereira[5] and **Valéria C. Santos-Ebinuma[5,*]**

[1] *Department of Biochemical and Pharmaceutical Technology, School of Pharmaceutical Sciences, University of São Paulo–USP, São Paulo, SP, Brazil*

[2] *Bionanomanufacturing Center, Institute for Technological Research–IPT, São Paulo, SP, Brazil*

[3] *Serra Talhada Campus, University of Pernambuco–UPE, Serra Talhada, PE, Brazil*

[4] *Department of Technological and Environmental Processes, University of Sorocaba–UNISO, Sorocaba, SP, Brazil*

[5] *Department of Bioprocesses and Biotechnology, School of Pharmaceutical Sciences, Univ. Estadual Paulista – UNESP, Araraquara, SP, Brazil*

Abstract: Food additives are substances incorporated into foods to improve quality, nutritional value, functional properties, and consumer acceptance. There is a tendency to replace synthetic additives by natural ones not only because of toxicity of the first but also because natural additives can enhance the characteristics of foodstuff. In this sense, the use of bioprocess technologies can improve the production of natural substances by using wild or genetically modified microorganisms, metabolic engineering, or simply by developing new food formulations. The major goal of this chapter is to present the main food additives used nowadays, mainly focusing on the ones produced *via* biotechnology. The food additives discussed include amino acids, antimicrobial peptides, colorants, organic acids, vitamins, and sweeteners. Although there are many food additives biotechnologically produced on research level, a lot of effort is required to improve their production yields and reduce their overall cost, enabling their large industrial production and commercialization. Anyway, food additives need to be approved by the regulatory authorities before they become industrially favorable. Despite this, biotechnology seems to be very promising in producing natural food additives. Some of the advances in this area are described in the present chapter.

Keywords: Additives, Amino Acids, Antimicrobials, Biotechnology, Colorants, Natural Compounds, Organic Acids, Sweeteners, Vitamins.

[*] **Corresponding author Valéria C. Santos-Ebinuma**: Department of Bioprocesses and Biotechnology; Univ. Estadual Paulista - UNESP, Rodovia Araraquara-Jaú, Km 01, 14800-903, Araraquara, SP, Brazil; Tel: +55-16-33-1-4647; E-mail: valeriac@fcfar.unesp.br

Ali Osman (Ed.)